Universidade de Coimbra

Master Thesis

Chiral Dynamics with Explicit Symmetry Breaking Interactions

Author:
Jorge Morais

Supervisor:
Dr. Brigitte Hiller

A thesis submitted in fulfilment of the requirements for the Master's Degree in Physics

in the

Departamento de Física
Faculdade de Ciências e Tecnologia

September 2014

FCTUC FACULDADE DE CIÊNCIAS E TECNOLOGIA
UNIVERSIDADE DE COIMBRA

"Nowadays, the principle of Spontaneous Symmetry Breaking *is the key concept in understanding why the world is so complex as it is, in spite of the many symmetry properties in the basic laws that are supposed to govern it. The basic laws are very simple, yet this world is not boring; that is, I think, an ideal combination."*

Yoichiro Nambu

"E as pessoas nem sonham que quem acaba uma coisa nunca é aquele que a começou, mesmo que ambos tenham um nome igual, que isso só é que se mantém constante, nada mais."

José Saramago, in *O Ano da Morte de Ricardo Reis*

UNIVERSIDADE DE COIMBRA

Abstract

Faculdade de Ciências e Tecnologia
Departamento de Física

Master's Degree in Physics

Chiral Dynamics with Explicit Symmetry Breaking Interactions

by Jorge Morais

This thesis' aim is twofold: the review and study of a recently proposed NJL-type model extended to include, consistently with N_c counting arguments, a complete set of mass-dependent interaction terms which explicitly break chiral symmetry; and providing a thermodynamical analysis of this model. The study of this model goes through the steps which motivate its construction by presenting several theoretical and phenomenological aspects of QCD and hadron physics, with a special focus on aspects of chiral symmetry and its dynamical breaking. Then some of the features of NJL models and their analysis are reviewed, and a careful exposition of the extended model is given. Finally, the finite temperature and chemical potential dependence is introduced in the model. The associated quark mass profiles, the phase diagram, and quark matter subject to β-equilibrium and charge neutrality conditions are calculated and analyzed. Two first-order transition lines are obtained and the prospect of stable strange quark matter in view of these results is discussed.

Acknowledgements

First of all, I would like to express my heartfelt gratitude to my supervisor, Brigitte Hiller, for being so solicitous and regardful, for always showing confidence in my ability to carry through, and for all the warmth and kindness she has shown me throughout the time we have worked together. Without her ever present guidance, I would have hardly been able to finish off my work in such a gratifying and fulfilling way.

I would also like to thank João Moreira, whose helpfulness and goodwill fall nothing short of Brigitte's. I am very glad to have had him collaborating with me in the analysis and discussion of the results obtained in this thesis. His support in all the numerical computations and in the ellucidation of the results was extremely valuable. Moreover, I must express my sincere appreciation for Alex Blin's collaboration on several occasions.

Furthermore, there are a number of friends and colleagues whose affection and companionship have undoubtedly eased the strenuous process of preparing and writing a thesis. All the joyful moments they have shared with me, all their advices and insights; these things have helped in keeping me steady and motivated throughout my work. I will not make a list of names for fear of unjust omissions, but I am certain that those to whom I am grateful will known this is for them.

Last, but surely not the least, I would like to thank my family for the unwavering love and support they have always shown, through better and worse times. A very special thank you to my parents, to whom I owe most of what I am; all my accomplishments will always be yours.

Contents

List of Figures

List of Tables

Abbreviations

BCS	**B**ardeen **C**ooper **S**chrieffer
CEP	**C**ritical **E**nd**p**oint
ChPT	**Ch**iral **P**erturbation **T**heory
HIC	**H**eavy **I**on **C**ollisions
LSM	**L**inear **S**igma **M**odel
NJL	**N**ambu **J**ona-**L**asinio
OZI	**O**kubo **Z**weig **I**izuka
QCD	**Q**uantum **C**hromo**d**ynamics
QFT	**Q**uantum **F**ield **T**heory
SM	**S**tandard **M**odel
SPA	**S**tationary **P**hase **A**pproximation
SQM	**S**trange **Q**uark **M**atter
TOV	**T**olman **O**ppenheimer **V**olkoff

To my loving parents...

Chapter 1

Introduction

Since the discovery of the nucleons and, later, of a proliferation of other particles which have come to be known collectively as hadrons, the necessity of an adequate theoretical framework that could describe their properties and dynamics grew ever more pressing. After several tentative models which have been developed since the early days, each unravelling a piece of the full intricate picture, a general consensus has been established among investigators around the theory of Quantum Chromodynamics (QCD) as being the best candidate to a complete theory of the strong interactions, with the quark model as one of its foundations and gauge field theory as another. Some credit for this broad support is certainly due to the multiple successes of its older cousin in the family of gauge theories, Quantum Electrodynamics (QED). However, it was also soon realized that QCD was a much wilder beast to tame, and the techniques that had been so fruitfully applied in QED, in particular the perturbative approach, were of much more limited use in QCD. And there we were, faced with a presumedly fundamental theory and yet with no apparent way of using it to describe a good part of the relevant physical phenomena. Necessity, as always, is the mother of invention, and in this case it was necessary to find new, creative ways of tackling QCD and making it produce sensible predictions. It was not too long before a multitude of different approaches and approximations were again on the market for application to the strong interactions.

One might ask, "But are we not back where we started?". The observant reader would promptly answer a resounding "No!". It is true that we have yet to uncover some (or many) parts of the picture and, as it often is when something new is being born, while giving birth to new insight and more profound discernment things may get a little messy. But all the efforts, all the right and wrong paths we have traveled in the pursuit of a solid understanding, and all the pieces of the puzzle we have set along the way are undeniably more than what we had when we started. Today, we may not have a full

grip on the whimsical theory of QCD, and it may even come to the point when we realize QCD was not the foremost answer after all, but we have certainly learned many valuable things about what hadrons are and how they interact, we have aknowledged prior difficulties and limitations and we have refined our approaches, coming out of the journey wiser, more skilled and empowered in our ability to delve ever deeper into nature's inner workings.

So, what have we learned so far? We learned about the systematic ways in which hadrons seem to be categorized according to their quantum numbers: the multiplets. We dug more in-depth and learned how we could accomodate these features in terms of a constituent quark model. We learned about the gluons which keep quarks strongly bound within hadrons, about confinement. We learned about decays and interactions. We learned about the fundamental role of symmetries. We learned many things. We keep learning and, still, the universe seems to remain inexhaustible in elaborate richness and detail, never dull, sometimes elusive, always alluring.

1.1 Purpose and Motivation

In the low energy regime, QCD does not admit a perturbative treatment, and alternative approaches must be worked out in order to make predictions on physical phenomena. Some of the available methods are mentioned in Chapter 2, but in this thesis we will focus on NJL-type models. These models try to capture the essential features of chiral symmetry in the light sector of QCD, modelling the strong interactions through effective multi-quark vertices and providing a mathematically tractable tool for studying the mechanism of dynamical mass generation through chiral symmetry breaking. The model, originally proposed in the 60's (thus prior to QCD itself) as an effective model for nucleon dynamics [1] [2], has been enhanced over decades and reformulated in terms of quark fields for two and three flavours, and also to include the effect of small current quark masses which explicitly break chiral symmetry. The model is non-renormalizable, so all results are explicitly dependent on some energy scale Λ which characterizes its domain of applicability.

Recently, in line with the reasoning behind the construction of effective field theories (EFTs), a new extension to the model has been proposed [3] [4] which includes a complete set of current quark mass dependent interaction terms which contribute at the same order as the $U(1)_A$ symmetry breaking interaction and other vertices that are important in four dimensions for dynamical chiral symmetry breaking. With this, there is a whole new set of terms whose phenomenological consequences have yet to be fully understood. This

fact gives us the main motivation behind this work: to study some of the phenomenology that these new terms bring into the model.

Models like this one are oriented towards the investigation of the non-perturbative scales of QCD, and they are specially useful to do analyses which are overly complicated to perform through lattice calculations. One such example, and a particularly interesting one, is the study of the QCD phase diagram at moderate temperatures and chemical potentials. Lattice techniques, despite many recent advances, are still plagued with problems at finite chemical potentials (known as the *sign problem*). Thus, model calculations may be the best theoretical alternative for studying this topic. This will be the main objective of this thesis: the construction of the phase diagram in light of the above-mentioned model and its discussion.

In order to present a sound argument, we will spend Chapters 2 and 3 reviewing a number of topics which are relevant for chiral dynamics, the NJL model and, of course, the new extended version that we wish to investigate. Then, in Chapter 4, we will perform our analysis and discuss our results.

We would like to note that natural units with $c = \hbar = k_B = 1$ are used throughout the entire thesis.

1.2 Discussion Layout

In Chapter 2, we present a series of theoretical aspects that underly and set the grounds for all the subsequent discussion. We start by giving a concise overview of QCD, addressing fundamental symmetry aspects with a special focus on chiral symmetry, the problem of low energy non-perturbativity, and the construction of effective models. Additionally, we give a brief review of some phenomenological aspects, and we end with an exposition of the Nambu-Jona-Lasinio (NJL) model.

In Chapter 3 we aim to establish the rigorous form of the model we wish to investigate, starting from the analysis of a preceding version of the NJL model wich includes the usual 't Hooft determinantal interaction term in the functional bosonization framework. We argue that this version has no stable vacuum for the three flavour case, which motivates the inclusion of 8-quark interaction terms in order attain stability. These vertices are, like the 't Hooft interaction, $1/N_c$ suppressed with regard to the 4-quark interactions and the mass term. The final extension that is considered at next to leading order (NLO) includes also the $1/N_c$ suppressed interactions which break explicitly the chiral symmetry through the coupling of the quark fields to an external source. We end by reviewing some important aspects of this extension.

In Chapter 4 we study the effects of including finite temperature and chemical potential on the model. We derive the one-loop thermodynamical potential and find the dynamical quark masses for several values of the thermodynamic variables. Furthermore, we build the phase diagram and discuss its most important features. The prospect of stable strange quark matter (SQM) is also investigated within physically reasonable conditions.

In Chapter 5 we summarize the results and the main conclusions, and we propose some directions for further investigation.

Chapter 2

Theoretical and Phenomenological Background

2.1 Quantum Chromodynamics

Quantum Chromodynamics (QCD) is a non-Abelian SU(3) gauge theory that describes the strong interaction of quarks in the Standard Model (SM). [5] The generators of the gauge symmetry group are given in terms of the well-known Gell-Mann matrices λ^a, which obey the algebra

$$\left[\lambda^a, \lambda^b\right] = 2if^{abc}\lambda^c, \tag{2.1}$$

where the f^{abc} are the group structure constants [see Appendix A]. The quark field q belongs to the fundamental triplet representation of the symmetry group, and one speaks of a colour quantum number to label each of the three members of the triplet. Furthermore, q transforms as a spinor under Lorentz transformations, and it carries an additional flavour quantum number underlying the distinction between different quarks in terms of physical variables such as electrical charge or mass. As for the gluon field $A_\mu = A_\mu^a \frac{\lambda^a}{2}$, it resides in the adjoint octet representation, carrying two colour quantum numbers. Under Lorentz transformations, it behaves as a vector.

The QCD Lagrangian density may be written as

$$\mathcal{L}_{QCD} = \bar{q}\left(i\gamma^\mu\partial_\mu - m_0\right)q - \frac{1}{4}F^a_{\mu\nu}F_a^{\mu\nu} + g\bar{q}\gamma^\mu A_\mu q. \tag{2.2}$$

Here, F is the gluon field tensor defined as

$$F^a_{\mu\nu} = \partial_\mu A_\nu - \partial_\nu A_\mu + g f^{abc} A^b_\mu A^c_\nu \tag{2.3}$$

For simplicity, quark field indices are all omitted. The formal content of this Lagrangian density is most transparent: we have a Dirac term that expresses quark kinetic and mass terms; then there is a Yang-Mills term quadratic in F which contains the kinetic and self-interaction terms for the gluon field; finally there is a quark-gluon coupling term, describing quark-quark interactions by means of intermediary gluon exchange.

QCD has an important feature which is worth noting: *asymptotic freedom*. [6] Due to the gauge boson self-interactions, vacuum polarization contributes an antiscreening effect that effectively reduces the running coupling constant at large momenta. This is in contrast with what is observed in QED, where vacuum polarization due to fermion bubbles gives rise to an effective screening effect. Quantitatively, one can resort to the one-loop beta function for strong interactions [7]

$$\beta(\alpha_s) = -(11N_c - 2N_f)\frac{\alpha_s^2}{6\pi} \tag{2.4}$$

It is evident that with number of colours $N_c = 3$ and number of flavours $N_f = 6$, $\beta(\alpha_s) < 0$, which leads to quarks being asymptotically free at sufficiently high energies, and very strongly bound at smaller energies. Presumably, this might give rise to a mechanism for colour confinement, i.e. the impossibility of observing colour degrees of freedom. [5]

2.1.1 Symmetries

The QCD Lagrangian density (2.2) is manifestly Lorentz covariant, as is expected of any realistic QFT. Additionally, the discrete symmetries of parity, time reversal and charge conjugation are also present. Furthermore, it enjoys (by construction) an SU(3) gauge symmetry, i.e., the Lagrangian density (2.2) is invariant under the combined transformations

$$q \to U_c q \qquad \bar{q} \to \bar{q} U_c^\dagger \tag{2.5a}$$

$$A_\mu \to U_c A_\mu U_c^\dagger - \frac{i}{g} U_c \partial_\mu U_c^\dagger \tag{2.5b}$$

where the unitary transformation U_c is given in terms of a set of eight local colour rotation angles $\theta^a(x)$ as

$$U_c = e^{i\theta^a(x)\frac{\lambda^a}{2}} \tag{2.6}$$

Another symmetry of (2.2) arises from the fact that gluons are flavour blind. If we take the quark mass matrix m_0 to be degenerate, it is straightforward to show that the Lagrangian density remains invariant under a general global rotation in flavour space

$$q \to U_f q \qquad \bar{q} \to \bar{q} U_f^\dagger \tag{2.7}$$

with the unitary transformation given by

$$U_f = e^{i\phi^a \frac{\tau^a}{2}} \tag{2.8}$$

where τ^a are the generators of the $U(N_f)$ flavour group (see Appendix A) and ϕ^a is an appropriately dimensioned set of flavour rotation angles. The singlet transformation with $a = 0$ is always an exact symmetry of the QCD Lagrangian, and is associated with baryon number conservation. [5]

Besides these symmetries, one can further consider an approximate chiral symmetry, which is related to a transformation similar to (2.7) but with

$$U_f^{'} = e^{i\phi^{'a}\gamma_5 \frac{\tau^a}{2}} \tag{2.9}$$

In this case, due to the Dirac algebra (see Appendix B), the adjoint spinor transforms as

$$\bar{q} \to \bar{q} U_f^{'} \tag{2.10}$$

This would be an exact symmetry of the Lagrangian density (2.2) for zero current quark masses m_0. Despite not being an exact symmetry as it is, it has been shown to be of great importance for further understanding of the dynamics of quarks and hadrons, namely by showing up as a dynamically broken symmetry in several models. This subject is more deeply developed in section 2.2.

2.1.2 Low Energy Non-Perturbativity

As a standard renormalization procedure in perturbation theory, one takes the interaction term as a small perturbation to the free Lagrangian density and expands it in powers of the coupling constant. This procedure relies on the assumption that the coupling constant is small, so that higher powers will contribute progressively less to the calculation of physical observables. [8] This works exceedingly well in Quantum Electrodynamics (QED), but fails when one tries to apply it to QCD, and the reason for this is its characteristic feature of asymptotic freedom.

At high energies, the strong coupling constant may be sufficiently small for perturbation theory to be applicable. However, at lower energies, the coupling becomes large enough for higher order terms in the perturbation series to be ever more important, raising convergence issues. This theoretically unsatisfactory feature shows that, at low energies, QCD is non-perturbative and, therefore, difficult to employ directly in the actual calculation of observables.

With this fact arises a pressing need for alternative approaches to conventional perturbation theory. One such approach which has become fairly popular is Lattice QCD. Its description falls way beyond the scope of the present work, but there is no way of going about these topics without at least mentioning it. Very briefly, it attempts to circumvent the infinite set of divergent diagrams crowding the continuous space version of the theory by discretizing spacetime into a hypercubic lattice, introducing as a new parameter the lattice spacing a. Naturally, some aspects of the original formalism, e.g. fundamental symmetries, must be put in an adequate form for the discretized description. If a is sufficiently small, lattice calculations constitute a very powerful approximation to the continuous version of the theory. It has already provided some of the most accurate predictions available today concerning strong processes. As a major setback, in the Lattice QCD framework, even the simplest calculations require tremendous computational power, which might not be widely available and be extremely time consuming. [7]

Another popular trend in the study of strong interactions comes in the shape of *Effective Field Theories* (EFTs), whose general aspects we succinctly describe in the following section.

2.1.3 Effective Models

A number of effective models and toy QFTs, either pre-QCD or post-QCD, have been developed in an attempt to better understand physical phenomena and to overcome the inherent difficulties of QCD. The Fermi theory of beta decay [9], for example, might be

considered one of the first effective models, and a successful one as well. The primary inspiration for the model we will be studying in the later sections of this thesis is the Nambu-Jona-Lasinio (NJL) model. We shall discuss it a little further in section 2.4. Its features are closely related to those of the Fermi model, as well as the toy models of Thirring [10] in one dimension, Gross-Neveu [11] in two dimensions, and Soler [12] in four dimensions. Their common feature is the description of self-interacting chiral fermions through local quartic interaction terms.

Other models include the Chiral model [13], Sigma models [14], the Skyrme model [15], the Vector Meson Dominance model [16], Chiral Perturbation Theory [17] [18] [19] [20] [21] [22], Unitarized Quark Models [23], and the Heavy Quark Effective Theory [24]. From a more contemporary perspective, we can identify some of these models as EFTs.

2.1.3.1 Effective Field Theories

The SM intends to give a dynamical description of physics based on fundamental degrees of freedom. However, this beautiful and important framework has its own shortcomings when it comes to the application to specific problems where calculations may become exceedingly complex and even intractable. An example of this has already been mentioned, the low energy regime of QCD, but there are a number of situations where the direct application of the SM is prohibitingly complicated. We would greatly benefit from building approximate (effective) models that could give the same results as the SM within a given range of applicability. Such systematic procedure for constructing EFTs has been introduced by Weinberg in [25].

The idea is that each specific problem or system may have its own set of relevant degrees of freedom distinct from the fundamental degrees of freedom that appear in the SM. In the case of low energy QCD, for example, heavier quarks may be disregarded altogether, since they are not expected to be involved in processes at energy scales significantly lower than their own masses. The mere introduction of an explicit energy scale Λ leads already to some simplification of the QCD Lagrangian density, discarding the heavier quark degrees of freedom. We can still go further in identifying the truly relevant low energy degrees of freedom as pions and nucleons. Finally, we can do an expansion in $\frac{p}{\Lambda}$, where p are momenta or masses which are lower than the effective energy scale Λ, in a similar fashion to conventional perturbation theory.

For the construction of the effective Lagrangian density, it is suggested that *"if one writes down the most general possible Lagrangian, including all terms consistent with the assumed symmetry principles, and then calculates matrix elements to any given order of perturbation theory, the result will simply be the most general possible S-matrix*

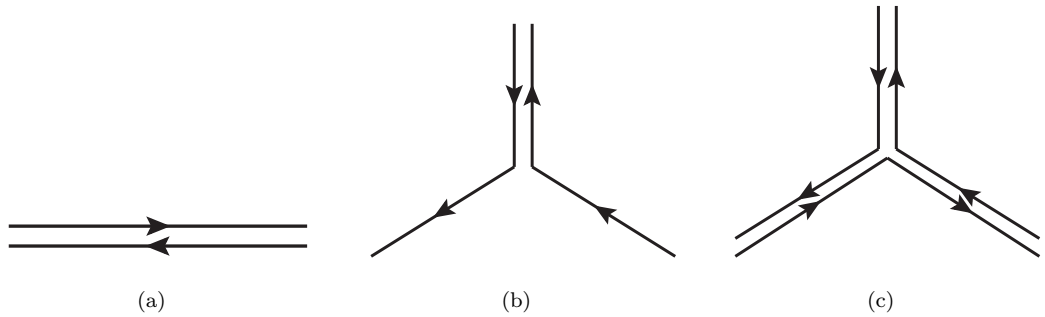

FIGURE 2.1: Double-line notation for the gluon propagator (a), with the quark-gluon vertex (b) and the three gluon vertex (c) shown.

consistent with analyticity, perturbative unitarity, cluster decomposition and the assumed symmetry principles". [25] This prescription emphasizes the significance of symmetry considerations as the underlying guiding principle for the construction of EFTs. For each term in the Lagrangian we introduce an effective low energy coupling, and the full Lagrangian is actually an infinite sum of terms respecting the assumed symmetries. A consistent perturbation approach then requires us to work with terms up to some power of $\frac{p}{\Lambda}$. This consistency check is known as *power counting*.

In the context of strong interactions, this has led to what is now known as *Chiral Perturbation Theory* (ChPT), which is commonly written in terms of mesonic degrees of freedom. An underlying spontaneously broken chiral symmetry with a $U(1)_A$ anomaly is assumed (see sections 2.2 and 2.3) and used to construct an effective Lagrangian, usually including the three lighest flavours. Alternatively, we can build an effective chiral Lagrangian based on quark degrees of freedom, and then bosonize the theory. This is the approach taken in the model we will be studying.

2.1.3.2 $1/N_c$ Expansion

It has been stated above that QCD doesn't allow for a perturbative expansion in terms of the coupling g, at least for sufficiently low energies, and that this feature stems from the asymptotic freedom associated with the non-Abelian gauge group $SU(3)$. Besides EFTs built around mass or momentum expansions, another possible expansion scheme based on the number of colours N_c has been suggested in the limit $N_c \longrightarrow \infty$. [26] This is usually performed by considering a $U(N_c)$ version of QCD.[1] Quark fields carry a colour index while gauge fields carry two colour indices, and a double line notation is introduced for the gluon propagator in order to explicitly represent colour flow in the diagrams. Examples are shown in figure 2.1.

[1]The same arguments are valid with $SU(N_c)$ in the large N_c limit.

We may rescale the coupling as $g \longrightarrow \frac{\tilde{g}}{\sqrt{N_c}}$ and the fields as $gA_\mu \longrightarrow \tilde{A}_\mu$ and $\psi \longrightarrow \sqrt{N_c}\tilde{\psi}$. With this, the QCD Lagrangian (2.2) is rewritten as

$$\mathcal{L}_{QCD} = N_c \left\{ \tilde{\bar{q}} \left(i\gamma^\mu \partial_\mu - m_0 \right) \tilde{q} - \frac{1}{4\tilde{g}^2} \tilde{F}^a_{\mu\nu} \tilde{F}^{\mu\nu}_a + \tilde{\bar{q}} \gamma^\mu \tilde{A}_\mu \tilde{q} \right\} \tag{2.11}$$

From this it is straightforward to extract a new set of Feynman rules: vertices carry a factor of N_c, propagators carry a factor of $\frac{1}{N_c}$, and colour loops introduce a factor of N_c.

We may systematically look at diagrams from a topological point of view: they consist of glued polygons that form more or less complicated surfaces. If we view propagators as polygon edges and colour loops as faces, then any connected diagram with no external legs has an overall factor given by

$$N_c^{V-E+F} \tag{2.12}$$

where V is the number of vertices, E is the number of edges, and F is the number of faces. This topological invariant combination is commonly known as the Euler characteristic $\chi = V - E + F$. For $\chi = 2$, the diagrams are said to be planar (they have the topology of the sphere); these give the dominant contribution in an expansion in powers of N_c. Non-planar diagrams have $\chi < 2$ and are thus suppressed in the expansion. For connected orientable surfaces, we have

$$\chi = 2 - 2h - b \tag{2.13}$$

where h is the number of handles and b is the number of distinct boundaries. This provides us with a way of systematically finding the order of any diagram in N_c, enabling us to use N_c as a perturbative expansion parameter. In figure 2.2 we can see some examples of diagrams which contribute at different orders in N_c power counting.

The N_c power counting may be used as a tool for the construction of effective QCD Lagrangians: we should decide which order in N_c we want to go, and then include all effective terms up to that power. In this way, we ensure the consistency of the effective expansion. A more complete exposition of these ideas may be found in [27].

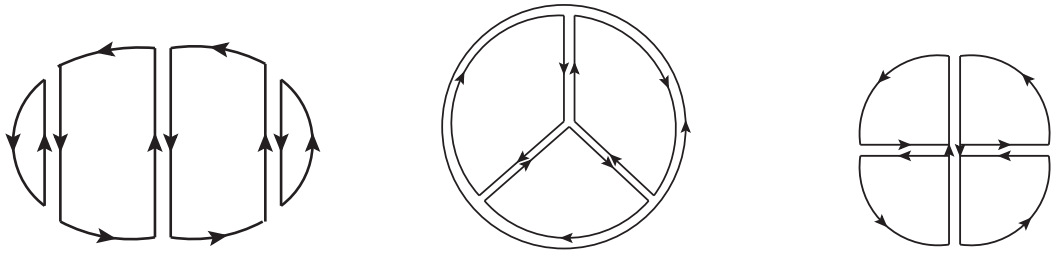

(a) (b) (c)

FIGURE 2.2: (a) An $\mathcal{O}(N_c)$ diagram, with one colour boundary and no handles. (b) An $\mathcal{O}(1)$ diagram, with two colour boundaries and no handles. (c) An $\mathcal{O}\left(N_c^{-1}\right)$ diagram, with one colour boundary and one handle.

2.2 Chiral Symmetry

As was briefly mentioned in the previous section (subsection 2.1.1), in the limit of vanishing current quark masses m_0 the QCD Lagrangian displays an additional invariance property known as *chiral symmetry*. It should be apparent that, for the heavier quarks, this approximation of zero current quark mass is overly crude. Therefore, it is costumary to restrict the discussion of chiral symmetry to the three lightest quark flavours, which are then taken as belonging to the triplet representation of an SU(3) flavour symmetry group.

In order to clarify what is meant by chiral symmetry, we refer to the unitary flavour transformations given in (2.7) and (2.10). We rewrite (2.8) and (2.9) respectively as

$$U_V = e^{i\theta_V^a \frac{\tau^a}{2}} = e^{i\theta_V} \tag{2.14a}$$

$$U_A = e^{i\gamma_5\theta_A^a \frac{\tau^a}{2}} = e^{i\gamma_5\theta_A} \tag{2.14b}$$

where the τ^a are then the generators of the U(3) group in flavour space and we define

$$\theta_{V,A} = \theta_{V,A}^a \frac{\tau^a}{2} \tag{2.15}$$

The τ^a are closely related to the Gell-Mann matrices λ^a of $SU(3)$ we had previously introduced. There are nine τ^a matrices, which can be taken identical to the λ^a for a between 1 and 8, and the remaining matrix is conventionally written τ^0 and taken as $\tau^0 = \sqrt{\frac{2}{3}}\mathbb{1}_{3\times3}$.[2] (see Appendix A)

[2] This amounts to the realization that the group $U(3)$ can be decomposed as $U(1) \otimes SU(3)$.

Chiral symmetry is then usually defined as invariance under the combined group $U(3)_V \otimes U(3)_A$. By making use of the chiral projection operators

$$P_{R,L} = \frac{1}{2}(1 \pm \gamma_5) \tag{2.16}$$

we can define left and right-handed spinors as

$$q_{R,L} = P_{R,L} q \qquad \bar{q}_{R,L} = \bar{q} P_{L,R} \tag{2.17}$$

Since $P_{R,L}$ are projection operators (see Appendix B), the spinors can always be decomposed as

$$q = q_R + q_L \qquad \bar{q} = \bar{q}_R + \bar{q}_L \tag{2.18}$$

With these definitions, we are led to an alternative perspective on chiral transformations by noting that the QCD Lagrangian density (2.2) naturally decomposes in terms of left and right handed spinors as

$$\begin{aligned} \mathcal{L}_{QCD} = {} & \bar{q}_R (i\gamma^\mu \partial_\mu) q_R + \bar{q}_L (i\gamma^\mu \partial_\mu) q_L - \frac{1}{4} F^a_{\mu\nu} F^{\mu\nu}_a \\ & + g\bar{q}_R \gamma^\mu A_\mu q_R + g\bar{q}_L \gamma^\mu A_\mu q_L - \bar{q}_L m_0 q_R - \bar{q}_R m_0 q_L \end{aligned} \tag{2.19}$$

In the limit of vanishing current quark mass (i.e., $m_0 = 0$), we see that no term remains in (2.19) that mixes left and right-handed spinors. This means that we can independently transform q_R and q_L under an $U_V(3)$ symmetry transformation. This is known as the *chiral limit*.

These two ways of understanding chiral symmetry must, of course, be equivalent. We can sketch a simple illustration of their equivalence following [5]. The effect of applying both transformations (2.14) is given by

$$\begin{aligned} U_V(\theta_V) U_A(\theta_A) &= U_V(\theta_V) \left(U_V(\theta_A)\right)^{\gamma_5} \\ &= \left(U_V(\theta_V)\right)^{P_R + P_L} \left(U_V(\theta_A)\right)^{P_R - P_L} \\ &= e^{i\theta_V (P_R + P_L)} e^{i\theta_A (P_R - P_L)} \end{aligned} \tag{2.20}$$

By expanding the exponentials in (2.20) in Taylor series and using the idempotence of $P_{R,L}$, we get

$$\begin{aligned} U_V(\theta_V)\,U_A(\theta_A) &= \left[P_R e^{i\theta_V} + P_L e^{i\theta_V}\right]\left[P_R e^{i\theta_A} + P_L e^{-i\theta_A}\right] \\ &= P_R e^{i\theta_V} e^{i\theta_A} + P_L e^{i\theta_V} e^{-i\theta_A} \\ &= P_R e^{i\theta_R} + P_L e^{i\theta_L} \end{aligned} \tag{2.21}$$

In this way, we can see that the joint action of transformations (2.14) with parameters θ_V and θ_A simply amounts to independently transforming left and right-handed spinors with parameters θ_R and θ_L consistent with

$$e^{i\theta_{R,L}} = e^{i\theta_V} e^{\pm i\theta_A} \tag{2.22}$$

We can say that the chiral symmetry group may equivalently be decomposed as $U(3)_V \otimes U(3)_A$ or $U(3)_L \otimes U(3)_R$. Furthermore, each $U(3)$ symmetry group admits a decomposition as $SU(3) \otimes U(1)$. Hence, the full chiral symetry group may be written as

$$\boxed{SU(3)_V \otimes SU(3)_A \otimes U(1)_V \otimes U(1)_A} \tag{2.23}$$

2.2.1 Chiral Currents

According to Noether's Theorem, there should be 18 conserved currents associated with the degrees of freedom of the chiral symmetry group (2.23). Applying the formalism described in Appendix C to the Lagrangian density (2.19) in the chiral limit (i.e. $m_0 = 0$), we find the conserved currents

$$J_R^{\mu,a} = \bar{q}_R \gamma^\mu \frac{\tau^a}{2} q_R \tag{2.24a}$$

$$J_L^{\mu,a} = \bar{q}_L \gamma^\mu \frac{\tau^a}{2} q_L \tag{2.24b}$$

Each of the currents in (2.24) comprises a singlet current for $a = 0$ and an octet for a between 1 and 8:[3]

[3] Multiplication of these currents by a constant factor does not alter anything about the physics they describe. We may then conveniently to drop the $\frac{1}{\sqrt{6}}$ factor that would appear in the expression for the singlet currents.

$$J^{\mu,(s)}_{R,L} = \bar{q}_{R,L}\gamma^{\mu}q_{R,L} \qquad J^{\mu,a}_{R,L} = \bar{q}_{R,L}\gamma^{\mu}\frac{\tau^a}{2}q_{R,L}\,, \qquad a \text{ between 1 and 8} \tag{2.25}$$

We can also define vector and axial vector chiral currents as

$$J^{\mu,a}_{V} = J^{\mu,a}_{R} + J^{\mu,a}_{L} = \bar{q}\gamma^{\mu}\frac{\tau^a}{2}q \tag{2.26a}$$

$$J^{\mu,a}_{A} = J^{\mu,a}_{R} - J^{\mu,a}_{L} = \bar{q}\gamma^{\mu}\gamma_5\frac{\tau^a}{2}q \tag{2.26b}$$

Furthermore, from each of these currents we can define a conserved charge as

$$Q^a_X = \int d^3x J^{0,a}_X(\vec{x},t) \tag{2.27}$$

2.2.2 Partial Conservation of Axial Current and Goldberger-Treiman Relations

One good example of the success of chiral symmetry as a good (approximate) symmetry of low energy phenomenology is given by a treatment of pion weak decay within a simple Fermi model. [9] In such a treatment, interactions are described through the direct coupling of the relevant currents. The decay can be summarized as $\pi^+ \longrightarrow l^+ + \nu_l$ or $\pi^- \longrightarrow l^- + \bar{\nu}_l$. The leptonic current consists of a sum of vector and axial vector currents between the charged lepton and corresponding neutrino. As for the pions, which have negative parity, the transition to the vacuum state takes place by means of some axial current $J^{\mu}_{A,\pi}(x)$. The only kinematically independent four-vector available is the pion momentum, and so the transition amplitude must be proportional to it. If the pion is initially in a state of definite momentum p, then the pionic transition current can be written as [28]

$$\langle 0|\,\hat{J}^{\mu}_{A,\pi}(x)\,|\pi(p)\rangle = if_{\pi}p^{\mu}e^{-ix^{\nu}p_{\nu}} \tag{2.28}$$

where f_π is the so-called pion decay constant and its empirical value is around 90 MeV. From this expression we can now take the four-divergence to obtain

$$\begin{aligned}\langle 0|\,\partial_{\mu}\hat{J}^{\mu}_{A,\pi}(x)\,|\pi(p)\rangle &= f_{\pi}p^{\mu}p_{\mu}e^{-ix^{\nu}p_{\nu}} \\ &= f_{\pi}m^2_{\pi}e^{-ix^{\nu}p_{\nu}}\end{aligned} \tag{2.29}$$

We have here a direct connection between the four-divergence of the axial current $J^{\mu}_{A,\pi}$ and the pion mass m_{π}. In fact, an exact conservation of the axial current (i.e., $\partial_{\mu} J^{\mu}_{A,\pi}(x) = 0$) would lead to massless pions. In this way, the relative smallness of the pions' actual masses serves as a good indicator that the axial current is at least partially conserved.

As a spin-0 particle, the pion field obeys a Klein-Gordon equation,

$$\left(\partial^{\mu}\partial_{\mu} + m_{\pi}^{2}\right)\phi(x) = 0 \tag{2.30}$$

and its solutions with definite momentum are simply plane waves (apart from a normalization factor) $\phi(x) = \exp\left(-ix^{\mu}p_{\mu}\right)$. This allows us to rewrite (2.29), apart from a constant factor, as

$$\begin{aligned} \partial_{\mu} J^{\mu}_{A,\pi}(x) &= f_{\pi}\partial^{\mu}\partial_{\mu}\phi(x) \\ \Rightarrow J^{\mu}_{A,\pi}(x) &= f_{\pi}\partial^{\mu}\phi(x) \end{aligned} \tag{2.31}$$

Another successful example of these ideas is given by the investigation of nucleon axial currents and pion-nucleon interactions. [28] The nucleon axial currents are given by

$$J^{\mu}_{A,N}(x) = g_a \bar{\psi}_N \gamma^{\mu}\gamma_5 \frac{\tau}{2}\psi_N \tag{2.32}$$

where g_a is a factor due to renormalization of the nucleon axial current, and τ is an element of the $SU(2)$ isospin group. Using the fact that the nucleon fields obey Dirac equations like

$$\left(i\gamma^{\mu}\partial_{\mu} - M_N\right)\psi_N(x) = 0 \tag{2.33a}$$

$$\bar{\psi}_N(x)\left(i\gamma^{\mu}\overleftarrow{\partial}_{\mu} + M_N\right) = 0 \tag{2.33b}$$

we can write the four-divergence of the axial current (2.32) as

$$\partial_{\mu} J^{\mu}_{A,N}(x) = i g_a M_N \bar{\psi}_N \gamma_5 \tau \psi_N \tag{2.34}$$

The high nucleon mass M_N does not allow for axial current conservation. We can, however, change the picture a bit if we recall how pions strongly interact with the

nucleons. Perhaps if we consider the sum of both currents, we can still speak of a partially conserved axial current. Using relation (2.2.2), we can write the total axial current as

$$J^{\mu}_{A,N+\pi}(x) = g_a \bar{\psi}_N \gamma^{\mu} \gamma_5 \frac{\tau}{2} \psi_N + f_{\pi} \partial^{\mu} \phi(x) \tag{2.35}$$

If we now require the total axial current to be conserved, we arrive at the relation

$$\partial^{\mu} \partial_{\mu} \phi(x) = -i g_a \frac{M_N}{f_{\pi}} \bar{\psi}_N \gamma_5 \tau \psi_N \tag{2.36}$$

This has the form of a Klein-Gordon equation for a massless pion interacting with the nucleon. Relaxing the condition of exact axial current conservation, we can introduce the appropriate pion mass term in the equation, which gives us

$$\left(\partial^{\mu} \partial_{\mu} + m_{\pi}^2\right) \phi(x) = -i g_a \frac{M_N}{f_{\pi}} \bar{\psi}_N \gamma_5 \tau \psi_N \tag{2.37}$$

We now inspect the interaction term in the right-hand side of (2.37). The pion-nucleon coupling constant arises in a simple fashion in terms of M_N and f_{π} as

$$g_{\pi NN} = g_a \frac{M_N}{f_{\pi}} \tag{2.38}$$

Equation (2.38) is known as the *Goldberger-Treiman relation* [29], and its predicted value of $g_{\pi NN} \approx 12.5$ is remarkably close to the empirical value of 13.4. Again, we were led to this result largely based on considerations of axial current conservation. It is remarkable that the strong interaction coupling $g_{\pi NN}$ contains information about the weak decay process of the pion through f_{π}. The quantitative agreement between prediction and experiment seems too good to be accidental.

These examples served to illustrate how a partially conserved axial current can be used as a good assumption for the phenomenological description of some low energy phenomena involving strongly interacting particles. Results like these have provided convincing empirical evidence for the establishment of chiral symmetry as a useful and important tool in the treatment of such problems.

2.3 Spontaneous Breaking of Chiral Symmetry

In the light quark sector of QCD, chiral symmetry appears to be a good symmetry of the system. It is, of course, explicitly broken through the quark mass terms in the Lagrangian density, although the deviation is scaled by small current quark masses. This can be expressed through the divergences of the chiral currents: [30]

$$\partial_\mu J_V^{\mu,a} = i\bar{q}\left[m_0, \frac{\tau^a}{2}\right] q \tag{2.39a}$$

$$\partial_\mu J_A^{\mu,a} = i\bar{q}\gamma_5\left\{m_0, \frac{\tau^a}{2}\right\} q \tag{2.39b}$$

$$\partial_\mu J_V^{\mu} = 0 \tag{2.39c}$$

$$\partial_\mu J_A^{\mu} = 2i\bar{q}\gamma_5 m_0 q + \frac{N_f g^2}{32\pi^2}\epsilon_{\mu\nu\rho\sigma}F_a^{\mu\nu}F_a^{\rho\sigma} \tag{2.39d}$$

Here, the first two equations give the four-divergence of the flavour octet vector and axial vector currents, respectively. The other two concern the singlet currents, where the axial anomaly has been included. Thus, taking into account the finite current quark masses, we see that the axial current is always spoiled independently of the actual values in m_0. However, the octet vector current is still conserved if we assume equal current masses for all the quark flavours in consideration, i.e., if $m_0 \propto \mathbb{1}$.

But this is not the whole story. A small explicit breaking of chiral symmetry is not enough to explain, for example, the hadron mass spectrum. In particular, the constituent quark model by itself is unable to explain the huge difference between the masses of a pion (2 up/down quarks, 150 MeV) and a nucleon (3 up/down quarks, 980 MeV). In the following subsection, the inconsistencies are developed and more clearly exposed.

2.3.1 Meson Mass Spectrum and Chiral Symmetry

The light mesons[4] can be represented by quark bilinears with the appropriate transformation properties. Thus, one can write (see also Appendix B): [28]

$$s^a = \bar{q}\frac{\tau^a}{2}q \qquad \text{scalar states} \tag{2.40a}$$

$$p^a = i\bar{q}\frac{\tau^a}{2}\gamma_5 q \qquad \text{pseudoscalar states} \tag{2.40b}$$

$$v^a_\mu = \bar{q}\frac{\tau^a}{2}\gamma_\mu q \qquad \text{vector states} \tag{2.40c}$$

$$a^a_\mu = \bar{q}\frac{\tau^a}{2}\gamma_\mu\gamma_5 q \qquad \text{axial vector states} \tag{2.40d}$$

$$t^a_\mu = \bar{q}\frac{\tau^a}{2}\sigma_{\mu\nu} q \qquad \text{tensor states} \tag{2.40e}$$

Under axial transformations, we find that states of different kinds mix together, or better, are rotated unto each others. For example, if we consider an infinitesimal axial transformation of pseudoscalar states, we get

$$\begin{aligned} p^a \longrightarrow p'^a &= i\bar{q}\left(1 + i\varepsilon^b\frac{\tau^b}{2}\gamma_5\right)\frac{\tau^a}{2}\gamma_5\left(1 + i\varepsilon^b\frac{\tau^b}{2}\gamma_5\right)q \\ &= p^a - \varepsilon^b\bar{q}\left\{\frac{\tau^a}{2}, \frac{\tau^b}{2}\right\}q \\ &= p^a - d^{abc}\varepsilon^b s^c \end{aligned} \tag{2.41}$$

Here, scalar and pseudoscalar states are rotated unto each other. We find a similar relationship between vector and axial vector states. These connections provided by axial transformations between different kinds of states suggest that those states which are rotated unto each others should, in the case of an exact axial symmetry, possess the same mass. For a small degree of asymmetry, the mass differences should be relatively small in comparison with the value of the masses themselves. Putting it in other words, we would expect a meson spectrum with approximately degenerate states of opposite parity. This is, however, not even close to what is experimentally found. Comparing as an example the masses of the ρ vector meson and the a_1 axial vector meson, we see a huge discrepancy ($m_\rho \approx 775\text{MeV}$ and $m_{a_1} \approx 1260\text{MeV}$) that cannot be explained in the basis of a small deviation from perfect symmetry. Something else must be at play. [28]

[4] By light mesons we mean those that have light constituent quarks only; these can be taken to be only up and down quarks, or extended to include the strange quark, but no further.

The discussion in section 2.2.2 offers compelling evidence on chiral symmetry being a good symmetry of strongly interacting systems, but the meson mass spectrum openly contradicts this observation. The answer to this puzzle is provided on the basis of *spontaneous breaking of chiral symmetry*, i.e., although the Lagrangian density is (approximately) chirally symmetric, this symmetry is spontaneously broken for the actual physical states of the theory, in particular the vacuum state. The mechanism of spontaneous symmetry breaking has been well established in the literature [31], going back to the Heisenberg theory of ferromagnetism, and dynamical versions of symmetry breaking have greatly risen in popularity with the advent of the well-known Higgs mechanism [32]. The appearance of massless bosonic modes associated with broken symmetry degrees of freedom is known as the Goldstone theorem. [33] The prototypical example for the mechanism is the linear sigma model, which we briefly describe in the following section.

2.3.2 Aspects of Symmetry Breaking within a Linear Sigma Model

The *Linear Sigma Model* (LSM) attempts to illustrate how massless bosons can arise starting from a formulation where all bosons are degenerate. An analogy can be made between the fields in this model and the pion and sigma meson fields. [28] We begin by writing an $SU(2)$ chirally symmetric effective Lagrangian density as

$$\mathcal{L}_{LSM} = \frac{1}{2}\partial_\mu\phi\partial^\mu\phi - \frac{\mu^2}{2}\phi^2 - \frac{\lambda}{4}\phi^4 \tag{2.42}$$

Here, $\phi = (\sigma, \vec{\pi})$ is a composite field whose components correspond to the isosinglet sigma meson and the isotriplet pion meson fields. We can then identify the nature of all terms in the Lagrangian density (2.42): we have a kinetic term; a mass term; and a quartic potential term.

We now analyze the ground state of the system. Classically, the potential density for this Lagrangian is

$$\mathcal{V}_{LSM} = \frac{\mu^2}{2}\phi^2 + \frac{\lambda}{4}\phi^4 \tag{2.43}$$

and the ground state corresponds to field expectation values that minimize this potential, i.e., we look for solutions to

$$\frac{d\mathcal{V}_{LSM}}{d\phi} = 0 \tag{2.44}$$

subject to the condition that

$$\frac{d^2\mathcal{V}_{LSM}}{d\phi^2} > 0 \tag{2.45}$$

Solutions to these equations are given by

$$|\phi| = 0, \qquad \mu^2 > 0 \tag{2.46}$$

$$|\phi| = \sqrt{\frac{-\mu^2}{\lambda}}, \qquad \mu^2 < 0 \tag{2.47}$$

We are then confronted with two very distinct pictures. The first one is very simple and uninteresting for the point we are trying to make here: for $\mu^2 > 0$ all field expectation values vanish in the ground state and everything remains perfectly symmetric. This is commonly known as the *Wigner-Weyl phase*. It is the second case that presents the interesting situation: for $\mu^2 < 0$ the fields (or at least some of them) acquire some finite expectation value in the ground state. There are, of course, many ways to realize the condition (2.47), and as soon as we pick one of them as the true vacuum the symmetry of the ground state is spoiled: there is a spontaneous symmetry breaking. This is known as the *Nambu-Goldstone phase*.

Finally, we wish to show how the situation described in (2.47) leads to a degeneracy lifting of the meson fields of the model. To that end, we pick the ground state expectation values in the Nambu-Goldstone phase as

$$\vec{\pi}_0 = 0 \qquad \sigma_0 = \sqrt{\frac{-\mu^2}{\lambda}} \tag{2.48}$$

and rewrite the Lagrangian density (2.42) in terms of fluctuations around these ground state values. This can be achieved through the substitution

$$\vec{\pi} \longrightarrow \vec{\pi} \qquad \sigma \longrightarrow \sigma + \sqrt{\frac{-\mu^2}{\lambda}} \tag{2.49}$$

where the new field variables (for which we keep the same notation as the old ones) are now representing these fluctuations around the ground state. With this, the Lagrangian density becomes

$$\mathcal{L}_{LSM} = \frac{1}{2}\partial_\mu\phi\partial^\mu\phi + \mu^2\sigma^2 - \frac{\lambda}{4}\phi^4 - \sqrt{-\mu^2\lambda}\sigma\phi^2 + \frac{\mu^4}{4\lambda} \tag{2.50}$$

Some differences have arisen in relation to the original form of the Lagrangian density. The last term in the right-hand side of (2.50) is just an irrelevant constant, but two new important features are clearly visible: cubic interactions have appeared (second to last term) and there remains a mass term (second term) solely for the σ field, with a mass $m_\sigma = \sqrt{-2\mu^2}$, while the $\vec{\pi}$ fields are now massless. The appearance of massless modes are related with the Nambu-Goldstone theorem; this loosely states that, for each symmetry degree of freedom that is spontaneously broken, there exists a massless bosonic mode in the theory. Another way of stating the theorem is through the effect of currents in the vacuum state. If there is some symmetry with an associated conserved charge Q that is realized in the ground state $|0\rangle$, then $Q|0\rangle = 0$; however, if this equality is not obeyed, the symmetry is spontaneously broken, and there appear massless poles in the commutator $\langle 0|\,[Q,\phi]\,|0\rangle$. [28]

By exploring the LSM, we were able to exemplify how large mass differences can arise within a chirally symmetric model with spontaneous symmetry breaking. We can then be reasonably justified in attributing the meson mass spectrum discrepancies to a spontaneously broken chiral symmetry of the QCD Lagrangian density.

2.3.3 Axial Anomaly and the η' Puzzle

Besides the previous discussion on spontaneous symmetry breaking, our analysis of the symmetries of the QCD Lagrangian (2.2) has been done essentially from a classical point of view, i.e., we have treated the fields as classical fields. A full quantum field theoretical treatment is usually done in a path integral formalism [34] by defining the vacuum persistence amplitude. In the case of QCD, we can write it as

$$Z_{QCD} = \int \mathcal{D}q\,\mathcal{D}\bar{q}\,\mathcal{D}A^a_\mu\, e^{i\int d^4x \mathcal{L}_{QCD}} \tag{2.51}$$

This object serves as a calculational tool for determining any correlation function of the theory. At a quantum level, invariance considerations must then go beyond the sole invariance of the Lagrangian density. More specifically, the functional integration measure must also be invariant with respect to a given symmetry transformation of the classical Lagrangian density. Whenever this is not the case, we speak of an *anomalous symmetry*, i.e., a classical symmetry that is broken at the quantum level due to quantum fluctuations. [35]

In the context of low energy chiral QCD, such an anomaly arises associated with the $U(1)_A$ symmetry transformation. [30] The integral measure $\mathcal{D}q\,\mathcal{D}\bar{q}$ transforms under such transformations as

$$\begin{aligned}\mathcal{D}q\,\mathcal{D}\bar{q} \longrightarrow & \mathcal{D}\left(e^{i\theta(x)\gamma_5}q\right)\,\mathcal{D}\left(\bar{q}e^{i\theta(x)\gamma_5}\right) \\ & = J\left(\theta\right)\mathcal{D}q\,\mathcal{D}\bar{q}\end{aligned} \tag{2.52}$$

where $J\left(\theta\right) \neq 1$ is a transformation dependent phase.[5] Even in the chiral limit, this gives rise to an anomalous divergence for the singlet axial current of the form

$$\partial_\mu J^\mu_A = \frac{N_f g^2}{32\pi^2}\epsilon_{\mu\nu\rho\sigma}F^{\mu\nu}_a F^{\rho\sigma}_a \tag{2.53}$$

So, at a quantum level, the full symmetry group of the QCD Lagrangian density in the chiral limit is

$$\boxed{SU\left(3\right)_L \otimes SU\left(3\right)_R \otimes U\left(1\right)_V} \tag{2.54}$$

The axial anomaly is phenomenologically connected with the so-called $\eta^{'}$ puzzle. The $\eta^{'}$ meson has a mass $m_{\eta'} \approx 958\text{MeV}$, way higher than any other meson of the pseudoscalar nonet. On the basis of the previous discussion, it would be expected for all the nonet mesons to arise as massless Goldstone-Nambu modes, with masses generated by the joint effect of small current quark masses and spontaneous breaking of chiral symmetry. The other eight modes seem to fit reasonably well within this scheme, but the $\eta^{'}$ meson clearly doesn't. It was later proposed by t'Hooft that this could be accounted for by instanton solutions that couple with the quarks through (2.53). [36] [37] This fact has since been shown by several authors. [38] There are other phenomenological manifestations of this anomaly, namely in the two-photon decays of the π^0 and and η mesons. [39] [40]

2.4 The NJL Model

We now summarize the picture we have been building up for the prominent and elaborate role of chiral symmetry in the phenomenology of quarks and hadrons. We assume an underlying chirally symmetric theory which is slightly broken through small explicit current quark mass terms. Furthermore, chiral symmetry is spontaneously broken for the physical states of the system, turning some of the hadronic states into massive states while others remain massless. Of course, the small explicit symmetry breaking provides these otherwise massless states with some small but finite masses. Finally, the chiral

[5] Actually, we may regard this term as the Jacobian of a coordinate transformation on the quark fields.

anomaly is taken into account to refine the description of the meson spectrum and decay schemes. Qualitatively, this picture appears to be able to match the physical phenomena.

Everything that has been discussed so far motivates the introduction of the *Nambu-Jona-Lasinio (NJL) Model*. What it tries to do is precisely to capture the essential role of spontaneously broken chiral symmetry and employ it in the construction of an effective model for strong interactions. Its original formulation goes back to the early 60's and is due to Yoichiro Nambu and Giovanni Jona-Lasinio. In two groundbreaking papers ([1] and [2]), they explore an inspired analogy between the Bardeen-Cooper-Schrieffer (BCS) theory of superconductivity [41] and nucleon dynamics. We will now briefly present the general lines along which this analogy was made.

In the BSC theory, *"elementary excitations in a superconductor can be conveniently described by means of a coherent mixture of electrons and holes"* [1] obeying a set of coupled equations, where the coupling is given in terms of a gap parameter ϕ related to electron-electron interactions. The quasi-particles possess two energy eigenstates separated by an energy gap $\Delta \geq 2\,|\phi|$, and all such quasi-particles should occupy the lower level in the ground state of the system. It would then take a finite energy Δ to excite a particle to the upper state. This picture bares a striking resemblance to the behaviour of Dirac particles, where the ground state was viewed as consisting of a completely filled negative Dirac sea, and the creation of excited states requiring an energy $E \geq 2m$. Just like ϕ arises from electron-electron interactions, we might assume that the Dirac masses have their origin in some interaction between bare massless fermions.

Again, in the BCS theory, collective excitations of quasi-particle pairs can arise, and if we take the analogy seriously, we would then expect a similar feature for the Dirac particles. *"If a Dirac particle is actually a quasi-particle, which is only an approximate description of an entire system where chirality is conserved, then there must also exist collective excitations of bound quasi-particle pairs."* [1] These collective excitations are compatible with the mesons.

They then propose a chirally symmetric Lagrangian density for isodoublet nucleon fields ψ in the form[6]

$$\mathcal{L}_{NJL} = i\bar{\psi}\gamma^{\mu}\partial_{\mu}\psi + G\left[\left(\bar{\psi}\psi\right)^2 + \left(\bar{\psi}i\gamma_5\vec{\tau}\psi\right)^2\right] \tag{2.55}$$

[6]We could include vector and axial vector quartic interactions, but this would just amount to making a Fierz transformation of the given terms, which doesn't bring about noticeable consequences for the discussion at hand. These terms' significance arises mainly in the discussion of collective states.

The paper goes on to show the existence of a mass gap and, thus, that the model exhibits a chirally asymmetric ground state populated with a finite condensate of nucleon-antinucleon pairs. They also study properties of collective states (mesons) on the basis of the Bethe-Salpeter equation.

After the advent of QCD, this Lagrangian was soon reinterpreted in terms of up and down quark fields instead of nucleon fields. Some of the early contributions on the development of related models and analysis techniques include [42], [43], [44], [45], [46], [47], [48], [49], [50], [51], [52]. In these articles, topics like inclusion of strangeness, functional integral bosonization, quark matter, meson and nuclear phenomenology, radiative corrections and thermodynamical analysis have been extensively studied, setting forth the very prolific subject of NJL-models and making way for a subsequent great deal of work from a multitude of investigators. A more complete summary of contributions may be found in [53].

In the next sections, we present an analysis of the model based on a mean-field approximation. The discussion is mainly based on the review articles [53] and [54]. Other useful reviews are [55] and [56].

2.4.1 Self-Consistent Mass Gap Equation

The NJL Lagrangian (2.55) includes quartic interaction terms for the fermionic fields, which give rise to a renormalization of fermion bare masses m_0 (which we temporarily take as finite for argument's sake) in terms of the proper self-energy tensor Σ as

$$m = m_0 + \Sigma\left(m, \Lambda\right) \tag{2.56}$$

$\Sigma\left(m, \Lambda\right)$ depends on the fermion's physical mass m and on some regularization parameter Λ.

FIGURE 2.3: Dyson series for the dressed fermion propagator.

The proper self-energy tensor Σ is defined through the Dyson equation depicted diagrammatically in figure 2.3. It consists of all the irreducible Feynman diagrams with no external legs that can be inserted in the propagator. Analytically, one can write the dressed fermion propagator S in terms of the bare propagator S_0 as

$$S = S_0 + S_0 \Sigma S \Rightarrow S = \frac{1}{S_0^{-1} - \Sigma} \tag{2.57}$$

We can evaluate Σ using a (Hartree) mean field approximation, which can be achieved by suitable linearization[7] of the interaction term in the Lagrangian (2.55). The Euler-Lagrange equations for ψ give the equation of motion:

$$\left\{ i\gamma^\mu \partial_\mu + 2G \left(\bar{\psi}\psi - \bar{\psi}\gamma_5 \vec{\tau} \psi \gamma_5 \vec{\tau} \right) \right\} \psi = 0 \tag{2.58}$$

This can be put in a form similar to the free Dirac equation if we make the substitutions:

$$\bar{\psi}\psi \longrightarrow \left\langle \bar{\psi}\psi \right\rangle = -i \mathrm{Tr} S\left(0\right) \tag{2.59a}$$

$$\bar{\psi}\gamma_5 \vec{\tau} \psi \longrightarrow \left\langle \bar{\psi}\gamma_5 \vec{\tau} \psi \right\rangle = -i \mathrm{Tr} \gamma_5 \vec{\tau} S\left(0\right) \tag{2.59b}$$

where the traces are taken over all internal indices (colour, flavour, spinor). This, together with equation (2.56) with $m_0 = 0$, allows us then to write a self-consistent equation as

$$\begin{aligned} \Sigma &= -2G \left\{ \left\langle \bar{\psi}\psi \right\rangle - \gamma_5 \vec{\tau} \left\langle \bar{\psi}\gamma_5 \vec{\tau} \psi \right\rangle \right\} \\ &= 2iG \left\{ \mathrm{Tr} S\left(0\right) - \gamma_5 \vec{\tau} \mathrm{Tr} \gamma_5 \vec{\tau} S\left(0\right) \right\} \end{aligned} \tag{2.60}$$

Recall that S depends on Σ through the operator Dyson series as given in (2.57). It is now easy to show that the second term is zero because of the traces involving γ_5 (see Appendix B). Had we included vector and axial vector terms, these would vanish as well. We can say that only the scalar quark bilinear has a nonvanishing vacuum expectation value.[8] Following this, we can finally write

$$\Sigma = 2iG \mathrm{Tr} \lim_{\epsilon \to 0} \int \frac{d^4 p}{\left(2\pi\right)^4} \frac{\gamma^\mu p_\mu + \Sigma}{p^2 - \Sigma^2 + i\epsilon} \tag{2.61}$$

The integral in the above expression is divergent, and we need to include an adequate regularization in order to obtain a finite result. The model is non-renormalizable and, in

[7] Here, we illustrate the linearization of the interaction by analogy of the equations of motion with Dirac's equation. Perhaps a more common alternative to perform this linearization in the context of mean-field QFTs is by Wick contracting pairs of fermionic fields until we are left with an interaction of the desired degree. In the present case, the two approaches are perfectly equivalent.

[8] And it should be so for a Lorentz and parity invariant vacuum.

the end, all calculated observables will depend explicitly on the regularization parameter Λ. Identifying Σ with the effective physical mass m (actually, $m = \Sigma + m_0$, so we are considering $m_0 = 0$), we get

$$m = 8iGN_cN_f m \lim_{\epsilon\to 0}\int \frac{d^4p}{(2\pi)^4}\frac{1}{p^2 - m^2 + i\epsilon}\rho\left(p,\Lambda\right)$$

$$\boxed{1 = 8iGN_cN_f \lim_{\epsilon\to 0}\int \frac{d^4p}{(2\pi)^4}\frac{1}{p^2 - m^2 + i\epsilon}\rho\left(p,\Lambda\right) \qquad , \qquad m \neq 0} \tag{2.62}$$

where $\rho\left(p,\Lambda\right)$ is a regulator. Equation (2.62) is a self-consistent mass gap equation, which may have solutions for $m \neq 0$ for certain values of G. In these conditions, a condensate $\langle\bar{\psi}\psi\rangle$ appears with a finite vacuum expectation value, fermions acquire mass m and chiral symmetry is dynamically broken.[9]

In order to proceed, we need to select some suitable regularization scheme. For simplicity, we use a 3-momentum cutoff Λ just for illustration, yielding

$$\begin{aligned} 1 &= \frac{2GN_cN_f}{\pi^2}\int_0^\Lambda dp \frac{p^2}{\sqrt{p^2+m^2}} \\ &= \frac{2GN_cN_f\Lambda^2}{\pi^2}\left\{\sqrt{1+\frac{m^2}{\Lambda^2}} - \frac{m^2}{\Lambda^2}\ln\left(\frac{\Lambda}{m} + \sqrt{1+\frac{\Lambda^2}{m^2}}\right)\right\} \\ \Leftrightarrow \frac{\pi^2}{N_cN_fG\Lambda^2} &= \sqrt{1+\frac{m^2}{\Lambda^2}} - \frac{m^2}{\Lambda^2}\ln\left(\frac{\Lambda}{m} + \sqrt{1+\frac{\Lambda^2}{m^2}}\right) \end{aligned} \tag{2.63}$$

We can define the critical coupling G_{crit} in the limit $m \to 0$ as

$$\frac{\pi^2}{N_cN_fG_{crit}\Lambda^2} = 1 \qquad \Leftrightarrow \qquad G_{crit} = \frac{\pi^2}{N_cN_f\Lambda^2} \tag{2.64}$$

Then, chiral symmetry is dynamically broken for values of the coupling $G > G_{crit}$, leading to a finite quark-antiquark condensate vacuum expectation value.

It should be noted that we could have included an explicit breaking of chiral symmetry by some small current mass term $\bar{\psi}m_0\psi$ in the Lagrangian density (2.55). This leads to a very simple modification of the mass gap equation (2.62) to

[9] We speak of a dynamically broken symmetry because this effect is brought about by the very dynamics of the fermions which are subject to strong attractive forces in the scalar channel and end up forming a finite pair condensate in the ground state. We may wish to distinguish this from what is commonly called a spontaneously broken symmetry due to the presence of elementary bosonic fields as occurs, for example, in the linear sigma model.

$$m = m_0 + 8iGN_cN_f m \lim_{\epsilon\to 0}\int \frac{d^4p}{(2\pi)^4}\frac{1}{p^2 - m^2 + i\epsilon}\rho\left(p,\Lambda\right) \tag{2.65}$$

2.4.2 Three-Flavour Model and the 't Hooft Determinant

We can go on to include a third quark flavour into our Lagrangian, extending the flavour $SU\left(2\right)$ symmetry group of (2.55) to $SU\left(3\right)$. The inclusion of the strange quark flavour begs for special attention regarding the axial anomaly discussed in section 2.3.3. The $U\left(1\right)_A$ symmetry is severely broken, and this should be expressed in the construction of an effective Lagrangian. It has been pointed out by 't Hooft [37], following previous work by Kobayashi and Maskawa [57], that we can include an instanton induced effective interaction of the form

$$K\left[\det\bar{\psi}\left(1+\gamma_5\right)\psi + \det\bar{\psi}\left(1-\gamma_5\right)\psi\right] \tag{2.66}$$

in our chirally symmetric Lagrangian. Here, the determinant is to be taken in flavour space. This six-quark interaction term preserves all other symmetries in consideration while explicitly breaking $U\left(1\right)_A$ symmetry.

It should be noted that a similar $U\left(1\right)_A$-breaking interaction could have been included in the two-flavour version of the model, but in that case it would have been a quartic interaction with a structure at all similar to the term already present in (2.55). A simple redefinition of the coupling would suffice for such a t'Hooft term to be absorbed into the original term. However, in a three-flavour version, the t'Hooft term is a six-quark interaction. Its identity is fundamentally different from the quartic interaction terms, and so its separate inclusion becomes of sensitive importance.

We can then define a general Lagrangian density (with an explicit current mass term) as

$$\begin{aligned}\mathcal{L}_{NJL} =& \bar{\psi}\left(i\gamma^\mu\partial_\mu - m_0\right)\psi + G\sum_{a=0}^{8}\left[\left(\bar{\psi}\tau^a\psi\right)^2 + \left(\bar{\psi}i\gamma_5\tau^a\psi\right)^2\right] \\ &+ K\left[\det\bar{\psi}\left(1+\gamma_5\right)\psi + \det\bar{\psi}\left(1-\gamma_5\right)\psi\right]\end{aligned} \tag{2.67}$$

where we use the flavour $U\left(3\right)$ generators τ^a. We may use the mean-field approximation again to obtain the mass gap equation. The 't Hooft term complicates things a bit,

requiring the contraction of four quark fields to be linearized. The mass gap equation has been determined by Bernard, Jaffe and Meissner in [58] as

$$m_i = m_{i0} + 4iGN_c Tr_D S_i - K\left(2N_c^2 + 3N_c + 1\right)\left(\mathrm{Tr}_D S_j\right)\left(\mathrm{Tr}_D S_k\right) \qquad , \qquad i \neq j \neq k \tag{2.68}$$

for each flavour i. $S_i \equiv S_i(0)$ are the dressed propagators for quark flavour i, and the trace Tr_D is taken over spinor indices. If we assume $KN_c^2 \sim \mathcal{O}(1)$ in $\frac{1}{N_c}$ counting, a lowest order consistent expansion would then be

$$m_i = m_{i0} + 4iGN_c Tr_D S_i - 2KN_c^2\left(Tr_D S_j\right)\left(Tr_D S_k\right) \qquad , \qquad i \neq j \neq k \tag{2.69}$$

In (2.67) we have only considered colour singlet interaction terms. Through a convenient Fierz transformation, it is possible to also include colour octet interactions of the form

$$\left(\bar{\psi}\Gamma\frac{\lambda^\alpha}{2}\tau^a\psi\right)^2 \tag{2.70}$$

where λ^α are generators of the colour $SU(3)$ group (see Apendix A) and Γ is some conventional combination of Dirac matrices (see Appendix B). The most general NJL-type Lagrangian density may be built by including all quartic interaction terms that can be built in the form (2.70) and respect the assumed symmetries. More detailed discussions may be found in [54] and [53].

2.4.3 Hadrons and the Bethe-Salpeter Equation

It is possible to describe hadrons within an NJL quark model, mesons being easier to describe than baryons. The former can be treated as bound quark-antiquark pairs through the Bethe-Salpeter equation in the ladder approximation. [59] [60] This is shown diagrammatically in figure 2.4. There, T is a mesonic transition matrix, $\mathcal{K}$ is the effective vertex function and J is a loop integral.

Analytically, the Bethe-Salpeter equation may be written as

$$T = \mathcal{K} + \mathcal{K}JT \qquad \Leftrightarrow \qquad T = \left(1 - \mathcal{K}J\right)^{-1}\mathcal{K} \tag{2.71}$$

The meson masses appear as poles in the transition matrix T, i.e., they are solutions to

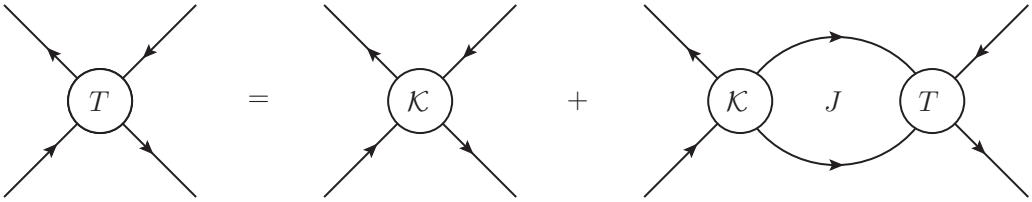

FIGURE 2.4: Bethe-Salpeter equation for mesonic states.

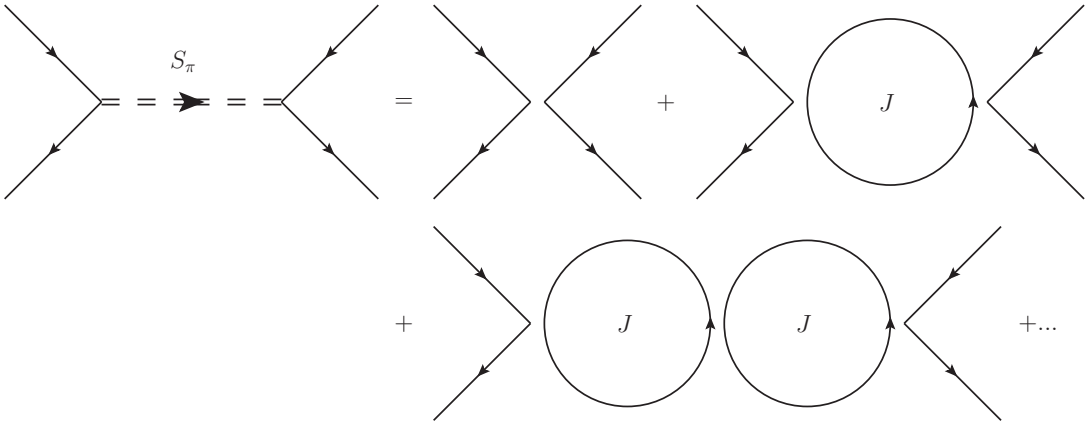

FIGURE 2.5: Dyson series for the pion propagator in the ladder approximation.

$$1 - \mathcal{K}J = 0 \tag{2.72}$$

As an example of this formalism, we will show that the transition matrix in the pseudoscalar channel for the two-flavour model given in (2.55) has a set of massless poles which may be identified as the Goldstone-Nambu pions. The Bethe-Salpeter formalism is represented again in figure 2.5, from which we can extract the pion propagator as

$$iS_\pi = \mathcal{K} + \mathcal{K}J\mathcal{K} + \mathcal{K}J\mathcal{K}J\mathcal{K} + ... = \mathcal{K}\left(J\mathcal{K} + J\mathcal{K}J\mathcal{K} + J\mathcal{K}J\mathcal{K}J\mathcal{K} + ...\right) = \frac{\mathcal{K}}{1 - \mathcal{K}J} \tag{2.73}$$

In this example, $\mathcal{K} = 2G$. The loop integral depends on the pion we are considering, but may be written

$$J\left(p^2\right) = -i\mathrm{Tr}\int \frac{d^4p'}{(2\pi)^4} i\gamma_5 T^a iS\left(p' + \frac{p}{2}\right) i\gamma_5 T^b iS\left(p' - \frac{p}{2}\right) \tag{2.74}$$

where $T^a = T^b = \tau^3$ for the π^0 meson and $T^a = T^{b\dagger} = \tau^\pm$ for the $\pi^\pm$ mesons, with $\tau^\pm = \frac{1}{2}\left(\tau^1 \pm i\tau^2\right)$. This ensures the correct description of the pions in terms of quark

content and the consistency of the coupling between the external quark currents and the internal quark loop. The S represent dressed quark propagators. So, for the π^0 meson and in the isospin limit, we have

$$\begin{aligned} J_{\pi^0}\left(p^2\right) &= -i\mathrm{Tr}\int \frac{d^4p'}{(2\pi)^4}\gamma_5\tau^3\frac{\gamma^\mu\left(p'+\frac{p}{2}\right)_\mu + m}{\left(p'+\frac{p}{2}\right)^2 - m^2}\gamma_5\tau^3\frac{\gamma^\mu\left(p'-\frac{p}{2}\right)_\mu + m}{\left(p'-\frac{p}{2}\right)^2 - m^2} \\ &= -4iN_cN_f\int \frac{d^4p'}{(2\pi)^4}\frac{-p'^2+\frac{p^2}{4}+m^2}{\left[\left(p'+\frac{p}{2}\right)^2 - m^2\right]\left[\left(p'-\frac{p}{2}\right)^2 - m^2\right]} \\ &= 4iN_cN_f\int \frac{d^4p'}{(2\pi)^4}\frac{1}{p'^2-m^2} - 2iN_cN_fp^2I\left(p^2\right) \end{aligned} \tag{2.75}$$

(2.76)

with

$$I\left(p^2\right) = \int \frac{d^4p'}{(2\pi)^4}\frac{1}{\left[\left(p'+\frac{p}{2}\right)^2 - m^2\right]\left[\left(p'-\frac{p}{2}\right)^2 - m^2\right]} \tag{2.77}$$

We can then resort to the mass gap equation (2.65) to write

$$J_{\pi^0}\left(p^2\right) = \frac{1}{2G}\left(1-\frac{m_0}{m}\right) - 2iN_cN_fp^2I\left(p^2\right) \tag{2.78}$$

Finally, employing the pole condition (2.72), the mass of the pion is given by the condition

$$\frac{m_0}{m} + 4iGN_cN_fm_{\pi^0}^2I\left(m_{\pi^0}^2\right) = 0 \Rightarrow m_{\pi^0}^2 = \frac{m_0}{m}\frac{1}{4iGN_cN_fI\left(m_{\pi^0}^2\right)} \tag{2.79}$$

From this expression, it is evident that, in the chiral limit $m_0 = 0$, the pion is automatically massless. It can be shown that the $\pi^\pm$ mesons masses obey the same identity. For finite current quark masses, a pion mass is dynamically generated which is proportional to the ratio $\frac{m_0}{m}$. This is in perfect agreement with the previous heuristic discussion on the pseudoscalar meson masses.

If we include the strange quark, with $m_{u0} = m_{d0} \neq m_{s0}$, the whole pseudoscalar octet is described in reasonably good agreement with the empirical spectrum. [54] With three-flavours, the effective vertex $\mathcal{K}$ needs to take into account the 't Hooft interaction which

is adequately reduced to an effective four-quark term by Wick contracting a pair of quark fields. The spectra of other families of mesons are also well described, namely the vector mesons. [55]

The description of baryons is somewhat more involved. One approach, described in [54], is to construct a diquark bound state via the Bethe-Salpeter equation, and then couple the diquark to a third quark. This is beyond the scope of this thesis, and more details can be found, for example, in [61]. A description of baryons as chiral solitons may be found in [62].

2.4.4 Functional Integral Bosonization

At low energies, the actually relevant degrees of freedom for strong interactions are usually hadrons and not quarks, in particular the light mesons and possibly the nucleons. In light of this, we might wish to regard the NJL model as an effective theory for mesons. To that end, we need to somehow eliminate the quark degrees of freedom in favour of mesonic ones. This *bosonization* procedure [53] is best taken in the path integral formalism, in which we define the vacuum to vacuum transition amplitude as

$$Z\left[\eta,\bar{\eta}\right]=\int\mathcal{D}\psi\mathcal{D}\bar{\psi}e^{i\int d^4x\mathcal{L}_{NJL}\left(\bar{\psi},\psi\right)+\bar{\psi}\eta+\bar{\eta}\psi} \tag{2.80}$$

The η and $\bar{\eta}$ serve as external sources for the quark fields. We will use here the two-flavor Lagrangian density (2.55) to briefly describe the procedure. Since this Lagrangian includes quartic terms, the functional integration cannot be performed exactly, but we can still use the known Gaussian functional integral to our advantage, which is given by

$$\int\mathcal{D}\phi e^{i\int d^4x\left[\frac{1}{2}\phi A\phi+J\phi\right]}=e^{-\frac{i}{2}\int d^4xd^4yJ(x)A^{-1}(x-y)J(y)} \tag{2.81}$$

Using this expression, we introduce boson fields σ and $\vec{\pi}$ and rewrite the interaction part of the action exponential as

$$e^{i\int d^4xG\left[\left(\bar{\psi}\psi\right)^2+\left(\bar{\psi}i\gamma_5\vec{\tau}\psi\right)^2\right]}=\int\mathcal{D}\sigma\mathcal{D}\vec{\pi}e^{-i\int d^4x\left[\bar{\psi}\psi\sigma+\bar{\psi}i\gamma_5\vec{\tau}\psi\cdot\vec{\pi}+\frac{\sigma^2+\vec{\pi}^2}{4G}\right]} \tag{2.82}$$

With this, the functional integral in (2.80) becomes

$$Z\left[\eta,\bar{\eta}\right]=\int\mathcal{D}\psi\mathcal{D}\bar{\psi}\mathcal{D}\sigma\mathcal{D}\vec{\pi}e^{i\int d^4x\left[\bar{\psi}(i\gamma^\mu\partial_\mu-\sigma-i\gamma_5\vec{\tau}\cdot\vec{\pi})\psi+\bar{\psi}\eta+\bar{\eta}\psi-\frac{\sigma^2+\vec{\pi}^2}{4G}\right]} \tag{2.83}$$

In this way, we now have a Gaussian integral for the fermionic sector, which we can perform explicitly in order to eliminate the quark degrees of freedom from the functional. The result is

$$Z\left[\eta,\bar{\eta}\right]=\int\mathcal{D}\sigma\mathcal{D}\vec{\pi}e^{i\left\{\int d^{4}x\left[-\frac{\sigma^{2}+\vec{\pi}^{2}}{4G}+\bar{\eta}(i\gamma^{\mu}\partial_{\mu}-\sigma-i\gamma_{5}\vec{\tau}\cdot\vec{\pi})^{-1}\eta\right]-i\tilde{\mathrm{Tr}}\ln(i\gamma^{\mu}\partial_{\mu}-\sigma-i\gamma_{5}\vec{\tau}\cdot\vec{\pi})\right\}} \tag{2.84}$$

In this expression, the trace $\tilde{\mathrm{Tr}}$ is a functional trace, which can be defined for any operator A as

$$\tilde{\mathrm{Tr}}A=\mathrm{Tr}\int d^{4}x\left\langle x\right|A\left|x\right\rangle \tag{2.85}$$

Tr being the usual trace over internal indices. We can interpret (2.84) as giving us an effective bosonized Lagrangian density. If we scale the boson fields by a constant factor g_0, this may be written as

$$\mathcal{L}_{\mathrm{bos}}=-\frac{\mu_{0}^{2}}{2}\left(\sigma^{2}+\vec{\pi}^{2}\right)-i\mathrm{Tr}\left\langle x\right|\ln\left[i\gamma^{\mu}\partial_{\mu}-g_{0}\left(\sigma+i\gamma_{5}\vec{\tau}\cdot\vec{\pi}\right)\right]\left|x\right\rangle \tag{2.86}$$

where $\mu_0^2=\frac{g_0^2}{2G}$ might be regarded as some mass parameter for the bosons. We may also extract the dressed quark propagator as

$$S\left(x-y\right)=\left[i\gamma^{\mu}\partial_{\mu}-g_{0}\left(\sigma+i\gamma_{5}\vec{\tau}\cdot\vec{\pi}\right)\right]^{-1}\delta^{(4)}\left(x-y\right) \tag{2.87}$$

or, in momentum space,

$$S\left(p\right)=\frac{1}{\gamma^{\mu}p_{\mu}-\sigma-i\gamma_{5}\vec{\tau}\cdot\vec{\pi}} \tag{2.88}$$

It is possible to derive a mass gap equation from (2.86) by requiring that $\left.\frac{\delta\mathcal{S}}{\delta\phi}\right|_{\phi=\langle\phi\rangle}=0$ for $\phi=(\sigma,\vec{\pi})$.[10] If we assume that only $\langle\sigma\rangle=v_0$ is nonvanishing, this leads to

$$m=2iG\tilde{\mathrm{Tr}}\frac{1}{i\gamma^{\mu}\partial_{\mu}-m} \tag{2.89}$$

with $m=g_0v_0$.

[10] $\mathcal{S}$ is the usual action defined as the integral in four-space of the Lagrangian density.

The form (2.86) for the bosonized Lagrangian density obscures its full dynamical content. We would like to be able to solve $\tilde{\mathrm{Tr}} \ln \left[i\gamma^\mu \partial_\mu - g_0 \left(\sigma + i\gamma_5 \vec{\tau} \cdot \vec{\pi} \right) \right]$ explicitly. This is actually an infinite sum of terms, some of which are actually divergent. The result presented in [53] with only the divergent terms is:

$$\begin{aligned} \mathcal{L}_{\mathrm{bos}} = & -\frac{1}{2}\left(\mu^2 - 2I_2 g_0^2 + 2I_0 g_0^2 \left(g_0 v_0\right)^2\right)\left(\sigma^2 + \vec{\pi}^2\right) + \frac{1}{2} I_0 g_0^2 \left[(\partial_\mu \sigma)^2 + (\partial_\mu \vec{\pi})^2\right] \\ & - \frac{1}{2} I_0 g_0^4 \left(\sigma^2 + \vec{\pi}^2\right)^2 \end{aligned} \tag{2.90}$$

In this expression,

$$I_0 = -4iN_c \int \frac{d^4p}{(2\pi)^4} \frac{1}{\left(p^2 - m^2\right)^2} \tag{2.91a}$$

$$I_2 = 4iN_c \int \frac{d^4p}{(2\pi)^4} \frac{1}{p^2 - m^2} \tag{2.91b}$$

which are just quark loop integrals. In this way, we can explicitly see the form of the usual kinetic, mass and interaction terms for the meson fields. In the next chapter, we shall use a generalized heat kernel technique to expand this functional trace in a chirally invariant series.

Chapter 3

NJL Models and Multi-Quark Interactions

The original NJL model (see section 2.4) has spawned several enhanced versions over the years, with the introduction of new elements and considerations, namely the reinterpretation of nucleon fields in terms of quark fields and the inclusion of the strange flavour, although its essential character has remained more or less intact. It works as an effective model for strongly interacting particles below some energy scale Λ by exploiting the dynamical breaking of chiral symmetry. The phenomenological success of this class of models (some examples may be found in [63], [64], [65], [66], [67], [68], [69]) has proven their usefulness as predictive tools for a number of phenomena in the context of strongly interacting systems. We will be studying features of a particular NJL-type model in the following sections. In this chapter, we will attempt to motivate the introduction of the model under study, as well as to carefully describe its formulation and technical features.

3.1 Analysis of the Three-Flavour Model with a 't Hooft Interaction Term

We will furnish an analysis of the NJL model's version of section 2.4.2 with the Lagrangian density of the form (2.67). We rewrite it here (with a slight redefinition of the couplings and notation) as

$$\mathcal{L} = \bar{q}\left(i\gamma^{\mu}\partial_{\mu} - m\right)q + \mathcal{L}_{NJL} + \mathcal{L}_{H} \tag{3.1}$$

with the usual NJL quartic interaction term

$$\mathcal{L}_{NJL} = \frac{G}{2}\left[(\bar{q}\lambda_a q)^2 + (\bar{q}i\gamma_5\lambda_a q)^2\right] \tag{3.2}$$

and the 't Hooft $U(1)_A$-breaking determinantal interaction term

$$\mathcal{L}_H = \kappa\left[\det \bar{q}P_R q + \det \bar{q}P_L q\right] \tag{3.3}$$

Here, λ_a are the Gell-Mann matrices in flavour space extended to $U(3)$ (see Appendix A). Summation over flavour indices a is understood. $P_{R,L}$ are the chiral projection operators defined in (2.16), and the quark fields are denoted by q. This Lagrangian matches the model studied in [70], where a generalized Schwinger-DeWitt heat kernel expansion is employed for regularization as a way of ensuring a full term by term covariance in the presence of a non-commutative quark mass matrix. We will reproduce here the main steps of its treatment, which will be relevant later for the full model. The analysis is performed in the functional integral formalism at the mean-field level. [71]

3.1.1 Bosonization of the Three-Flavour Model using the SPA

The model is bosonized following the technique in [72]. We define bosonic fields $\sigma = \sigma_a\lambda_a$ and $\phi = \phi_a\lambda_a$ and auxiliary fields $s = s_a\lambda_a$ and $p = p_a\lambda_a$. Using the functional unit

$$\begin{aligned} 1 &= \int \prod_a \mathcal{D}s_a\mathcal{D}p_a\delta\left(s_a - \bar{q}\lambda^a q\right)\delta\left(p_a - \bar{q}i\gamma_5\lambda^a q\right) \\ &= \int \prod_a \mathcal{D}s_a\mathcal{D}p_a\mathcal{D}\sigma_a\mathcal{D}\phi_a e^{i\int d^4x[\sigma_a(s_a-\bar{q}\lambda^a q)+\phi_a(p_a-\bar{q}i\gamma_5\lambda^a q)]} \end{aligned} \tag{3.4}$$

and multiplying it by the vacuum persistence amplitude

$$Z = \int \mathcal{D}q\mathcal{D}\bar{q}e^{i\int d^4x[\bar{q}(i\gamma^\mu\partial_\mu - m)q + \mathcal{L}_{NJL} + \mathcal{L}_H]} \tag{3.5}$$

we get

$$Z = \int \prod_a \mathcal{D}\sigma_a \mathcal{D}\phi_a \mathcal{D}q \mathcal{D}\bar{q} e^{i\int d^4x \mathcal{L}_q(\bar{q},q,\sigma,\phi)} \times \int \prod_a \mathcal{D}s_a \mathcal{D}p_a e^{i\int d^4x \mathcal{L}_r(\sigma,\phi,s,p)} \tag{3.6}$$

with a quark dependent Lagrangian

$$\mathcal{L}_q = \bar{q}\left(i\gamma^\mu \partial_\mu - M - \sigma - i\gamma_5 \phi\right) q \tag{3.7}$$

and an auxiliary Lagrangian

$$\mathcal{L}_r = \frac{G}{2}\left(s_a^2 + p_a^2\right) + s_a\left(\sigma_a + \Delta_a\right) + p_a\phi_a + \frac{\kappa}{32} A_{abc} s_a \left(s_b s_c - 3p_b p_c\right) \tag{3.8}$$

The symmetric constants A_{abc} are defined in Appendix A. m_a is defined through the relation $m = m_a \lambda_a$. We have shifted $\sigma_a \longrightarrow \sigma_a + M_a$ so that, in the Nambu-Goldstone phase, σ has a vanishing vacuum expectation value, and M may be interpreted as a constituent quark mass matrix. Also, we define $\Delta_a = M_a - m_a$. This prescription is in line with the previous discussion: we expect that, in the Nambu-Goldstone phase, the scalar channel exhibits a finite vacuum expectation value, and we shift the scalar field in order to describe fluctuations around this vacuum.

The functional integral in the auxiliary fields s_a and p_a is evaluated using a stationary phase approximation (SPA) [73] by assuming an asymptotic expansion in bosonic fields [74]

$$s_a^{st} = h_a + h_{ab}^{(1)}\sigma_b + h_{abc}^{(1)}\sigma_b\sigma_c + h_{abc}^{(2)}\phi_b\phi_c + ... \tag{3.9a}$$

$$p_a^{st} = h_{ab}^{(2)}\phi_b + h_{abc}^{(3)}\phi_b\sigma_c + ... \tag{3.9b}$$

and using it with $\frac{\delta\mathcal{L}_r}{\delta s_a} = 0$ and $\frac{\delta\mathcal{L}_r}{\delta p_a} = 0$ to obtain the stationary phase conditions

$$Gs_a + (\sigma + \Delta)_a + \frac{3\kappa}{32} A_{abc}\left(s_b s_c - p_b p_c\right) = 0 \tag{3.10a}$$

$$Gp_a + \phi_a - \frac{3\kappa}{16} A_{abc} s_b p_c = 0 \tag{3.10b}$$

Through these relations, higher order h coefficients may be recursively expressed in terms of lower order ones. The lowest order coefficient is given by

$$Gh_a + \Delta_a + \frac{3\kappa}{32} A_{abc} h_b h_c = 0 \tag{3.11}$$

From the structure of this expression, it is straightforward to realize that the only non-zero h_a coefficients are those with indices 0, 3 and 8 (corresponding to the diagonal $U(3)$ matrices). This may be understood if we notice that Δ is a diagonal matrix in flavour space, so that only the components associated with diagonal $U(3)$ matrices are non-vanishing. Also, if the index a is either 0, 3 or 8, then the coefficients A_{abc} are non-vanishing only if b and c are 0, 3 or 8 as well. By exploiting the fact that the mass matrix is a diagonal matrix with a structure given by $m = m_a \lambda_a = \mathrm{diag}\,(m_u, m_d, m_s)$, one can define transformation matrices between the set of indices $a \in \{0, 3, 8\}$ and $i \in \{u, d, s\}$ as [75] (summation over repeated indices implied)

$$m_i = \omega_{ia} m_a \qquad , \qquad m_a = e_{ai} m_i \tag{3.12}$$

with

$$\omega_{ia} = \frac{1}{\sqrt{3}} \begin{pmatrix} \sqrt{2} & \sqrt{3} & 1 \\ \sqrt{2} & -\sqrt{3} & 1 \\ \sqrt{2} & 0 & -2 \end{pmatrix} \qquad , \qquad e_{ai} = \frac{1}{2\sqrt{3}} \begin{pmatrix} \sqrt{2} & \sqrt{2} & \sqrt{2} \\ \sqrt{3} & -\sqrt{3} & 0 \\ 1 & 1 & -2 \end{pmatrix} \tag{3.13}$$

These matrices satisfy the identities

$$e_{ai} = \frac{\omega_{ia}}{2} \qquad , \qquad e_{ai} e_{aj} = \frac{\delta_{ij}}{2} \qquad , \qquad A_{abc} e_{bj} e_{ck} = \frac{e_{ai} t_{ijk}}{3} \tag{3.14}$$

where t_{ijk} is a fully symmetric tensor with entries equal to 1 for $i \neq j \neq k$ and all other entries null. With the definition of these objects, we can rewrite (3.11) in terms of flavour indices u, d, s as

$$\Delta_i + G h_i + \frac{\kappa}{32} t_{ijk} h_j h_k = 0 \tag{3.15}$$

It is evident that this equation admits the trivial solution $h_i = 0$, corresponding to the chirally symmetric Wigner-Weyl phase where $\Delta_i = 0$. Besides this, it also admits

solutions for non-zero h_i, which induce a finite mass shift; this corresponds to the dynamically broken Goldstone-Nambu phase. More about the SPA solutions and their consequences is said in section 3.1.5.

A full algebraic manipulation of the results obtained so far allows us to write the effective bosonized auxiliary Lagrangian as [75]

$$\mathcal{L}_r^{st} = h_a\sigma_a + \frac{1}{2}h_{ab}^{(1)}\sigma_a\sigma_b + \frac{1}{2}h_{ab}^{(2)}\phi_a\phi_b + \frac{1}{3}\sigma_a\left[h_{abc}^{(1)}\sigma_b\sigma_c + \left(h_{abc}^{(2)} + h_{abc}^{(3)}\right)\phi_b\phi_c\right] + ... \quad (3.16)$$

leaving us with the functional integral

$$Z = \int \prod_a \mathcal{D}\sigma_a\mathcal{D}\phi_a e^{i\int d^4x\mathcal{L}_r^{st}(\sigma,\phi)} Z_q\left[\sigma,\phi\right] \quad (3.17)$$

with

$$\begin{aligned} Z_q &= \int \mathcal{D}q\mathcal{D}\bar{q}e^{i\int d^4x\bar{q}(i\gamma^\mu\partial_\mu - M - \sigma - i\gamma_5\phi)q} \\ &= \det\left(i\gamma^\mu\partial_\mu - M - \sigma - i\gamma_5\phi\right) \\ &= e^{\ln\det(i\gamma^\mu\partial_\mu - M - \sigma - i\gamma_5\phi)} \end{aligned} \quad (3.18)$$

All that remains to be done to achieve a full bosonized model is to explicitly evaluate the functional integral over the quark fields Z_q.

3.1.2 Heat Kernel Expansion

Heat kernel techniques, which are a classical subject in mathematics, have found wide application in physical problems. [76] A very good review of the subject may be found in [77]. The method used in [70] is a generalization of the Schwinger-DeWitt proper time heat kernel expansion introduced in [78] and [79]. A naive version of the technique's fundamentals is discussed below following [77]. Another approach to the heat kernel expansion is through the use of ζ-function regularization. [80]

The basic idea of heat kernel techniques is to rewrite the Green's functions of some elliptic operator D as integrals over an auxiliary variable (the proper time τ) of a heat kernel

$$K\left(\tau, r, r'; D\right) = \langle r| e^{-\tau D} \left|r'\right\rangle \tag{3.19}$$

satisfying the heat equation

$$\left(\frac{\partial}{\partial \tau} + D\right) K\left(\tau, r, r'; D\right) = 0 \tag{3.20}$$

with initial conditions

$$K\left(0, r, r'; D\right) = \delta\left(r - r'\right) \tag{3.21}$$

It is then possible to write

$$D^{-1}\left(r, r'\right) = \int_0^\infty d\tau K\left(\tau, r, r'; D\right) \tag{3.22}$$

For $D = D_0 \equiv -\nabla^\mu \nabla_\mu + m^2$, where ∇_μ is the covariant derivative and m is some constant (usually a mass), the heat kernel in $\mathbb{R}^n$ is

$$K\left(\tau, r, r'; D_0\right) = (4\pi\tau)^{-\frac{n}{2}} e^{-\frac{(r-r')^2}{4\tau} - \tau m^2} \tag{3.23}$$

If $D = D_0 + V$ contains some other objects like potential terms or other fields, this expression may be generalized to the expansion

$$K\left(\tau, r, r'; D\right) = K\left(\tau, r, r'; D_0\right) F\left(\tau, r, r'; V\right) \tag{3.24}$$

$$F\left(\tau, r, r'; V\right) = \sum_{n=0}^{\infty} \tau^n a_n\left(r, r'; V\right) \tag{3.25}$$

where $a_i\left(r, r'; V\right)$ are the heat kernel coefficients which, for coinciding arguments $r = r'$, are just polynomials of background fields and their derivatives. This expression is actually an asymptotic approximation to the full heat kernel [81] in the limit $\tau \to 0$, and its convergence issues are far from being trivial. [82]

Substituting (3.24) in (3.20), we find

$$\frac{\partial F}{\partial \tau} = \frac{\partial^2 F}{\partial r^2} - \frac{r' - r}{\tau} \frac{\partial F}{\partial r} - V\left(r\right) F \tag{3.26}$$

From this and the initial condition (3.21) which in terms of F reads $F(0,r,r')=1$ we find $a_0(r,r')=1$ and a recursion relation

$$na_n(r,r')+(r-r')\frac{\partial}{\partial r}a_n(r,r')=\frac{\partial^2}{\partial r^2}a_{n-1}(r,r')-V(r)a_{n-1}(r,r') \tag{3.27}$$

Another useful representation for the heat kernel may be achieved if, in some regular domain, we expand V in Taylor series

$$V(r)=\sum_{k=0}^{\infty}\frac{(r-r')^k}{k!}V^{(k)}(r') \tag{3.28}$$

with $V^{(k)}(r')=\frac{d^kV(r)}{dr^k}\Big|_{r=r'}$, and we rewrite F as

$$F(\tau,r,r')=1+\sum_{n=1}^{\infty}\sum_{k=0}^{\infty}\tau^n(r-r')^k b_{nk}(r') \tag{3.29}$$

Evidently, $a_n(r,r')=\sum_{k=0}^{\infty}(r-r')^k b_{nk}(r')$ for $n\neq 0$, and a recursion relation can be established for the b_{nk} coefficients as well.

Suppose we want to evaluate a one-loop effective action of the form

$$W=\frac{1}{2}\ln\det D \tag{3.30}$$

We can write an identity for each positive eigenvalue λ of D as

$$\ln\lambda=-\int_0^{\infty}\frac{d\tau}{\tau}e^{-\tau\lambda} \tag{3.31}$$

Using $\ln\det D=\operatorname{Tr}\ln D$, this allows us to write the Schwinger proper time representation of the effective action W

$$W=-\frac{1}{2}\int_0^{\infty}\frac{d\tau}{\tau}K(\tau;D) \tag{3.32}$$

with

$$K(\tau;D)=\tilde{\operatorname{Tr}}e^{-\tau D}=\int d^nrK(\tau,r,r;D) \tag{3.33}$$

Together with the expansion (3.24), (3.32) allows for an evaluation of W in terms of the heat kernel coefficients a_i. It is now patent that the asymptotic behaviour of the heat kernel trace at $\tau = 0$ is of special importance for the integrals in (3.32), since these exhibit ultraviolet divergences in this limit. [83] This fact is reassuring of the validity of the asymptotic expansion (3.24).

Application to specific physical models might require additional considerations concerning symmetries and algebra, in which case expansion (3.24) might not be appropriate. The Schwinger-DeWitt proper time expansion has been worked out to yield relativistically covariant and gauge invariant coefficients, but it does not take into account the possibility that m might be a non-degenerate mass matrix, in which case the usual expansions do not work because m does not commute with the rest of the fields. So, application of heat kernel techniques to the explicit evaluation of the effective action in (3.18) requires a suitable generalization of expansion (3.24) that is algebraically sound and that preserves the transformation pattern of the model Lagrangian.

A good account of available approches to the heat kernel expansion may be found in [84]. In what follows, we will present a generalized heat kernel technique that is suited for the model in study. [85] [86] [87]

3.1.3 Quark Functional Integral in a Generalized Heat Kernel Expansion

We wish to evaluate the quark functional integral (3.18). By performing a Wick rotation

$$x^0 \to -ix_4^{(E)} \qquad x^i \to x_i^{(E)} \tag{3.34a}$$

$$\gamma^0 \to -i\gamma_4^{(E)} \qquad \gamma^i \to \gamma_i^{(E)} \tag{3.34b}$$

and defining the Euclidean vectors $x^{(E)} = (\vec{x}, x_4)$ and $\gamma^{(E)} = (\vec{\gamma}, \gamma_4)$, we can rewrite the quark integral as[1]

$$Z_q = e^{W[\sigma,\phi]} \tag{3.35}$$

with the Euclidean action defined as

$$W = \ln\det\left(i\gamma_\alpha^{(E)}\partial_\alpha^{(E)} - M - \sigma - i\gamma_5\phi\right) = \ln\det D_E \tag{3.36}$$

[1]Note that, in Euclidean space, we assume the definition $\gamma_5^{(E)} = \gamma_1^{(E)}\gamma_2^{(E)}\gamma_3^{(E)}\gamma_4^{(E)} = \gamma_5$.

For the real part of this effective action we can write

$$W = \ln\det|D_E| = \frac{1}{2}\ln\det\left(D_E^\dagger D_E\right) \tag{3.37}$$

with

$$\begin{aligned} D_E^\dagger D_E &= M^2 - \partial_E^2 + Y \\ Y &= i\gamma_\alpha\left(\partial_\alpha\sigma + i\gamma_5\partial_\alpha\phi\right) + \sigma^2 + \phi^2 + \{M,\sigma\} + i\gamma_5\left[\sigma + M, \phi\right] \end{aligned} \tag{3.38}$$

Using now (3.32) and (3.33), we can write

$$W = -\frac{1}{2}\tilde{\mathrm{Tr}}\int_0^\infty \frac{d\tau}{\tau}\rho\left(\tau\Lambda^2\right)e^{-\tau D_E^\dagger D_E} = -\frac{1}{2}\mathrm{Tr}\int_0^\infty \frac{d\tau}{\tau}\rho\left(\tau\Lambda^2\right)\int d^4x^{(E)}\left\langle x^{(E)}\right|e^{-\tau D_E^\dagger D_E}\left|x^{(E)}\right\rangle \tag{3.39}$$

where $\tilde{\mathrm{Tr}}$ denotes a functional trace as defined in (2.85), and Tr is the trace over internal indices. We have included a regulator function $\rho\left(\tau\Lambda^2\right)$ since the τ integrals are, in general, divergent at $\tau = 0$. In this way, the results will be regularization dependent, and for them to satisfy the invariance requirements of the model it is important to choose a suitable regularization scheme. A Pauli-Villars type regularization is employed [88], with a regulator of the form [89]

$$\rho\left(\tau\Lambda^2\right) = 1 - \left(1 + \tau\Lambda^2\right)e^{-\tau\Lambda^2} \tag{3.40}$$

This regularization procedure effectively subtracts the contributions arising from energies greater than the regularization parameter Λ in a covariant way.

At this point, we would like to take advantage of the expansion (3.24), but for that we need to work out a suitable generalization of the heat kernel expansion (3.24) that is valid in the case of the explicit appearance of a non-degenerate mass matrix $M = \mathrm{diag}\left(M_u, M_d, M_s\right)$ in D_E. We then turn to the procedure described in [86] and [87], which avoids expanding the mass dependent part of the heat kernel, performing a necessary resummation of the series expansion of the remainder of the heat kernel fleshed out to preserve the chiral transformation properties of the effective bosonized Lagrangian at every order in the expansion. Of course, the presence of the current quark masses will then break this invariance explicitly. The main steps of this procedure are laid out in [85]

for the broken $SU(2)$ case and may be outlined as follows (we omit for now the explicit Euclidean notation, recovering it in the final result). We may use a fictitious Hilbert space basis to rewrite (3.39) as

$$W = -\frac{1}{2}\int d^4x \int \frac{d^4p}{(2\pi)^4}\int_0^\infty \frac{d\tau}{\tau^3}\rho\left(\tau\Lambda^2\right)e^{-p^2}\mathrm{Tr}e^{-\tau\left(M^2+A\right)} \tag{3.41}$$

with

$$A = -\partial^2 - \frac{2ip}{\sqrt{\tau}}\partial + Y \tag{3.42}$$

We then resort to a Dyson series expansion [90] for the heat kernel as

$$\mathrm{Tr}e^{-\tau\left(M^2+A\right)} = \mathrm{Tr}\left[e^{-\tau M^2}\left(1+\sum_{n=1}^{\infty} f_n\left(\tau, A\right)\right)\right] \tag{3.43}$$

where

$$f_n\left(\tau, A\right) = \int_0^t ds_1 \int_0^{s_1} ds_2 ... \int_0^{s_{n-1}} ds_n A\left(s_1\right) A\left(s_2\right) ... A\left(s_n\right) \tag{3.44}$$

and

$$A\left(s\right) = e^{sM^2} A e^{-sM^2} \tag{3.45}$$

With this we can write the first few terms of expansion (3.43) explicitly, and then insert them into (3.41). It is instrumental to exploit the cyclic property of the traces and the properties of the Gaussian integral over p to manipulate the expression into a useful form. The several terms of the series (3.43) end up clustering into nice new coefficients which multiply similarly structured integrals of the form

$$I_n = \frac{1}{3}\sum_{i=0}^{3} J_n\left(M_i^2\right) = \frac{1}{3}\sum_{i=0}^{3}\int_0^\infty \frac{d\tau}{\tau^{2-n}}\rho\left(\tau\Lambda^2\right)e^{-\tau M_i^2} \tag{3.46}$$

satisfying the identity

$$J_l\left(M_j^2\right) - J_l\left(M_i^2\right) = \sum_{n=1}^{\infty}\frac{\Delta_{ij}^n}{2^n n!}\left[J_{l+n}\left(M_i^2\right) - \left(-1\right)^n J_{l+n}\left(M_j^2\right)\right] \tag{3.47}$$

with $\Delta_{ij} = M_i^2 - M_j^2$. These J_n correspond to one-loop quark integrals with $n+1$ vertices. Some explicit J_n integrals evaluated with the regulator (3.40) are

$$J_1\left(M_i^2\right) = \ln\left(1 - \frac{\Lambda^2}{M_i^2}\right) - \frac{\Lambda^2}{\Lambda^2 + M_i^2} \tag{3.48a}$$

$$J_0\left(M_i^2\right) = \Lambda^2 - M_i^2 \ln\left(1 + \frac{\Lambda^2}{M_i^2}\right) \tag{3.48b}$$

After a long algebraic and analytic calculation, we may state the final result for the heat kernel expansion as [86] [87]

$$W = -\int \frac{d^4x^{(E)}}{32\pi^2} \sum_{n=0}^{\infty} I_{n-1} \mathrm{Tr}\left(a_n\right) \tag{3.49}$$

where the a_n are the new generalized Seeley-DeWitt coefficients. The first few are

$$\begin{aligned} a_0 &= 1 \\ a_1 &= -Y \\ a_2 &= \frac{Y^2}{2} + \frac{\Delta_{ud}}{2}\lambda_3 Y + \frac{1}{2\sqrt{3}}\left(\Delta_{us} + \Delta_{ds}\right)\lambda_8 Y \end{aligned} \tag{3.50}$$

In the isospin limit $M_u = M_d \neq M_s$, a_2 and higher order coefficients are considerably simplified.

It should be remarked that the series (3.49) may be interpreted as an inverse mass expansion, since $I_{n+1} \sim M_i^{-2n}$, and it can be shown that it is in perfect agreement with the known Schwinger-DeWitt expansion for a degenerate mass matrix $M = M_q \mathbb{1}$. It should also be noted that the coefficients (3.50) are indeed invariant under infinitesimal chiral transformations $\omega = \alpha + \beta\gamma_5$ if the operator $D_E^\dagger D_E$ transforms in the adjoint representation of the chiral group. [87]

3.1.4 Gap Equations and Quark Condensates

We proceed with the analysis of the model presented in [70]. Making use of the quark component of the effective action W obtained above (3.49), it is possible to write an Euclidean effective bosonized Lagrangian for the model.

$$\mathcal{L}_{bos} = -\mathcal{L}_r^{st} + \frac{1}{32\pi^2}\sum_{n=0}^{\infty} I_{n-1}\mathrm{Tr}\,(a_n) \tag{3.51}$$

An important remark is due. Our auxiliary Lagrangian (3.16) contains a linear term in σ which behaves as a source term, and hence the overall expression multiplying σ must be set to zero in the calculation of correlation functions from the vacuum persistence amplitude. This condition gives rise to the mass gap equations. The infinite heat kernel series (3.49) also contributes with its own set of tadpole terms. We truncate the series to order $n = 2$ and collect the tadpole contributions from the second and third order terms (the first one has no field dependence and can thus be discarded without concern). With this, we get a system of gap equations of the form

$$h_i + \frac{N_c}{6\pi^2} M_i \left[3I_0 - \left(3M_i^2 - M^2\right) I_1\right] = 0 \tag{3.52}$$

Here, the index i runs over the quark flavours u, d and s, and $M^2 = M_u^2 + M_d^2 + M_s^2$. In the isospin limit $M_u = M_d \neq M_s$, we get

$$\begin{aligned} h_u + \frac{N_c}{6\pi^2} M_u \left[3I_0 - \Delta_{us} I_1\right] &= 0 \\ h_s + \frac{N_c}{6\pi^2} M_s \left[3I_0 + 2\Delta_{us} I_1\right] &= 0 \end{aligned} \tag{3.53}$$

Remembering that the expansion (3.49) can be interpreted as an inverse mass expansion, we can effectively neglect terms J_n of order $n > 2$ for large constituent quark masses, in which case we can use (3.46) and (3.47) to rewrite the gap equation (3.52) as

$$h_i + \frac{N_c}{2\pi^2} M_i J_0\left(M_i^2\right) = 0 \tag{3.54}$$

The h_i coefficients are in direct connection with the chiral symmetry breaking quark condensates $\langle\bar{q}q\rangle$. To verify this fact, we recall the bosonization procedure in which we used $\delta\left(s_a - \bar{q}\lambda^a q\right)$ and $\delta\left(p_a - \bar{q}i\gamma_5\lambda^a q\right)$, effectively introducing the identities between the auxiliary fields and the quark bilinears in the arguments of the delta functions. Then, the SPA restricts s_a and p_a to the stationary values expressed through (3.9). We may then write

$$\bar{q}\lambda_a q = 2e_{ai}\bar{q}\lambda_a q = s_a^{st} = e_{ai}s_i^{st} \qquad \Leftrightarrow \qquad \langle\bar{q}_i q_i\rangle = \frac{\left\langle s_i^{st}\right\rangle}{2} \tag{3.55}$$

The fields σ and ϕ are defined to have zero vacuum expectation value, which results in

$$h_i = 2\langle \bar{q}_i q_i \rangle \tag{3.56}$$

This asserts that we can indeed identify the h_i coefficients with the quark condensates (apart from a factor of 2).

3.1.5 Effective Potential and Vacuum Stability

The physical implications and mathematical subtleties arising from the t'Hooft term (3.3) have been meticulously studied in [91] and [75]. In particular, the issues of vacuum stability of the NJL model extended with the t'Hooft term and the hierarchy problem of multi-quark interactions are adressed. The two are intertwined, as is stated in [91] that the existence or not of a hierarchy in the multi-quark interaction terms may affect the ground state stability of the model. The main concern comes from the SPA employed in the functional integration over auxiliary fields s_a and p_a in (3.6). The resulting stationary phase conditions (3.15) may generally admit more than one real solution, which should equally be taken into account in the SPA result from a rigorous perspective. Furthermore, it is expected that in the limit $\kappa \to 0$, i.e., if we turn off the t'Hooft interaction, we should recover the familiar results [54] [53] of the simpler NJL model without the six-quark term.

In [75], the effective potential V is determined from the gap equation. The rationale is simple: the vacuum expectation value of the potential in the bosonized Lagrangian gives us the classical effective potential $V = \langle U(\sigma, \phi) \rangle$, or

$$\frac{\partial V}{\partial \langle \sigma \rangle} = \left\langle \frac{\partial U}{\partial \sigma} \right\rangle \tag{3.57}$$

This corresponds to the coefficient of the σ tadpole term. The solutions of the gap equation then correspond to extrema of the effective potential, and we have the relation

$$dV = \sum_i f_i dM_i \qquad , \qquad f_i = -\frac{h_i}{2} - \frac{N_c}{4\pi^2} M_i J_0\left(M_i^2\right) \tag{3.58}$$

From (3.15) we have

$$dM_i = -G dh_i - \frac{\kappa}{16} t_{ijk} h_j dh_k \tag{3.59}$$

We also note that

$$J_{n+1}\left(M_i^2\right) = -\frac{\partial}{\partial M_i^2} J_n\left(M_i^2\right) \tag{3.60}$$

This gives an exact differential

$$dV = d\left[\frac{G}{4}\sum_i h_i^2 + \frac{\kappa}{16} h_u h_d h_s + \frac{3N_c}{8\pi^2} I_{-1}\right] \tag{3.61}$$

from which we can define the effective potential (apart from a constant factor C) as

$$V = \frac{G}{4}\sum_i h_i^2 + \frac{\kappa}{16} h_u h_d h_s + \frac{3N_c}{8\pi^2} I_{-1} + C \tag{3.62}$$

The constant C is fixed by requiring that $V = 0$ for $M_i = 0$. The quark integrals J_{-1} may be written as

$$J_{-1}\left(M_i^2\right) = -\frac{1}{2}\left[M_i^2 J_0\left(M_i^2\right) + \Lambda^4 \ln\left(1 + \frac{M_i^2}{\Lambda^2}\right)\right] \tag{3.63}$$

In [75], besides studying the effect of quantum fluctuations (to first non-leading order) that tend to restore the chiral symmetric phase, an analysis of the structure of the vacuum and the effective potential is done. A more detailed and extended analysis is also performed in [91], where compelling arguments are presented to support the fact that this effective potential is unbounded from below, having at most a metastable non-tivial vacuum. In the general case, the stationary phase conditions (3.15) have multiple non-degenerate solutions, of which only one is regular at $\kappa \to 0$; this results in an unstable vacuum. The analysis has been conducted in perturbative expansion around the metastable vacuum, in loop expansion and in $1/N_c$ expansion.

Still in [91], it is suggested that the 't Hooft term should be $1/N_c$ suppressed relative to the four-quark term, thus hinting at a hierarchy of multi-quark interactions based on the $1/N_c$ expansion. The NJL model without the 't Hooft term, which corresponds to leading order in N_c counting, has a stable vacuum in the Nambu-Goldstone phase, whereas the introduction of the 't Hooft term spoils the model's stability. However, a full account of the next-to-leading order terms in N_c counting should not affect the stability of the model, since their contribution is suppressed. This is good indication that same order terms in N_c counting as the 't Hooft term are missing from the model. Inclusion of eight-quark interaction terms that are of the same order in N_c counting as the 't

Hooft term is proposed in [92] as a way to restore consistency with an N_c expansion and vacuum stability.

3.1.6 Eight-Quark Interactions

To implement the ideas discussed above, in [92] the most general chirally symmetric eight-quark terms are included in (2.67), so that the Lagrangian now reads

$$\mathcal{L} = \bar{\psi}\left(i\gamma^{\mu}\partial_{\mu} - m\right)\psi + \mathcal{L}_{NJL} + \mathcal{L}_{H} + \mathcal{L}_{8q} \tag{3.64}$$

with the new terms given by

$$\mathcal{L}_{8q}^{(1)} = g_1\left[\mathrm{tr}\left(\bar{q}P_R q\right)\left(\bar{q}P_L q\right)\right]^2 \tag{3.65}$$

$$\mathcal{L}_{8q}^{(2)} = g_2 \mathrm{tr}\left[\left(\bar{q}P_R q\right)\left(\bar{q}P_L q\right)\right]^2 \tag{3.66}$$

where tr denotes a trace in flavour space. With these new terms, the auxiliary Lagrangian in the bosonized theory becomes

$$\begin{aligned}\mathcal{L}_r = {} & s_a\left(\sigma_a + \Delta_a\right) + \frac{G}{2}\left(s_a^2 + p_a^2\right) + \frac{\kappa}{32}A_{abc}s_a\left(s_b s_c - 3p_b p_c\right) + \frac{g_1}{8}\left(s_a^2 + p_b^2\right)^2 \\ & + \frac{g_2}{8}\left[d_{abe}d_{cde}\left(s_a s_b + p_a p_b\right)\left(s_c s_d + p_c p_d\right) + 4f_{abe}f_{cde}s_a s_c p_b p_d\right]\end{aligned} \tag{3.67}$$

and the stationary phase conditions for the h_i coefficients read

$$Gh_i + \Delta_i + \frac{\kappa}{32}t_{ijk}h_j h_k + \frac{g_1}{4}h^2 h_i + \frac{g_2}{2}h_i^3 = 0 \tag{3.68}$$

where $h^2 = h_u^2 + h_d^2 + h_s^2$.

We now study the stability of a non-trivial vacuum in this model. The analysis in [92] and [93] shows that, if stability conditions are satisfied, the local minimum existing before in the model without eight-quark interactions gets stabilized with the inclusion of the new terms. A way to determine the stability constraint of the system is to study the solutions to the stationary phase condition (3.68), which yield fifth-order equations in the coefficients h_i and generally admit more than one real solution. The general solutions can only be found numerically, but the flavour $SU(3)$ symmetric case is simple

enough to solve analytically, and provides an approximate but compelling indication that it is possible to stabilize the Goldstone-Nambu phase vacuum (even in the general case, the values of the different h_i are very close). In this simplified case, the stationary phase conditions become

$$h^3 + \frac{\kappa}{12\lambda}h^2 + \frac{4G}{3\lambda}h + \frac{4\Delta}{3\lambda} = 0 \tag{3.69}$$

with $\lambda = g_1 + \frac{2}{3}g_2$. We may eliminate the quadratic term by making the substitution $h = \bar{h} - \frac{\kappa}{36\lambda}$, resulting in

$$\bar{h}^3 + A\bar{h} = B \tag{3.70}$$

with

$$A = \frac{4}{3}\left[\frac{G}{\lambda} - \left(\frac{\kappa}{24\lambda}\right)^2\right] \quad , \quad B = \frac{4}{3}\left\{\frac{\kappa}{36\lambda}\left[\frac{G}{\lambda} - \frac{2}{3}\left(\frac{\kappa}{24\lambda}\right)^2\right] - \frac{\Delta}{\lambda}\right\} \tag{3.71}$$

Equation (3.70) has one real root if its discriminant $-4A^3 - 27B^2$ is negative, i.e., if $A > 0$, or

$$\frac{G}{\lambda} > \left(\frac{\kappa}{24\lambda}\right)^2 \tag{3.72}$$

Finally, we just state the form of the effective potential V and its stability conditions. As in (3.62), we have

$$\begin{aligned} V = {} & \frac{G}{4}\sum_i h_i^2 + \frac{\kappa}{16}h_u h_d h_s + \frac{3g_1}{32}\left(\sum_i h_i^2\right)^2 \\ & + \frac{3g_2}{16}\sum_i h_i^4 + \frac{3N_c}{8\pi^2}I_{-1} + C \end{aligned} \tag{3.73}$$

and this potential has a stable Nambu-Goldstone ground state for[2]

$$g_1 > 0 \quad , \quad g_1 + 3g_2 > 0 \quad , \quad G > \frac{1}{g_1}\left(\frac{\kappa}{16}\right)^2 \tag{3.74}$$

[2]In the next section, the parameters are redefined as $g_1 \to 2g_1$ and $\kappa \to 8\kappa$.

3.2 NJL Model with Mass-Dependent Multi-Quark Interactions

We have thoroughly analyzed the three-flavour NJL-model with a t'Hooft six-quark interaction (3.3) by bosonizing the Lagrangian (3.1) in the functional integral formalism, to which end we have used the SPA and a generalized proper time heat kernel expansion. This model exhibits an unstable vacuum which is stabilized by extending the model with eight-quark interactions. On the basis of this entire discussion, we consider a final extension to our model in the form of generalized chiral symmetry breaking terms, following the material presented in [3] and [4]. In the context of chiral quark models, such terms have been mostly overlooked in the literature, and it is of great interest to understand their role in meson spectra and quark matter thermodynamics. In what follows, we summarize the relevant points of the model's formulation and manipulation.

3.2.1 External Source and Power Counting

So far, we have vehemently argued for the central role of chiral symmetry (and its dynamical breaking) in the dynamics of strongly interacting particles, to the point that it should be an indispensable ingredient of any effective model of QCD. However, the presence of an explicit quark current mass is vital for the consistency of chiral models with QCD, as well as an accurate description of light hadron spectra, and should not be overlooked. While the bulk of the constituent mass of the quarks is generated through the mechanism of chiral symmetry breaking native to the strong interactions, the current quark masses have their origin someplace else, presumably in the Higgs and electroweak sectors of the theory. In this sense, current quark masses are foreign to the strong interactions. Current quark mass may then be seen as coming into the picture of an exactly chirally symmetric Lagrangian by letting the quarks interact with a source field χ extraneous to the strong interaction itself.

From an EFT perspective, we should include in our Lagrangian all such interaction terms that can be written up to the desired order in the expansion parameter. A good illustration of this principle that falls within the domain of QCD effective models comes from ChPT, [94] [95] where the expansion is usually made in terms of quark masses and hadronic degrees of freedom. In the present case, we wish to describe the dynamics of quark degrees of freedom in an effective expansion consistent with N_c counting, and we have argued that a consistent inclusion of the t'Hooft term requires eight-quark interactions to be included as well. Since we are working out a low energy effective model, there is an explicit cutoff $\Lambda \sim 1\text{GeV}$ appearing in the regularization of ultraviolet

divergences which presents itself as a natural expansion parameter. Additionally, mass terms must also be generalized to include all possibilities consistent with the N_c counting order and dimensional analysis. We will then have a chiral Lagrangian which is complete up to order N_c^0 in an $1/N_c$ expansion and also up to order in Λ^0 in a mass expansion, with explicit mass terms and mass-dependent interactions introduced as interaction terms between quarks and the source field χ. [96] [97]

As is done in [4], we will show how to build the most general collection of effective terms that include quark fields q and a source field χ, and which belong to an expansion on the basis of the explicit cutoff Λ. For this purpose, it is convenient to define, as before, scalar and pseudoscalar bilinears $s_a = \bar{q}\lambda_a q$ and $p_a = i\bar{q}\lambda_a\gamma_5 q$, and also a $U(3)$ valued field (the λ_a are flavour space $U(3)$ Gell-Mann matrices defined in Appendix A)

$$\Sigma = \frac{1}{2}(s_a - ip_a)\lambda_a \tag{3.75}$$

which transforms under chiral transformations as $\Sigma \longrightarrow U_R \Sigma U_L^\dagger$ (the unitary transformations U_L and U_R are defined in section 2.2). Furthermore, we assume the source field transforms in the same way as Σ, i.e., $\chi \longrightarrow U_R \chi U_L^\dagger$. With this assumption, we may build multi-quark effective interaction terms for the chiral Lagrangian by imposing chiral invariance alongside the other exact symmetries of QCD, namely the discrete symmetries of charge conjugation, parity and time reversal. Also, we should not forget that the six-quark interaction terms are of the 't Hooft determinantal form and explicitly break the $U_A(1)$ axial symmetry.

For a dimensional analysis of these terms, we begin by noticing the general structure of any (non-derivative) interaction term, which may be given as

$$\mathcal{L}_i \sim \frac{\bar{g}_i}{\Lambda^\gamma}\Sigma^\alpha \chi^\beta \tag{3.76}$$

where $\bar{g}_i$ are dimensionless couplings. Since the action must be dimensionless, the Lagrangian density must have dimension $[mass]^4$ (in four space-time dimensions). The dimensions of quark fields are well known [8] to be $[mass]^{\frac{3}{2}}$, and both Λ and χ have dimensions $[mass]^1$ Thus, the effective terms are restricted to integer values of α, β and γ obeying

$$3\alpha + \beta - \gamma = 4 \tag{3.77}$$

We impose a second restriction by only keeping terms whose contribution to the effective potential survive in the limit $\Lambda \to \infty$. These correspond to the relevant and marginal operators of the EFT we are building. [98] The effective potential refers to the bosonized Lagrangian, where the bosonic degrees of freedom may be seen as arising from contracting pairs of quark fields in the original Lagrangian. Each of these contractions introduces a quark loop, and each quark loop introduces an integral of a quark propagator and its respective trace, wich overall diverges as $[mass]^2$. When regularized for ultraviolet divergences, these loops then give off a factor of Λ^2. So, the overall $\mathcal{O}(\Lambda)$ to which terms (3.76) contribute to the effective potential is $2\alpha - \gamma$, and the term will survive at large Λ if

$$2\alpha - \gamma \geq 0 \tag{3.78}$$

If we join constraints (3.77) and (3.78), we get the condition

$$4 - \alpha - \beta \geq 0 \tag{3.79}$$

This condition, together with (3.77), severely narrows the relevant terms to the following combinations:

1. $\beta = 0$: $(\alpha, \gamma) = \{(2,2), (3,5), (4,8)\}$
2. $\beta = 1$: $(\alpha, \gamma) = \{(1,0), (2,3), (3,6)\}$
3. $\beta = 2$: $(\alpha, \gamma) = \{(1,1), (2,4)\}$
4. $\beta = 3$: $(\alpha, \gamma) = \{(1,2)\}$

The first group encompasses all the previously discussed four, six and eight-quark interaction terms which were studied together in section 3.1.6. The mass-dependent interactions appear in the subsequent groups in linear, quadratic and cubic combinations. It is then just a matter of systematically constructing chirally invariant terms following the prescriptions above. This procedure is facilitated by first constructing the $\beta = 0$ terms and then using them as prototypes for the mass-dependent terms by simply replacing the appropriate number of Σ fields by χ fields (remember that Σ and χ transform in the same fashion under chiral transformations). Also, we note that the first possibility with $\beta = 1$ coincides with the explicit mass term we have previously considered.

The $\beta = 0$ terms should be equivalent to those already described in the previous analysis of the NJL model, but translated into Σ fields instead of q fields. It is useful to notice from (3.75) that we can write the Σ field's flavour space matrix components as

$$\Sigma_{ab} = 2\bar{q}_b P_R q_a \qquad , \qquad \Sigma^\dagger_{ab} = 2\bar{q}_b P_L q_a \tag{3.80}$$

Likewise, we highlight that any expression of the form $\mathrm{tr}\Sigma^\dagger\Sigma$ is chirally invariant, where tr is the trace in flavour space. With these features and some algebra, it can be shown that the interaction terms may be written as

$$\mathcal{L}_{int} = \frac{\bar{G}}{\Lambda^2}\mathrm{tr}\left(\Sigma^\dagger\Sigma\right) + \frac{\bar{\kappa}}{\Lambda^5}\left(\det\Sigma + \det\Sigma^\dagger\right) + \frac{\bar{g}_1}{\Lambda^8}\left[\mathrm{tr}\left(\Sigma^\dagger\Sigma\right)\right]^2 + \frac{\bar{g}_2}{\Lambda^8}\mathrm{tr}\left(\Sigma^\dagger\Sigma\Sigma^\dagger\Sigma\right) \tag{3.81}$$

and that these terms have the same structure as those in (3.2), (3.3) and (3.65). With these prototypical terms in place, we now present a series of ten possible mass-dependent terms:

$$\begin{aligned}
\mathcal{L}_0 &= -\mathrm{tr}\left(\Sigma^\dagger\chi + \chi^\dagger\Sigma\right) \\
\mathcal{L}_1 &= -\frac{\bar{\kappa}_1}{\Lambda}\epsilon_{ijk}\epsilon_{lmn}\Sigma_{il}\chi_{jm}\chi_{kn} + \mathrm{h.c.} \\
\mathcal{L}_2 &= \frac{\bar{\kappa}_2}{\Lambda^3}\epsilon_{ijk}\epsilon_{lmn}\Sigma_{il}\Sigma_{jm}\chi_{kn} + \mathrm{h.c.} \\
\mathcal{L}_3 &= \frac{\bar{g}_3}{\Lambda^6}\mathrm{tr}\left(\Sigma^\dagger\Sigma\Sigma^\dagger\chi\right) + \mathrm{h.c.} \\
\mathcal{L}_4 &= \frac{\bar{g}_4}{\Lambda^6}\mathrm{tr}\left(\Sigma^\dagger\Sigma\right)\mathrm{tr}\left(\Sigma^\dagger\chi\right) + \mathrm{h.c.} \\
\mathcal{L}_5 &= \frac{\bar{g}_5}{\Lambda^4}\mathrm{tr}\left(\Sigma^\dagger\chi\Sigma^\dagger\chi\right) + \mathrm{h.c.} \\
\mathcal{L}_6 &= \frac{\bar{g}_6}{\Lambda^4}\mathrm{tr}\left(\Sigma^\dagger\Sigma\chi^\dagger\chi + \Sigma\Sigma^\dagger\chi\chi^\dagger\right) + \mathrm{h.c.} \\
\mathcal{L}_7 &= \frac{\bar{g}_7}{\Lambda^4}\left[\mathrm{tr}\left(\Sigma^\dagger\chi\right) + \mathrm{h.c.}\right]^2 \\
\mathcal{L}_8 &= \frac{\bar{g}_8}{\Lambda^4}\left[\mathrm{tr}\left(\Sigma^\dagger\chi\right) - \mathrm{h.c.}\right]^2 \\
\mathcal{L}_9 &= -\frac{\bar{g}_9}{\Lambda^2}\mathrm{tr}\left(\Sigma^\dagger\chi\chi^\dagger\chi\right) + \mathrm{h.c.} \\
\mathcal{L}_{10} &= -\frac{\bar{g}_{10}}{\Lambda^2}\mathrm{tr}\left(\Sigma^\dagger\chi\right)\mathrm{tr}\left(\chi^\dagger\chi\right) + \mathrm{h.c.}
\end{aligned} \tag{3.82}$$

The $\pm$h.c. appearing in the above expressions mean that we should add to the expression to the left its hermitean conjugate. We can then write the full Lagrangian density as

$$\mathcal{L} = \mathcal{L}_D + \mathcal{L}_{int} + \mathcal{L}_\chi \tag{3.83}$$

where

$$\mathcal{L}_D = i\bar{q}\gamma^\mu \partial_\mu q \tag{3.84}$$

is the free Dirac massless Lagrangian, $\mathcal{L}_{int}$ is defined in (3.81) and

$$\mathcal{L}_\chi = \sum_{i=0}^{10} \mathcal{L}_i \tag{3.85}$$

with $\mathcal{L}_i$ defined in (3.82).

We now summarize the N_c dependence of the terms. The leading-order $\mathcal{O}(N_c)$ terms correspond to the original NJL four-quark interaction (the first term in $\mathcal{L}_{int}$) and the simple current quark mass term $\mathcal{L}_0$. Σ fields count as N_c, since they each contribute a quark loop to the effective potential, and thus $\bar{G} \sim N_c^{-1}$. The other terms are all of order $\mathcal{O}(1)$ in N_c counting, which gives us $\bar{\kappa}_1, \bar{g}_9, \bar{g}_{10} \sim N_c^{-1}$, $\bar{\kappa}_2, \bar{g}_5, \bar{g}_6, \bar{g}_7, \bar{g}_8 \sim N_c^{-2}$, $\bar{\kappa}, \bar{g}_3, \bar{g}_4 \sim N_c^{-3}$, and $\bar{g}_1, \bar{g}_2 \sim N_c^{-4}$. It has been further shown in [3] that the N_c assignments match the counting rules based on arguments set by the scale Λ, i.e., the diagrams that survive in the large N_c limit are the same that do not vanish as $\Lambda \longrightarrow \infty$.

3.2.2 Dirac Mass and the Kaplan-Manohar Ambiguity

To leading order, the term $\mathcal{L}_0$ in (3.82) should correspond to the current quark mass term $-\bar{q}mq$. It can be shown that, for hermitean χ,

$$-\operatorname{tr}\left(\Sigma^\dagger \chi + \chi^\dagger \Sigma\right) = -2\bar{q}\chi q \tag{3.86}$$

To be able to identify this as the usual mass term, we set $\chi = \frac{\mathcal{M}}{2}$, where $\mathcal{M} = \operatorname{diag}(m_u, m_d, m_s)$. If we go beyond leading order, other linear terms in Σ will also contribute to the Dirac mass term, i.e., $\mathcal{L}_1$, $\mathcal{L}_9$ and $\mathcal{L}_{10}$; these read

$$\begin{aligned}\mathcal{L}_1 &= -\frac{\bar{\kappa}_1}{\Lambda}\bar{q}\left(\det\mathcal{M}\right)\mathcal{M}^{-1}q \\ \mathcal{L}_9 &= -\frac{\bar{g}_9}{4\Lambda^2}\bar{q}\mathcal{M}^3 q \\ \mathcal{L}_{10} &= -\frac{\bar{g}_{10}}{4\Lambda^2}\bar{q}\left(\mathrm{tr}\mathcal{M}^2\right)\mathcal{M}q\end{aligned} \tag{3.87}$$

So, if we include next-to-leading order terms, we get a Dirac mass term $-\bar{q}mq$ with

$$m = \mathcal{M} + \frac{\bar{\kappa}_1}{\Lambda}\left(\det\mathcal{M}\right)\mathcal{M}^{-1} + \frac{\bar{g}_9}{4\Lambda^2}\mathcal{M}^3 + \frac{\bar{g}_{10}}{4\Lambda^2}\mathrm{tr}\left(\mathcal{M}^2\right)\mathcal{M} \tag{3.88}$$

There is, however, a certain freedom in the definition of the parameters $\bar{\kappa}_1$, $\bar{g}_9$ and $\bar{g}_{10}$, or better, in the definition of the current quark masses introduced through the source field χ. This fact is related to earlier discoveries reported in [99] and other papers about an apparent ambiguity in the definition of current quark masses. This should not come as unexpected in light of colour confinement, which suggests that current quark masses should be unobservable, behaving more like running coupling constants which are explicitly dependent on the renormalization scale. Measurements of hadronic observables are only able to probe current mass ratios, and even these cannot all be fixed from the phenomenology, leaving the actual current masses essentially undefined.

In the present case, [3] we may address this point by first redefining the source term as

$$\chi \longrightarrow \chi' = \chi + \frac{c_1}{\Lambda}\left(\det\chi^\dagger\right)\chi\left(\chi^\dagger\chi\right)^{-1} + \frac{c_2}{\Lambda^2}\chi\chi^\dagger\chi + \frac{c_3}{\Lambda}\mathrm{tr}\left(\chi^\dagger\chi\right)\chi \tag{3.89}$$

where c_i are three free parameters. It can be shown that χ' transforms exactly as χ under chiral transformations, which guarantees that the redefinition is compatible with the symmetry requirements. Using this freedom it is possible to redefine the couplings in the Lagrangian in such a way that $m = \mathcal{M}$ and the final Lagrangian becomes

$$\mathcal{L} = \bar{q}\left(i\gamma^\mu\partial_\mu - m\right)q + \mathcal{L}_{int} + \sum_{i=2}^{8} L_i \tag{3.90}$$

3.2.3 Functional Integral Bosonization

The whole analysis performed in section 3.1 is directly applicable to the Lagrangian density (3.90). We start by using the functional identity (3.4) to write the vacuum persistence amplitude in the form (3.6). As before, we wish to describe the system in

the Nambu-Golsdtone phase, to which end we make again the shift $\sigma \longrightarrow \sigma + M$ so that $\langle\sigma\rangle = 0$ in the chirally broken ground state. The quark-dependent Lagrangian $\mathcal{L}_q$ is the same as before (3.7), but the auxiliary Lagrangian has a series of new terms coming from the mass-dependent part of the Lagrangian. As before, we use $\chi = \frac{\mathcal{M}}{2} = \frac{1}{2}\mathrm{diag}\,(m_u, m_d, m_s)$. Resorting to the $U\,(3)$ algebra, we can write

$$\mathcal{L}_r = s_a\,(\sigma_a + \Delta_a) + p_a\phi_a + \mathcal{L}_{int}\,(s,p) + \mathcal{L}_\chi\,(s,p) \tag{3.91}$$

with

$$\begin{aligned}\mathcal{L}_{int}\,(s,p) = {} & \frac{\bar{G}}{2\Lambda^2}\left(s_a^2 + p_a^2\right) + \frac{\bar{\kappa}}{4\Lambda^5}A_{abc}s_a\,(s_b s_c - 3p_b p_c) + \frac{\bar{g}_1}{4\Lambda^8}\left(s_a^2 + p_b^2\right)^2 \\ & + \frac{\bar{g}_2}{8\Lambda^8}\left[d_{abe}d_{cde}\,(s_a s_b + p_a p_b)\,(s_c s_d + p_c p_d) + 4f_{abe}f_{cde}s_a s_c p_b p_d\right]\end{aligned} \tag{3.92}$$

and

$$\begin{aligned}\mathcal{L}_r\,(s,p) &= \sum_{i=2}^{8}\mathcal{L}_i\,(s,p) \\ \\ \mathcal{L}_2\,(s,p) &= \frac{3\bar{\kappa}_2}{2\Lambda^3}A_{abc}m_a\,(s_b s_c - p_b p_c) \\ \mathcal{L}_3\,(s,p) &= \frac{\bar{g}_3}{4\Lambda^6}m_a\left[d_{abe}d_{cde}s_b\,(s_c s_d + p_c p_d) - 2f_{abe}f_{cde}p_b p_c s_d\right] \\ \mathcal{L}_4\,(s,p) &= \frac{\bar{g}_4}{2\Lambda^6}\left(s_a^2 + p_a^2\right)s_b m_b \\ \mathcal{L}_5\,(s,p) &= \frac{\bar{g}_5}{4\Lambda^4}\left(d_{abe}d_{cde} - f_{abe}f_{cde}\right)m_b m_d\,(s_a s_c - p_a p_c) \\ \mathcal{L}_6\,(s,p) &= \frac{\bar{g}_6}{4\Lambda^4}d_{abe}d_{cde}m_a m_b\,(s_c s_d + p_c p_d) \\ \mathcal{L}_7\,(s,p) &= \frac{\bar{g}_7}{\Lambda^4}\left(s_a m_a\right)^2 \\ \mathcal{L}_8\,(s,p) &= \frac{\bar{g}_8}{\Lambda^4}\left(p_a m_a\right)^2\end{aligned} \tag{3.93}$$

Following along the same lines, we use the SPA to perform the functional integration over the auxiliary fields s and p, expanding them as before (3.9) in powers of the bosonic fields σ and ϕ. To simplify the notation, we redefine the couplings by absorbing into them the explicit Λ dependence of its respective term. The stationary phase conditions

extend the ones obtained in (3.10) now including contributions coming from the eight-quark interactions [93] and the mass-dependent terms [3] [4],

$$\begin{aligned}
&\sigma_a + \Delta_a + Gs_a + \frac{3\kappa}{4}A_{abc}\left(s_b s_c - p_b p_c\right) + g_1 s_a\left(s^2+p^2\right) \\
&+\frac{g_2}{2}s_b\left[d_{abe}d_{cde}\left(s_c s_d + p_c p_d\right) + 2f_{ace}f_{bde}p_c p_d\right] + 3\kappa_2 A_{abc}s_b m_c \\
&+\frac{g_3}{4}\left[2d_{abe}d_{cde}s_b s_c + d_{ade}d_{bce}\left(s_b s_c + p_b p_c\right) - f_{abe}f_{cde}p_b p_c\right]m_d \\
&+\frac{g_4}{2}\left[2s_a s_b m_b + m_a\left(s^2+p^2\right)\right] + \frac{g_5}{2}\left(d_{ace}d_{bde} - f_{ace}f_{bde}\right)s_b m_c m_d \\
&+\frac{g_6}{2}d_{abe}d_{cde}s_b m_c m_d + 2g_7 m_a s_b m_b = 0
\end{aligned} \tag{3.94a}$$

$$\begin{aligned}
&\phi_a + Gp_a - \frac{3\kappa}{2}A_{abc}s_b p_c + g_1 p_a\left(s^2+p^2\right) \\
&+\frac{g_2}{2}p_b\left[d_{abe}d_{cde}\left(p_c p_d + s_c s_d\right) + 2f_{ace}f_{bde}s_c s_d\right] \\
&-3\kappa_2 A_{abc}p_b m_c + \frac{g_3}{2}\left(d_{ace}d_{bde} + f_{abe}f_{cde} - f_{ade}f_{bce}\right)s_b p_c m_d \\
&+g_4 p_a s_b m_b - \frac{g_5}{2}\left(d_{ace}d_{bde} - f_{ace}f_{bde}\right)p_b m_c m_d \\
&+\frac{g_6}{2}d_{abe}d_{cde}p_b m_c m_d - 2g_8 m_a p_b m_b = 0
\end{aligned} \tag{3.94b}$$

Using transformations (3.13) on (3.94a) and expanding it as in (3.9), we may write the lowest order equation for the h_i parameter as

$$\begin{aligned}
&\Delta_i + \frac{h_i}{2}\left(2G + g_1 h^2 + g_4 mh\right) + \frac{g_2}{2}h_i^3 + \\
&+\frac{m_i}{4}\left(3g_3 h_i^2 + g_4 h^2 + \left(g_5+g_6\right)m_i h_i + 4g_7 mh\right) \\
&+\frac{\kappa}{4}t_{ijk}h_j h_k + \kappa_2 t_{ijk}h_j m_k = 0
\end{aligned} \tag{3.95}$$

Here, $h^2 = h_u^2 + h_d^2 + h_s^2$ and $mh = m_u h_u + m_d h_d + m_s h_s$, and there is no summation over index i. The auxiliary Lagrangian can then be written as in (3.16) and the vacuum persistence amplitude as in (3.17).

For the integration over the quark fields, everything is exactly as before, since the quark dependent part of the Lagrangian is the same we had without the mass-dependent interactions. We may then use the result (3.49) for this part of the Euclidean effective bosonized action, so that we may write

$$Z = \int \mathcal{D}\sigma\mathcal{D}\phi e^{\int d^4x^{(E)}\mathcal{L}_r^{st}(\sigma,\phi)+W} \tag{3.96}$$

Proceeding with the analysis, the gap equations are obtained from the σ tadpole term, yielding the exact same relation (3.54), and the effective potential is again defined from the gap equation as in (3.58), but with

$$\begin{aligned} dM_i = &-Gdh_i - \frac{\kappa}{2}t_{ijk}h_j dh_k - \frac{g_1}{2}\left(h^2 dh_i + 2h_i \sum_j h_j dh_j\right) \\ &- \frac{3g_2}{2}h_i^2 dh_i - \kappa_2 t_{ijk} m_j dh_k - \frac{2g_3}{2}m_i h_i dh_i \\ &- \frac{g_4}{2}\left(mhdh_i + h_i \sum_j m_j dh_j + m_i \sum_j h_j dh_j\right) \\ &- \frac{g_5+g_6}{4}m_i^2 dh_i - g_7 m_i \sum_j m_j dh_j \end{aligned} \tag{3.97}$$

This results in an effective potential given by

$$\begin{aligned} dV = d\Bigg[&\frac{G}{4}\sum_i h_i^2 + \frac{\kappa}{2}h_u h_d h_s + \frac{3g_1}{16}\left(\sum_i h_i^2\right)^2 + \frac{3g_2}{16}\sum_i h_i^4 \\ &+ \frac{\kappa_2}{2}\sum_{i\neq j\neq k} m_i h_j h_k + \frac{g_3}{4}\sum_i m_i h_i^3 + \frac{g_4}{4}\sum_i h_i^2 \sum_j m_j h_j \\ &+ \frac{g_5+g_6}{8}\sum_i m_i^2 h_i^2 + \frac{g_7}{4}\left(\sum_i m_i h_i\right)^2 + \frac{3N_c}{8\pi^2}I_{-1}\Bigg] \end{aligned} \tag{3.98}$$

It is often convenient to distinguish between the stationary phase contribution to the effective potential and the quark integral contribution. We may write

$$V = V_{st} + V_q \tag{3.99}$$

with

$$V_{st} = \frac{1}{16}\Bigg[4G\sum_i h_i^2 + 8\kappa h_u h_d h_s + 3g_1\left(\sum_i h_i^2\right)^2 + 3g_2\sum_i h_i^4 + 8\kappa_2\sum_{i\neq j\neq k} m_i h_j h_k + 4g_3\sum_i m_i h_i^3 + 4g_4\sum_i h_i^2\sum_j m_j h_j + 2\left(g_5+g_6\right)\sum_i m_i^2 h_i^2 + 4g_7\left(\sum_i m_i h_i\right)^2\Bigg]\Bigg|_0^{M_i^2} \tag{3.100}$$

and

$$V_q = \frac{3N_c}{8\pi^2} I_{-1} \tag{3.101}$$

3.2.4 Parameter Fitting

In [4], all the kinetic and mass terms for σ and ϕ fields arising in $\mathcal{L}_{bos}$ (3.51) are collected. The kinetic terms are relatively simple,

$$\mathcal{L}_{kin} = \frac{N_c I_1}{16\pi^2}\mathrm{tr}\left[(\partial_\mu\sigma)^2 + (\partial_\mu\phi)^2\right] \tag{3.102}$$

and a comparison with standard Lagrangian kinetic terms imply a rescaling of the fields as

$$\sigma_a = g\sigma_a^R \quad , \quad \phi_a = g\phi_a^R \quad , \quad g^2 = \frac{4\pi^2}{N_c I_1} \tag{3.103}$$

On the other hand, the collection of mass terms is bulky. We can, however, use these terms to adjust the model's parameters by fitting their predicted effective masses to the physical meson spectrum. To that end, it is necessary to rewrite the flavour basis fields σ_a and ϕ_a as charge basis fields

$$\frac{\lambda_a}{\sqrt{2}}\sigma_a = \begin{pmatrix} \frac{\sigma_u}{\sqrt{2}} & a_0^+ & \kappa^+ \\ a_0^- & \frac{\sigma_d}{\sqrt{2}} & \kappa^0 \\ \kappa^- & \bar{\kappa}^0 & \frac{\sigma_s}{\sqrt{2}} \end{pmatrix} \quad , \quad \frac{\lambda_a}{\sqrt{2}}\phi_a = \begin{pmatrix} \frac{\phi_u}{\sqrt{2}} & \pi^+ & K^+ \\ \pi^- & \frac{\phi_d}{\sqrt{2}} & K^0 \\ K^- & \bar{K}^0 & \frac{\phi_s}{\sqrt{2}} \end{pmatrix} \tag{3.104}$$

with the identifications

m_π	m_K	m_η	$m_{\eta'}$	f_π	f_K	m_κ	m_{a_0}	m_{f_0}
138	494	547	958	92	113	850	980	980

TABLE 3.1: Empirical data used in the parameter fitting, with values given in MeV.

$$\phi_u = \phi_3 + \eta_{ns} \quad , \quad \phi_d = -\phi_3 + \eta_{ns} \quad , \quad \phi_s = \sqrt{2}\eta_s \tag{3.105}$$

and similarly for the scalar field. The physical π^0, η and η' states are related with the above by a unitary transformation which depends on the mixing angles. [4] Finally, interaction terms in (3.51) are computed to allow for a fitting of both mixing angles in the scalar and pseudoscalar channels, as well as of decay constants.

There are fourteen parameters to be fixed in the isospin limit: the current masses $m_u = m_d$ and m_s, the couplings G, κ, κ_2, g_1, g_2, g_3, g_4, g_5, g_6, g_7, g_8, and the energy scale Λ. The current quark masses are given as input based on commonly accepted values given in [100], with $m_u = m_d = 4$MeV and $m_s = 100$MeV. The mass ratio relation

$$\frac{M_s}{M_u} = 2\frac{f_K}{f_\pi} - 1 = 1.46 \tag{3.106}$$

is used in conjunction with the mass gap equations (3.54) and the stationary phase conditions (3.95) to fix Λ. The light pseudoscalar mass spectrum (π, K, η and η') , the respective weak decay constants (f_π and f_K), and the scalar mass spectrum (a_0 and f_0), which are experimentally well established, are used to fit some of the parameters as given in table 3.1. A light strange scalar meson κ (or $K_0^*(800)$) is also assumed with mass given in the same table.[3] This leaves three conditions to be able to fix all the parameters. These are provided by the σ meson mass and the two mixing angles θ_s and θ_{ps} in the scalar and pseudoscalar sectors, respectively. From an empirical viewpoint, these values are less well established, opening a considerable range of possible parameterizations using different values and different combinations within the experimental uncertainty. To this respect, four alternative parameterizations have been attempted in [4] for values of m_σ ranging from 550 to 600 MeV, and for mixing angles ranging from -12° to -15° for θ_{ps} and from 25° to 27.5° for θ_s.

The robustness of this parameterization procedure is then verified by using the fixed parameter values in the calculation of other empirical observables, like radiative and strong decay widths. The aforementioned paper [4] then performs a comparative study of four distinct parameter sets and reports on a collection of rather successful predictions

[3] There is a great amount of controversy concerning this state. Its large width makes it hard to pinpoint in experimental results. Moreover, there appear to be some phenomenological analyses in which a corresponding pole emerges in the S-matrix, and others in which this state plays no part. [100]

that are in sensible accordance with empirical data. This wide success in the description of meson spectra and decay widths is unprecedent in NJL-type models, indicating that the mass-dependent interactions do play an important role in the accurate modelling of strongly interacting systems. This is crucial for establishing enough confidence in the model's potential for giving a useful description of the finite temperature and chemical potential regime, which is the main goal in the following section.

Chapter 4

Thermodynamical Analysis and Results

4.1 Finite Temperature and Chemical Potential

In order to further understand the dynamics of many quarks, the study of the response of the system to external parameters, such as the temperature, is due. Furthermore, the number of quarks is not constant. This is described by including chemical potentials as coefficients of the $U_V(1)$ conserved charges' operators $q^\dagger q$. The interpretation of QFT in a thermodynamical sense is then usualy attained by an appropriate identification of the Euclidean vacuum persistence amplitude with the grand canonical partition function. The general formalism for functional calculations at finite temperature has been proposed in [101] by employing Matsubara frequency sums together with periodic or antiperiodic boundary conditions for bosonic or fermionic fields, respectively. Finite-temperature Feynman rules are developed in [102]. A good account of these matters is given in [103] and [104].

In the context of the model described in section 3.2, thermal fluctuations arise from the underlying, more fundamental, quark degrees of freedom. The quark content of the mesonic fields is contained in the heat kernel part of the bosonized effective action (3.49) or, more precisely, in the one-loop integrals J_i defined in (3.46). We follow the approach of [105] to obtain the pertinent quark loop integrals at finite T and μ in the following.

The J_n integrals can be written in a more transparent form as Euclidean four-momentum integrals

$$J_n\left(M_i^2\right) = \int_0^\infty d\tau \tau^n \rho\left(\tau\Lambda^2\right) \int \frac{d^4p}{\pi^2} e^{-\tau\left(M_i^2+p^2\right)}$$
$$= 16\pi^2 \int \frac{d^4p}{\left(2\pi\right)^4} \int_0^\infty d\tau \left[1 - \left(1+\tau\Lambda^2\right) e^{-\tau\Lambda^2}\right] \tau^n e^{-\tau\left(M_i^2+p^2\right)} \tag{4.1}$$

Keeping in mind the relationship (3.60), if suffices to determine the form of, say, $J_0\left(M_i^2\right)$; other J_n integrals may then be found by integration or differentiation with respect to M_i^2. Thus, we have for J_0

$$J_0\left(M_i^2\right) = 16\pi^2 \int \frac{d^4p}{\left(2\pi\right)^4} \int_0^\infty d\tau \left[1 - \left(1+\tau\Lambda^2\right) e^{-\tau\Lambda^2}\right] e^{-\tau\left(M_i^2+p^2\right)}$$
$$= 16\pi^2 \int \frac{d^4p}{\left(2\pi\right)^4} \left[\frac{1}{M_i^2+p^2} - \frac{1}{M_i^2+p^2+\Lambda^2} - \frac{\Lambda^2}{\left(M_i^2+p^2+\Lambda^2\right)^2}\right] \tag{4.2}$$

The Matsubara formalism then introduces the effects of finite temperature T and chemical potential μ through the substitutions [103]

$$\int dp_0 \longrightarrow 2\pi T \sum_{k=-\infty}^{\infty} \qquad , \qquad p_0 \longrightarrow \omega_n - i\mu \qquad , \qquad \omega_n = \left(2n+1\right)\pi T \tag{4.3}$$

We may then write

$$J_0\left(M_i^2, T, \mu\right) = 16\pi^2 T \int \frac{d^3\vec{p}}{\left(2\pi\right)^3} \sum_{n=-\infty}^{+\infty} \left\{ \frac{1}{\left(\omega_n - i\mu\right)^2 + E_p^2} \right.$$
$$\left. - \frac{1}{\left(\omega_n - i\mu\right)^2 + E_{p\Lambda}^2} - \frac{\Lambda^2}{\left[\left(\omega_n - i\mu\right)^2 + E_{p\Lambda}^2\right]^2} \right\} \tag{4.4}$$

with

$$E_p^2 = \left|\vec{p}\right|^2 + M_i^2 \qquad , \qquad E_{p\Lambda}^2 = \left|\vec{p}\right|^2 + M_i^2 + \Lambda^2 \tag{4.5}$$

The infinite sums in the expression above are more easily evaluated in the form

$$\sum_{n=-\infty}^{+\infty} \frac{1}{(\omega_n - i\mu)^2 + E_{p(\Lambda)}^2} = \frac{1}{4\pi^2 T^2} \sum_{n=-\infty}^{+\infty} \frac{1}{\left(n + a_{(\Lambda)}\right)\left(n + b_{(\Lambda)}\right)}$$
$$= \frac{1}{4\pi^2 T^2} \frac{1}{b_{(\Lambda)} - a_{(\Lambda)}} \sum_{n=-\infty}^{+\infty} \left[\frac{1}{n + a_{(\Lambda)}} - \frac{1}{n + b_{(\Lambda)}}\right] \tag{4.6}$$

and

$$\sum_{n=-\infty}^{+\infty} \frac{\Lambda^2}{\left[(\omega_n - i\mu)^2 + E_{p\Lambda}\right]^2} = \frac{\Lambda^2}{16\pi^4 T^4} \sum_{n=-\infty}^{+\infty} \frac{1}{(n + a_\Lambda)^2 (n + b_\Lambda)^2}$$
$$= \frac{\Lambda^2}{16\pi^4 T^4} \left\{ \frac{2}{(a_\Lambda - b_\Lambda)^3} \sum_{n=-\infty}^{+\infty} \left[\frac{1}{n + a_\Lambda} - \frac{1}{n + b_\Lambda}\right] \right.$$
$$\left. + \frac{1}{(a_\Lambda - b_\Lambda)^2} \sum_{n=-\infty}^{+\infty} \left[\frac{1}{(n + a_\Lambda)^2} + \frac{1}{(n + b_\Lambda)^2}\right] \right\} \tag{4.7}$$

with

$$a_{(\Lambda)} = \frac{1}{2} - \frac{i}{2\pi T}\left(\mu + E_{p(\Lambda)}\right)$$
$$b_{(\Lambda)} = \frac{1}{2} - \frac{i}{2\pi T}\left(\mu - E_{p(\Lambda)}\right) \tag{4.8}$$

We may now use the summation formulae

$$\sum_{k=-\infty}^{\infty} \frac{1}{k + a} = \pi \cot(\pi a) \qquad , \qquad \sum_{k=-\infty}^{\infty} \frac{1}{(k + a)^2} = \pi^2 \csc^2(\pi a) \tag{4.9}$$

to evaluate (4.6) as

$$\frac{1}{4\pi^2 T^2} \frac{1}{b_{(\Lambda)} - a_{(\Lambda)}} \sum_{n=-\infty}^{\infty} \left[\frac{1}{\left(n + a_{(\Lambda)}\right)} - \frac{1}{\left(n + b_{(\Lambda)}\right)}\right] =$$
$$= \frac{1}{4iTE_{p(\Lambda)}} \left[\cot\left(\frac{\pi}{2} - \frac{i}{2T}\left(\mu + E_{p(\Lambda)}\right)\right) - \cot\left(\frac{\pi}{2} - \frac{i}{2T}\left(\mu - E_{p(\Lambda)}\right)\right)\right]$$
$$= \frac{1}{4iTE_{p(\Lambda)}} \left[\tan\left(\frac{i}{2T}\left(\mu + E_{p(\Lambda)}\right)\right) - \tan\left(\frac{i}{2T}\left(\mu - E_{p(\Lambda)}\right)\right)\right] \tag{4.10}$$

and (4.7) as

$$\begin{aligned}
&\frac{\Lambda^2}{16\pi^4T^4}\left\{\frac{2}{(a_\Lambda-b_\Lambda)^3}\sum_{n=-\infty}^{+\infty}\left[\frac{1}{n+a_\Lambda}-\frac{1}{n+b_\Lambda}\right]\right.\\
&\left.+\frac{1}{(a_\Lambda-b_\Lambda)^2}\sum_{n=-\infty}^{+\infty}\left[\frac{1}{(n+a_\Lambda)^2}+\frac{1}{(n+b_\Lambda)^2}\right]\right\}=\\
&=\frac{\Lambda^2}{8iTE_{p\Lambda}^3}\left[\cot\left(\frac{\pi}{2}-\frac{i}{2T}\left(\mu+E_{p\Lambda}\right)\right)-\cot\left(\frac{\pi}{2}-\frac{i}{2T}\left(\mu-E_{p\Lambda}\right)\right)\right]\\
&-\frac{\Lambda^2}{16T^2E_{p\Lambda}^2}\left[\csc^2\left(\frac{\pi}{2}-\frac{i}{2T}\left(\mu+E_{p\Lambda}\right)\right)+\csc^2\left(\frac{\pi}{2}-\frac{i}{2T}\left(\mu-E_{p\Lambda}\right)\right)\right]\\
&=\frac{\Lambda^2}{8iTE_{p\Lambda}^3}\left[\tan\left(\frac{i}{2T}\left(\mu+E_{p\Lambda}\right)\right)-\tan\left(\frac{i}{2T}\left(\mu-E_{p\Lambda}\right)\right)\right]\\
&-\frac{\Lambda^2}{16T^2E_{p\Lambda}^2}\left[\sec^2\left(\frac{i}{2T}\left(\mu+E_{p\Lambda}\right)\right)+\sec^2\left(\frac{i}{2T}\left(\mu-E_{p\Lambda}\right)\right)\right]
\end{aligned}\tag{4.11}$$

In the last lines we have used

$$\cot\left(\frac{\pi}{2}-\theta\right)=\tan\theta\qquad,\qquad\csc\left(\frac{\pi}{2}-\theta\right)=\sec\theta\tag{4.12}$$

Finally, using the relation between regular and hyperbolic trigonometric functions, we may write

$$\begin{aligned}
&\sum_{n=-\infty}^{+\infty}\left\{\frac{1}{(\omega_n-i\mu)^2+E_p^2}-\frac{1}{(\omega_n-i\mu)^2+E_{p\Lambda}^2}-\frac{\Lambda^2}{\left[(\omega_n-i\mu)^2+E_{p\Lambda}^2\right]^2}\right\}=\\
&=\frac{1}{4TE_p}\left[\tanh\left(\frac{\mu+E_p}{2T}\right)-\tanh\left(\frac{\mu-E_p}{2T}\right)\right]\\
&-\frac{1}{4TE_{p\Lambda}}\left[\tanh\left(\frac{\mu+E_{p\Lambda}}{2T}\right)-\tanh\left(\frac{\mu-E_{p\Lambda}}{2T}\right)\right]\\
&-\frac{\Lambda^2}{8TE_{p\Lambda}^3}\left[\tanh\left(\frac{\mu+E_{p\Lambda}}{2T}\right)-\tanh\left(\frac{\mu-E_{p\Lambda}}{2T}\right)\right]\\
&+\frac{\Lambda^2}{16T^2E_{p\Lambda}^2}\left[\operatorname{sech}^2\left(\frac{\mu+E_{p\Lambda}}{2T}\right)+\operatorname{sech}^2\left(\frac{\mu-E_{p\Lambda}}{2T}\right)\right]
\end{aligned}\tag{4.13}$$

We can now use (4.13) in (4.4) to write

$$
\begin{aligned}
J_0\left(M_i^2,T,\mu\right) = 4\pi^2 \int \frac{d^3\vec{p}}{(2\pi)^3} \Bigg\{ & \frac{1}{E_p}\left[\tanh\left(\frac{\mu+E_p}{2T}\right) - \tanh\left(\frac{\mu-E_p}{2T}\right)\right] \\
& - \frac{1}{E_{p\Lambda}}\left[\tanh\left(\frac{\mu+E_{p\Lambda}}{2T}\right) - \tanh\left(\frac{\mu-E_{p\Lambda}}{2T}\right)\right] \\
& - \frac{\Lambda^2}{2E_{p\Lambda}^3}\left[\tanh\left(\frac{\mu+E_{p\Lambda}}{2T}\right) - \tanh\left(\frac{\mu-E_{p\Lambda}}{2T}\right)\right] \\
& + \frac{\Lambda^2}{4TE_{p\Lambda}^2}\left[\operatorname{sech}^2\left(\frac{\mu+E_{p\Lambda}}{2T}\right) + \operatorname{sech}^2\left(\frac{\mu-E_{p\Lambda}}{2T}\right)\right]\Bigg\} \\
= 4\int_0^\infty d\left|\vec{p}\right|\left|\vec{p}\right|^2 \Bigg\{ & \frac{1}{E_p}\left(1-n_{\bar{p}}-n_q\right) - \frac{1}{E_{p\Lambda}}\left(1+\frac{\Lambda^2}{2E_{p\Lambda}^2}\right)\left(1-n_{\bar{p}\Lambda}-n_{q\Lambda}\right) \\
& + \frac{\Lambda^2}{2TE_{p\Lambda}^2}\left(n_{\bar{p}\Lambda}+n_{q\Lambda}-n_{\bar{p}\Lambda}^2-n_{q\Lambda}^2\right)\Bigg\}
\end{aligned}
\tag{4.14}
$$

with

$$
n_{\bar{q}(\Lambda),q(\Lambda)} = \frac{1}{1+e^{\frac{E_{p(\Lambda)}\pm\mu}{T}}} = \frac{1}{2}e^{-\frac{E_{p(\Lambda)}\pm\mu}{2T}}\operatorname{sech}\left(\frac{E_{p(\Lambda)}\pm\mu}{2T}\right) \tag{4.15}
$$

In expression (4.14), we can clearly distinguish the contributions arising from the vacuum (T-independent terms) from those of the medium (T-dependent terms). We can write

$$
\begin{aligned}
J_0\left(M_i^2,T,\mu\right) &= J_0^{vac}\left(M_i^2\right) + J_0^{med}\left(M_i^2,T,\mu\right) \\
J_0^{vac}\left(M_i^2\right) &= 4\int_0^\infty d\left|\vec{p}\right|\left|\vec{p}\right|^2\left\{\frac{1}{E_p} - \frac{1}{E_{p\Lambda}} - \frac{\Lambda^2}{2E_{p\Lambda}^3}\right\} \\
&= \Lambda^2 - M_i^2\ln\left(1+\frac{\Lambda^2}{M_i^2}\right) \\
J_0^{med}\left(M_i^2,T,\mu\right) &= -4\int_0^\infty d\left|\vec{p}\right|\left|\vec{p}\right|^2\left\{\frac{n_{\bar{q}}+n_q}{E_p} - \frac{n_{\bar{q}\Lambda}+n_{q\Lambda}}{E_{p\Lambda}}\left(1+\frac{\Lambda^2}{2E_{p\Lambda}^2}\right)\right. \\
&\quad \left. - \frac{\Lambda^2}{2TE_{p\Lambda}^2}\left(n_{\bar{q}\Lambda}+n_{q\Lambda}-n_{\bar{q}\Lambda}^2-n_{q\Lambda}^2\right)\right\}
\end{aligned}
\tag{4.16}
$$

As can be seen, J_0^{vac} is, as it should, exactly equivalent to the expression we have already given for $J_0\left(M_i^2\right)$ in (3.48b), confirming its identification as the vacuum contribution. Furthermore, it is not difficult to show that

$$
\lim_{T,\mu\to 0} J_0^{med}\left(M_i^2,T,\mu\right) = 0 \qquad \Rightarrow \qquad \lim_{T,\mu\to 0} J_0\left(M_i^2,T,\mu\right) = J_0^{vac}\left(M_i^2\right) \tag{4.17}
$$

since

$$\lim_{T,\mu\to 0} n_{q(\Lambda),\bar{q}(\Lambda)} = 0 \qquad , \qquad \lim_{T,\mu\to 0} \frac{n_{q(\Lambda),\bar{q}(\Lambda)}}{T} = 0 \tag{4.18}$$

The distinction between vacuum and medium contributions is therefore well justified. One should stress, however, that at finite T and μ the values of M_i vary accordingly in the vacuum contribution.

4.1.1 Thermodynamical State Functions and the Gap Equation

We now use our results for $J_0\left(M_i^2, T, \mu\right)$ in order to obtain $J_{-1}\left(M_i^2, T, \mu\right)$, which enters the expression for the effective potential (3.99). Using (3.60) and (4.16), we can similarly write the expressions for the vacuum and the medium contributions to $J_{-1}\left(M_i^2, T, \mu\right)$. We have

$$\begin{aligned}
J_{-1}\left(M_i^2, T, \mu\right) &= J_{-1}^{vac}\left(M_i^2\right) + J_{-1}^{med}\left(M_i^2, T, \mu\right) \\
J_{-1}^{vac}\left(M_i^2\right) &= -\int_0^{M_i^2} dM_i^2 \left[\Lambda^2 - M_i^2 \ln\left(1 + \frac{\Lambda^2}{M_i^2}\right)\right] \\
&= -\frac{1}{2}\left[M_i^2\Lambda^2 - M_i^4 \ln\left(1 + \frac{\Lambda^2}{M_i^2}\right) + \Lambda^4 \ln\left(1 + \frac{M_i^2}{\Lambda^2}\right)\right] \\
J_{-1}^{med}\left(M_i^2, T, \mu\right) &= 4\int_0^{\infty} d\left|\vec{p}\right| \left|\vec{p}\right|^2 \int_0^{M_i^2} dM_i^2 \left\{\frac{n_{\bar{q}} + n_q}{E_p} - \frac{n_{\bar{q}\Lambda} + n_{q\Lambda}}{E_{p\Lambda}}\left(1 + \frac{\Lambda^2}{2E_{p\Lambda}^2}\right)\right. \\
&\quad \left. - \frac{\Lambda^2}{2TE_{p\Lambda}^2}\left(n_{\bar{q}\Lambda} + n_{q\Lambda} - n_{\bar{q}\Lambda}^2 - n_{q\Lambda}^2\right)\right\} \\
&= 8\int_0^{\infty} d\left|\vec{p}\right| \left|\vec{p}\right|^2 \left\{2\left(E_p + E_{p\Lambda 0} - E_{p0} - E_{p\Lambda}\right) + T\ln\left(\frac{n_q n_{\bar{q}} n_{q\Lambda 0} n_{\bar{q}\Lambda 0}}{n_{q0} n_{\bar{q}0} n_{q\Lambda} n_{\bar{q}\Lambda}}\right)\right. \\
&\quad \left. + \frac{\Lambda^2}{2}\left(\frac{n_{q\Lambda} + n_{\bar{q}\Lambda}}{E_{p\Lambda}} - \frac{n_{q\Lambda 0} + n_{\bar{q}\Lambda 0}}{E_{p\Lambda 0}}\right)\right\}
\end{aligned} \tag{4.19}$$

In these and subsequent expressions, the additional 0 subscript is to be understood as an instruction to set $M_i^2 = 0$ in the original expression. Once again, using (4.18) and

$$\lim_{T,\mu\to 0} T\ln\left(\frac{n_q n_{\bar{q}} n_{q\Lambda 0} n_{\bar{q}\Lambda 0}}{n_{q0} n_{\bar{q}0} n_{q\Lambda} n_{\bar{q}\Lambda}}\right) = -2\left(E_p + E_{p\Lambda 0} - E_{p0} - E_{p\Lambda}\right) \tag{4.20}$$

it is easy to show that

$$\lim_{T,\mu\to 0} J_{-1}^{med}\left(M_i^2,T,\mu\right)=0 \Rightarrow \lim_{T,\mu\to 0} J_{-1}\left(M_i^2,T,\mu\right)=J_{-1}^{vac}\left(M_i^2\right) \tag{4.21}$$

We have not yet explicitly shown the different chemical potentials μ_i, but as we have noted already, these are associated with the conserved flavour $U(1)_V$ charges, one for each quark flavour. Since the quark loop integrals $J_n\left(M_i^2\right)$ are defined for decoupled flavours i, we should in fact understand the μ appearing in the previous expressions as the i flavour chemical potential μ_i. The thermodynamical potential may then be written from (3.99), (3.100), (3.101) and (4.19) as

$$\Omega\left(T,\mu_u,\mu_d,\mu_s\right)=V_{st}+\frac{N_c}{8\pi^2}\sum_i J_{-1}\left(M_i^2,T,\mu_i\right)+C\left(T,\mu_u,\mu_d,\mu_s\right) \tag{4.22}$$

Here, $C\left(T,\mu_u,\mu_d,\mu_s\right)$ is an M_i-independent term (remember that V is calculated in (3.99) as an integral over M_i of the gap equation, and is always defined up to an M_i-independent term) that may be fixed by imposing some physical condition on the asymptotic behaviour of Ω or of other thermodynamical state functions. In [105], this term is determined by requiring consistency with the standard NJL approach, in particular by the condition that the medium contribution to the thermodynamical potential in both approaches must coincide in the absence of a regulator; it is given in the limit of vanishing μ_i as

$$C\left(T,\mu_u,\mu_d,\mu_s\right)=C\left(T\right)=-\frac{7N_c}{60}\pi^2T^4 \tag{4.23}$$

Similarly, we can rewrite the gap equation for the case of finite temperature and chemical potential. From (3.54) and (4.16), we get

$$h_i+\frac{N_c}{2\pi^2}M_iJ_0\left(M_i^2,T,\mu_i\right)=0 \tag{4.24}$$

The thermodynamical potential (4.22) corresponds to the grand or Landau potential of Statistical Mechanics [103], and thermodynamical averages for the state functions are expressible through the usual relationships. First, it should be remarked that the mean pressure p is just $-\Omega$. The mean entropy density s and the mean quark number densities ρ_i are given by

$$s=\frac{\partial p}{\partial T} \quad , \quad \rho_i=\frac{\partial p}{\partial \mu_i} \tag{4.25}$$

while the mean energy density ε is given by

$$\varepsilon = -p + Ts + \sum_i \mu_i \rho_i \tag{4.26}$$

4.2 Dynamical Masses and Phase Transitions

We have established the main equations for the finite temperature and chemical potential study of the model, namely the stationary phase conditions (3.95) (which remain the same as without T or μ), the gap equations (4.24), the thermodynamical potential (4.22) and the finite temperature quark integrals (4.16) and (4.19). With these, we are equipped to scrutinate the thermodynamical features of the model. Such a finite temperature study of NJL-type models has been presented or reviewed in some of the already mentioned publications, like [53] and [55]. A review of the QCD phase diagram may be found in [106].

Here we present for the first time the calculation of the thermodynamic potential subject to the explicit symmetry breaking terms of the extended Lagrangian discussed in section 3.

4.2.1 Constituent Mass Profiles

We start by studying the solutions to the gap equations (4.24), with the h_i determined self-consistently through the stationary phase conditions (3.95). We assume $\mu_u = \mu_d = \mu_s = \mu$, and we work in the isospin limit $m_u = m_d \neq m_s$. With these assumptions, we have a coupled system of four equations to solve for the constituent quark masses $M_u\,(= M_d)$ and M_s

G	κ	κ_2	g_1	g_2	g_3	g_4	g_5	g_6	g_7	g_8	Λ
9.834	-122.9	6.189	4436.7	211.0	-6647	1529	215.4	-1666	29.81	-63.20	0.8275
f_π	f_K	θ_{ps}	θ_s	m_π	m_K	m_η	$m_{\eta'}$	m_{a_0}	$m_{K^\star}$	m_σ	m_{f_0}
92	113	-12	27.5	138	494	547	958	980	850	500	980

TABLE 4.1: Parameter set of the model (first row), given in the following units: $[\Lambda] =$ MeV, $[G] = \text{GeV}^{-2}$, $[\kappa_2] = \text{GeV}^{-3}$, $[g_5] = [g_6] = [g_7] = [g_8] = \text{GeV}^{-4}$, $[\kappa] = \text{GeV}^{-5}$, $[g_3] = [g_4] = \text{GeV}^{-6}$, $[g_1] = [g_2] = \text{GeV}^{-8}$; the current quark masses values $m_u = m_d =$ 4 MeV, $m_s = 100$ MeV and the empirical input (second row) is used for their fitting (meson masses and weak decays in MeV). From the self-consistent resolution of the gap equations we obtain $M_u = M_d = 375$ MeV, $M_s = 546$ MeV for the constituent quark masses at $T, \mu = 0$. θ_{ps}, θ_s are the mixing angles in degrees in the pseudoscalar and scalar sectors, respectively.

$$
\begin{aligned}
h_u &= -\frac{N_c}{2\pi^2} M_u J_0\left(M_u^2, T, \mu\right) \\
h_s &= -\frac{N_c}{2\pi^2} M_s J_0\left(M_s^2, T, \mu\right) \\
M_u &= m_u - \frac{h_u}{2}\left(2G + g_1 h^2 + g_4 mh\right) - \frac{g_2}{2} h_u^3 \\
&\quad - \frac{m_u}{4}\left(3g_3 h_u^2 + g_4 h^2 + (g_5 + g_6)\, m_u h_u + 4g_7 mh\right) \\
&\quad - \frac{\kappa}{2} h_u h_s - \kappa_2\left(h_u m_s + h_s m_u\right) \\
M_s &= m_s - \frac{h_s}{2}\left(2G + g_1 h^2 + g_4 mh\right) - \frac{g_2}{2} h_s^3 + \\
&\quad - \frac{m_s}{4}\left(3g_3 h_s^2 + g_4 h^2 + (g_5 + g_6)\, m_s h_s + 4g_7 mh\right) \\
&\quad - \frac{\kappa}{2} h_u^2 - 2\kappa_2 h_u m_u = 0
\end{aligned}
\tag{4.27}
$$

with $h^2 = 2h_u^2 + h_s^2$ and $mh = 2m_u h_u + m_s h_s$. As stated in section 3.1.5, where the effective potential is obtained from the gap equations, solving the gap equation amounts to finding the extrema of the thermodynamical potential (4.22). Of these, only those solutions that minimize (4.22) correspond to thermodynamical equilibrium solutions, i.e., to the stable physical states.

The system (4.27) is solved numerically for given values of T and μ. The system is implemented in *Mathematica*® and the parameter set of table 4.1 is used. A series of mass profiles at fixed chemical potential μ are shown in figures 4.2 to 4.11.

It is interesting to inspect how the mass profiles change as μ is raised. Figure 4.2 is the starting point with $\mu = 0$. There, the prototypical mass profile is visible, with an essentially constant high constituent mass plateau for low T, followed by a smooth crossover to lower mass values which becomes more pronounced at $T \sim 150 MeV$. This crossover is significantly steeper for the light quark masses than it is for the strange

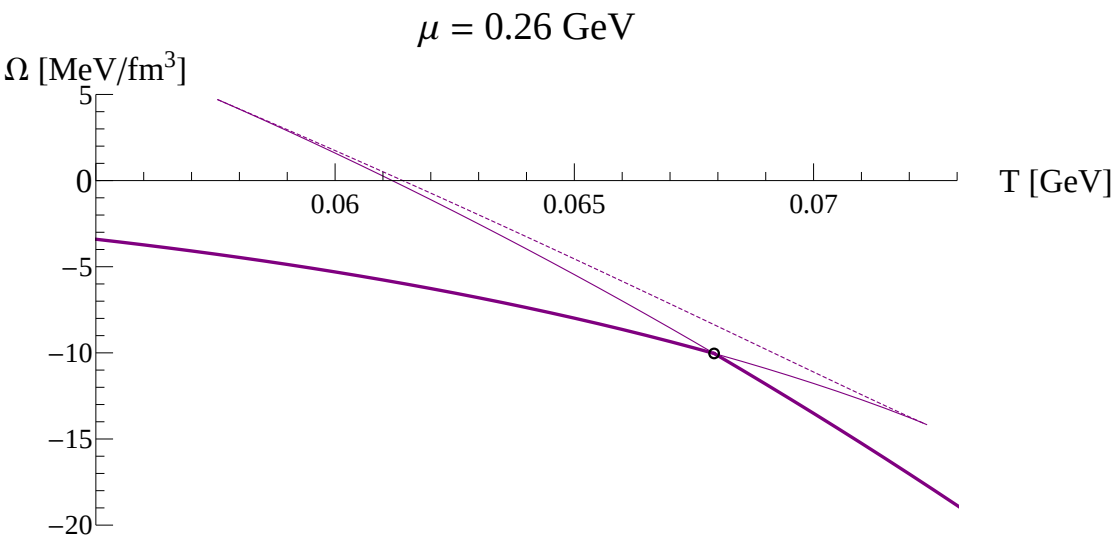

FIGURE 4.1: Thermodynamical potential at $\mu = 260$MeV.

quark mass, the latter decreasing more slowly and in what appears to be a two-step transition. In other words, there seems to be a first crossover between 100 MeV and 160 Mev associated with a pronounced decrease in the light quark masses and a slight decrease in the strange quark mass, followed closely by a second crossover in which the most significant decrease of the strange quark mass is seen. This pattern is maintained for higher chemical potential values, with the crossover regions progressively moving to lower temperatures and becoming steeper.

At some point, this pattern evolves into something else: a region begins to emerge where three solution branches overlap over some temperature domain. In order to ascertain the physical nature of these solution branches, we need to determine to which kind of extrema of the thermodynamical potential do they correspond. We find that the upper and lower branches correspond to minima, while the middle branch contains solutions that are maxima of the thermodynamical potential, and are therefore unstable. In figure 4.1, a plot of Ω is shown in the overlap region for $\mu = 260$MeV. The critical point of transition between the upper and lower branches is given by the intersection of the branches in the Ω plot. We can see that, to the left of this intersection point, the first branch lies lower than the second branch, and that to the right of the intersection they switch. Those portions of a branch that lie above the other branch are local minima of the thermodynamical potential and correspond to metastable solutions, while the lower lying portions represent the actual global minima and are, therefore, the stable physical solutions.

This feature is first visible in figure 4.6 for $\mu = 200$MeV, and it signals the onset of a first-order transition in the quark masses driven by a thermal restoration of chiral symmetry. In figures 4.6 to 4.9, we can see that the mass profiles get ever more distorted as the

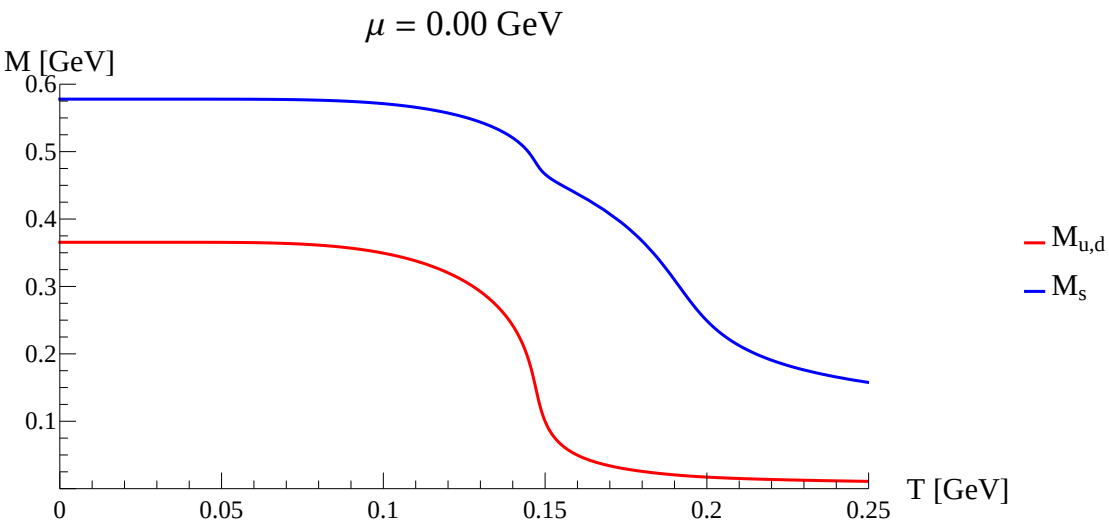

FIGURE 4.2: Mass profile at $\mu = 0$.

chemical potential is increased, with the overlapping regions becoming progressively larger. In these figures, the thick lines represent stable solutions, the thin lines represent metastable solutions, and the dashed lines represent unstable solutions. Also, the sharp first-order transitions are marked with a black dashed line connecting two circles which point out the mass values for which the jump occurs.

That chiral symmetry is approximately restored[1] can be understood by looking at figure 4.12, where the value of the condensates, which are the order parameters for chiral transitions, is shown for $\mu = 260$MeV. We can clearly see the light quark condensates (red line) jumping to values which get rapidly close to zero. A null condensate indicates a transition from the dynamically broken Nambu-Goldstone phase to the chirally symmetric Wigner-Weyl phase. Moreover, in figure 4.8, the light quark dynamical masses are seen to drop to values increasingly close to their current masses, with almost no dynamical contribution from the condensates.

There is yet another interesting feature: the emergence of a second first-order transition after $\mu \sim 300$MeV. This is almost exclusively noticeable for the strange quark mass, since the light quarks have already undergone a bulk decrease in mass in this chemical potential region. This second transition is illustrated in figures 4.10 and 4.11. The quark condensates are shown for $\mu = 350$MeV in figure 4.13, where a large jump in the strange quark condensate is visible.

[1] This restoration is only asymptotic, and it is much more significant for the light quarks than it is for the strange.

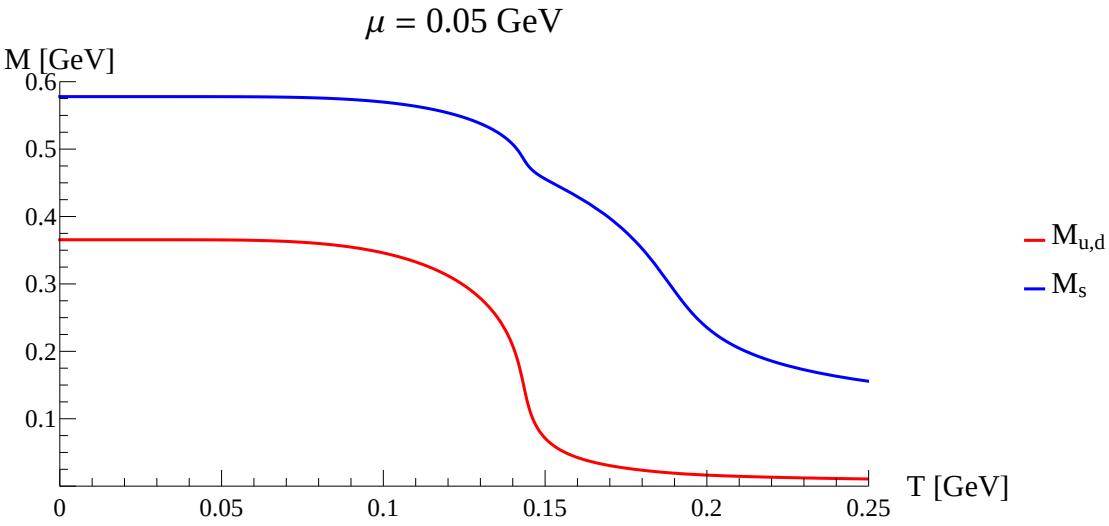

FIGURE 4.3: Mass profile at $\mu = 50$ MeV.

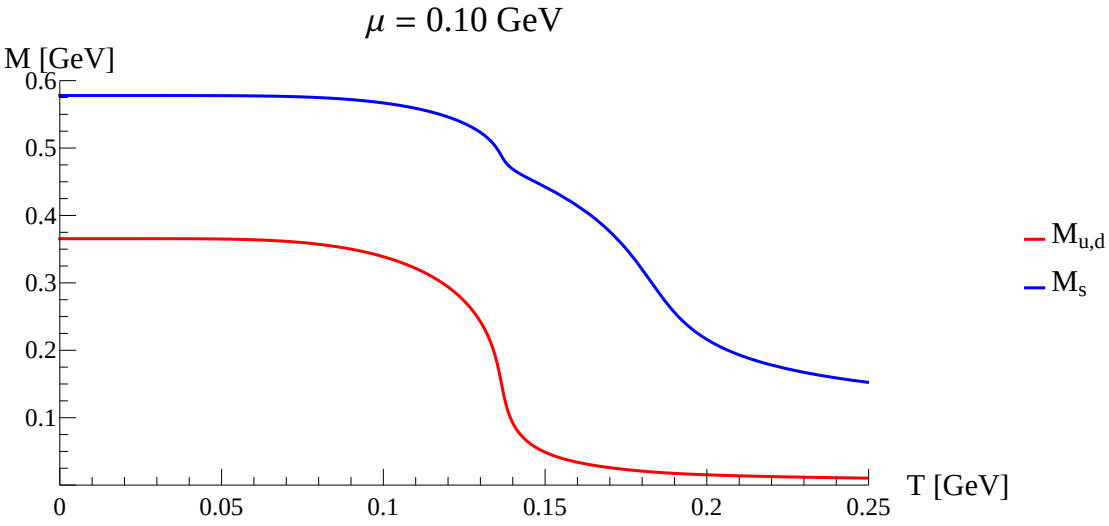

FIGURE 4.4: Mass profile at $\mu = 100$ MeV.

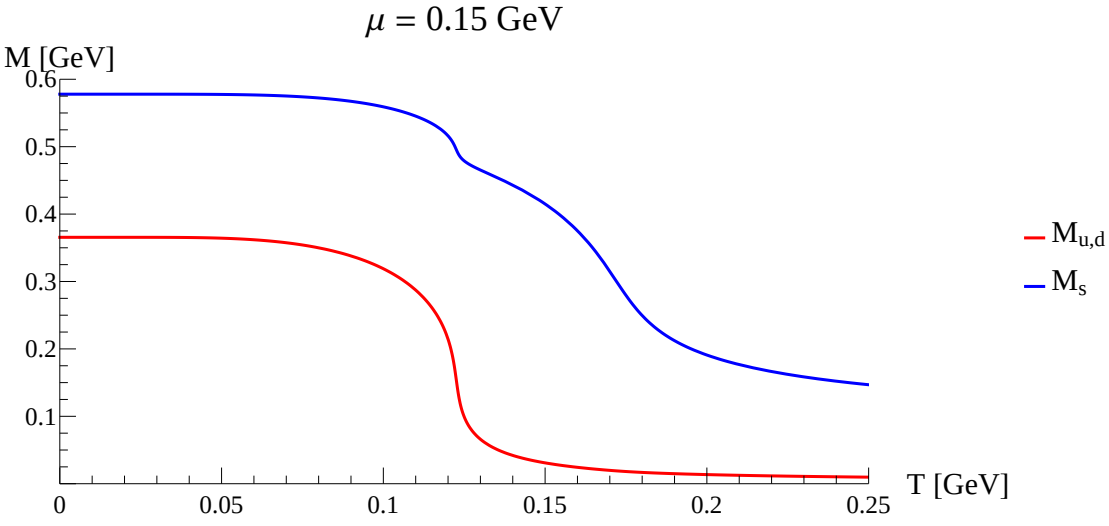

FIGURE 4.5: Mass profile at $\mu = 150$ MeV.

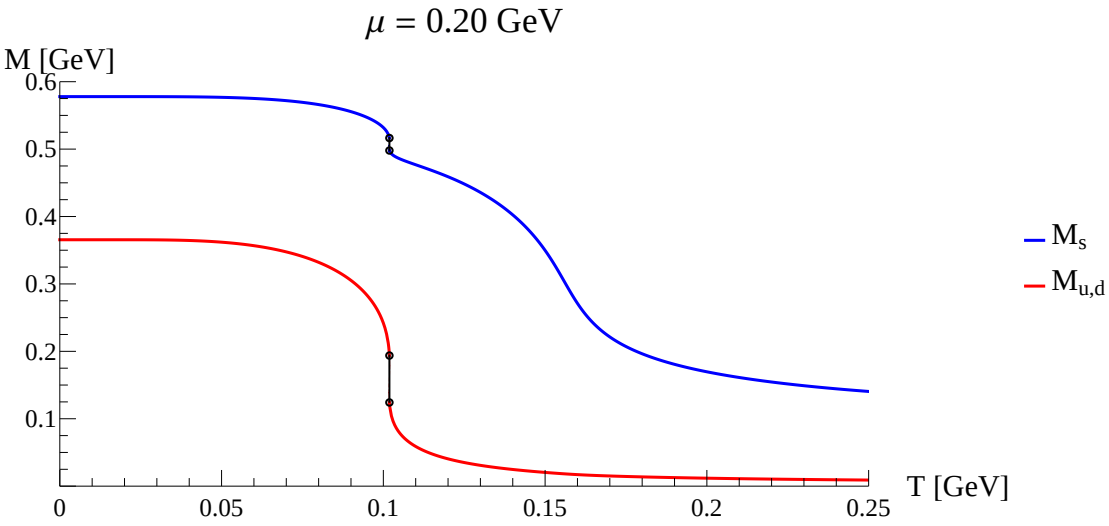

FIGURE 4.6: Mass profile at $\mu = 200$ MeV.

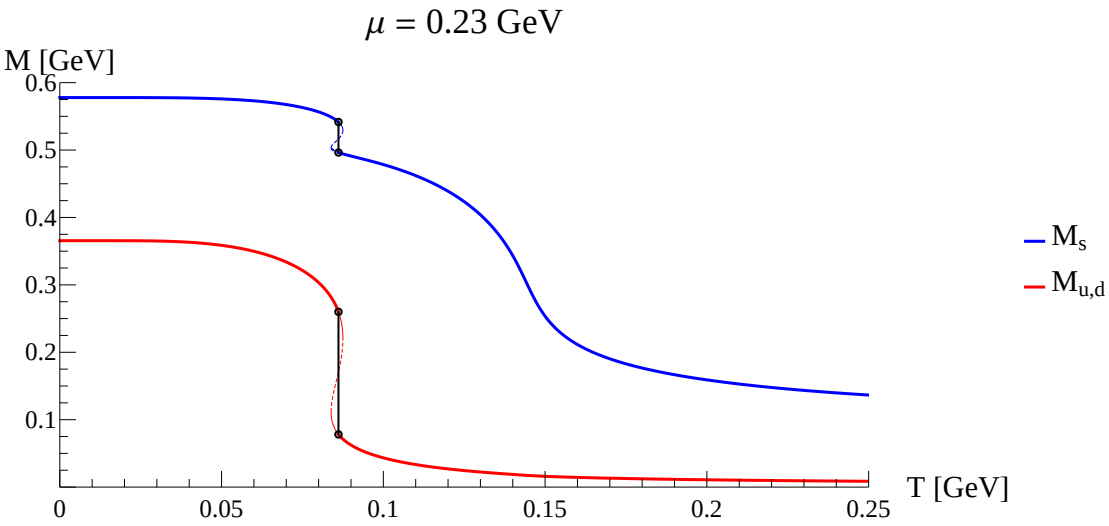

FIGURE 4.7: Mass profile at $\mu = 230$ MeV.

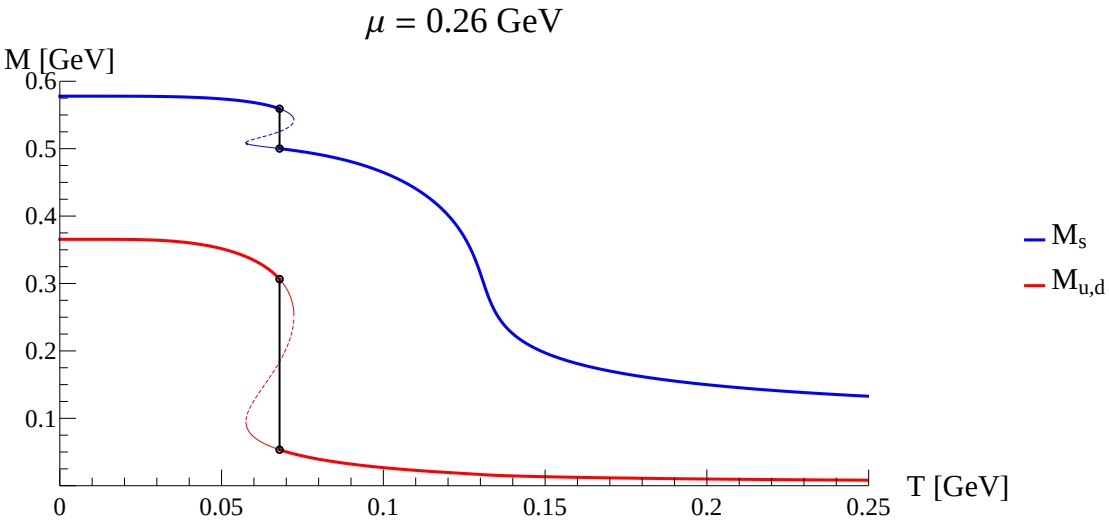

FIGURE 4.8: Mass profile at $\mu = 260$ MeV.

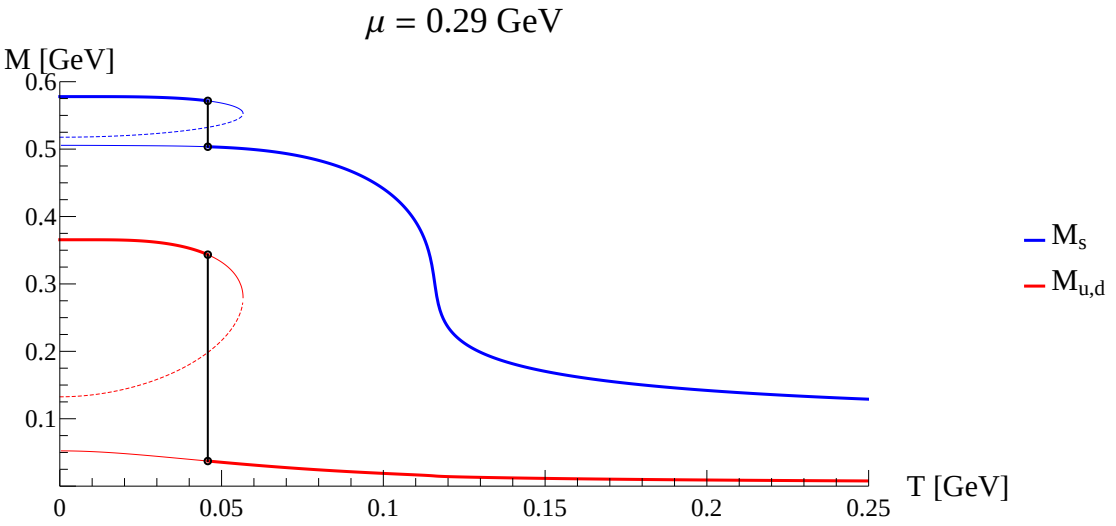

FIGURE 4.9: Mass profile at $\mu = 290$ MeV.

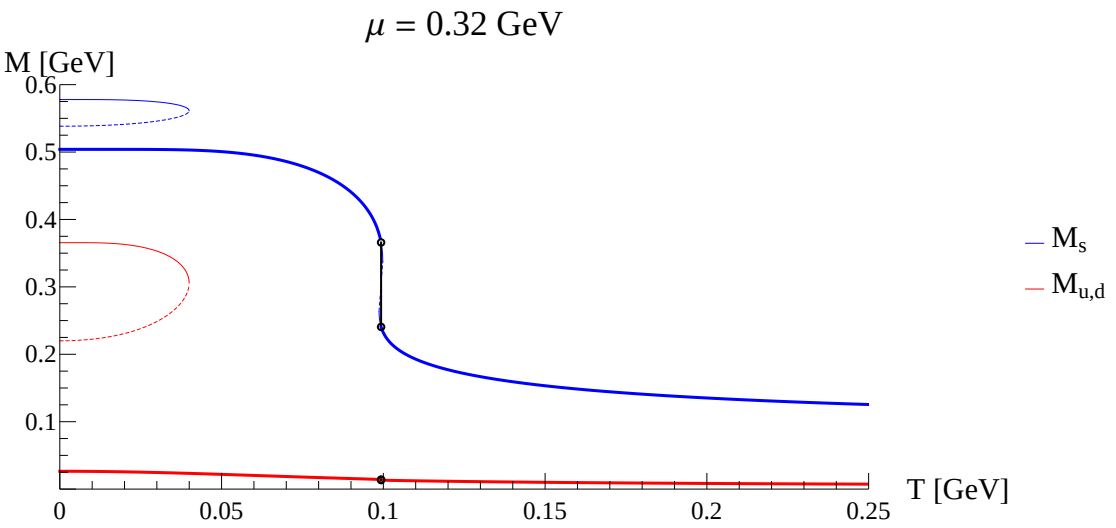

FIGURE 4.10: Mass profile at $\mu = 320$ MeV.

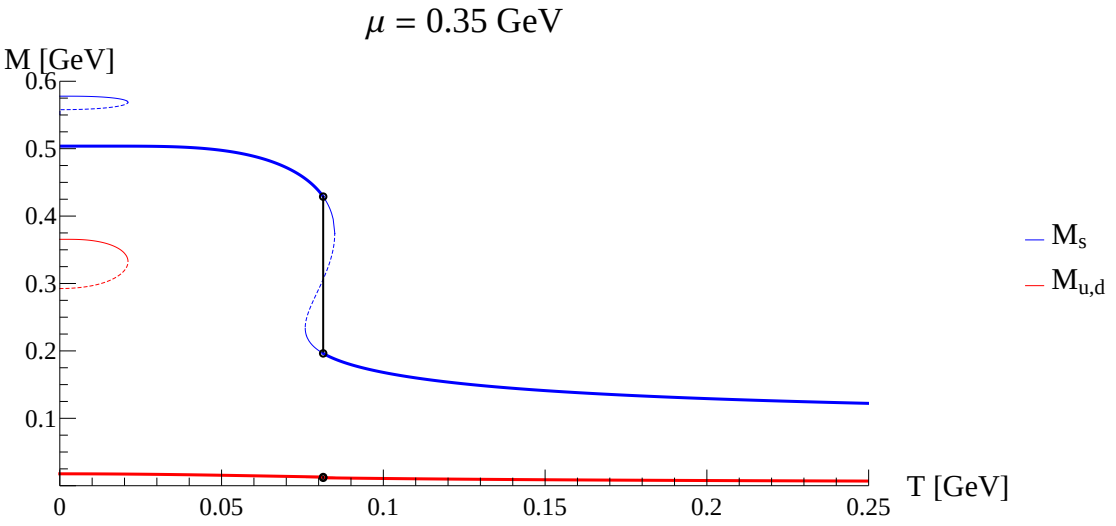

FIGURE 4.11: Mass profile at $\mu = 350$ MeV.

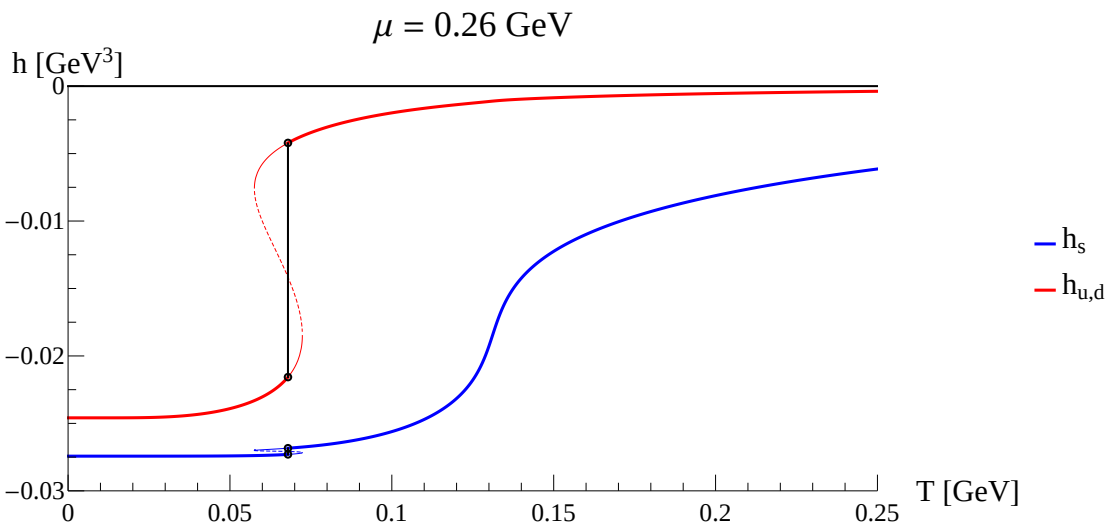

FIGURE 4.12: Quark condensates at $\mu = 260$ MeV.

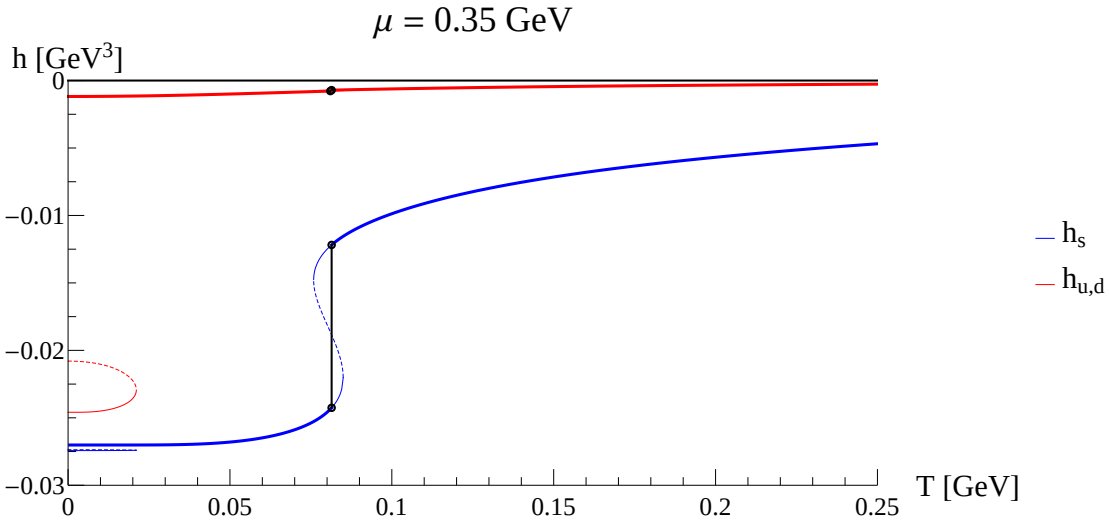

FIGURE 4.13: Quark condensates at $\mu = 350$ MeV.

4.2.2 Phase Diagram

Using the results from the mass profiles, we can determine the phase diagram of the model in the $\mu - T$ plane. This is done in figure 4.14, where two first-order transition boundaries are shown in thick lines, and with crossover regions represented as dashed lines. The crossover curves are determined from the points of maximal slope of $M(T)$. The two critical endpoints are marked with a circle. The results from the previous section allow us to identify the first line with a transition in the light quarks and the second line with the strange quarks. Of course, because the system is coupled, i.e., there are flavour mixing interaction terms in the Lagrangian, the masses of all the quarks jump down at the transition, although the jump is much more pronounced for light quarks in the first one and for strange quarks in the second.

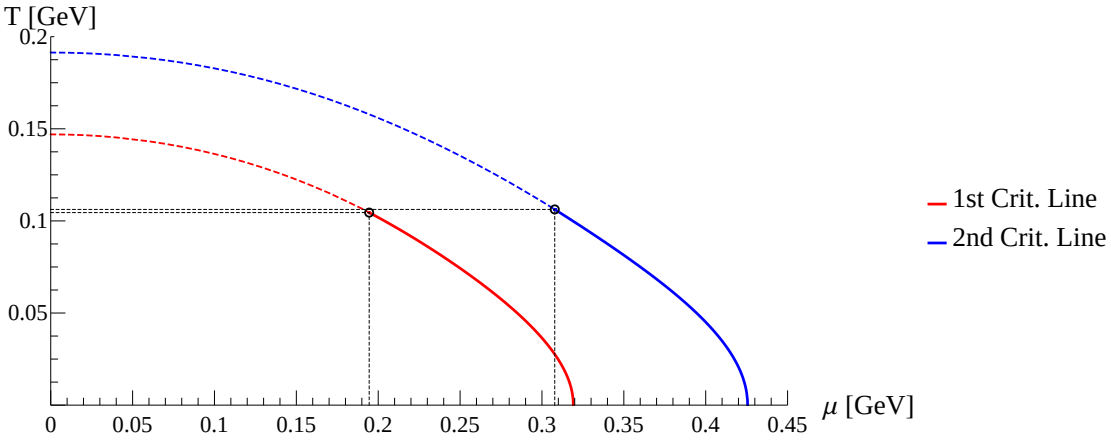

FIGURE 4.14: Phase diagram.

Data relative to some of the noteworthy points in the phase diagram is displayed is table 4.2. The closeness of the two CEP temperatures might catch the eye, but calculations performed with slightly different parameter sets (namely those given in [4]) show different vertical spacings for the two CEPs. In view of this, no special significance appears to exist in this feature, although it is not absolutely clear.

The existence of two first-order boundaries and hence two CEPs in this model makes it harder to make meaningful comparisons with results from other sources. Nevertheless, it is interesting to compare some of the values we obtained with those predicted in lattice calculations. For instance, in the review paper [106], a range between 150 and 200 MeV is reported as the likely range for the pseudocritical temperature at $\mu = 0$. The values obtained in the present work are more or less compatible with this range. For larger values of μ, lattice methods run into several problems[2] [107], and the reliability of the results is highly debated. Still, the predictions in [108] for the CEP coordinates are often cited: $T_{CEP} = 162 \pm 2\text{MeV}$ and $\mu_{CEP} = 360 \pm 40\text{MeV}$. Our results are significantly lower, which is probably related with the fact that we have used lower values for the current quark masses in our calculations.

We may also compare our results with those found in other effective models, particularly in what concerns the two critical lines feature. In [56], two and three flavour versions of the NJL model are studied, and it is shown that, for the conventional four and six quark interaction terms, two critical lines may exist only for unphysically low flavour mixing couplings. However, the same paper shows how the existence of the two CEPs arises in a sensible way if one introduces diquark terms. It is not clear whether there is any relation between the diquark terms and the mass-dependent terms introduced in

[2] A finite chemical potential results in a generelly complex action. From a computational point of view, this makes it hard to implement Monte Carlo importance sampling methods which are commonly used in lattice calculations for evaluating the QCD partition function.

	μ [MeV]	T [MeV]	M_{u1} [MeV]	M_{u2} [MeV]	M_{s1} [MeV]	M_{s2} [MeV]
$\mu = 0$	0	147.0	151.8	—	484.7	—
	0	191.4	19.9	—	300.5	—
CEPs	194.5	104.5	161.9	—	506.3	—
	307.8	106.2	14.3	—	295.4	—
$T = 0$	319.2	0	365.5	26.8	577.9	504.0
	425.6	0	9.1	8.6	503.7	144.6

TABLE 4.2: CEPs, $T = 0$ critical points, and $\mu = 0$ crossover points. Masses 1 and 2 refer to the high and low values of the jump, respectively. These are equal at the CEPs and at the $\mu = 0$ crossover points.

the version under present study, but it surely is intriguing that they both lead to such similarities in the phase structure.

As discussed in section 3.2.4, there is a certain freedom in the fitting of the model parameters, largely due to a significant empirical uncertainty in the σ meson mass. In [109] its value is given in the range 400 - 550 MeV. Also, both mixing angles in the scalar and pseudoscalar sectors are given as rough estimations. However, the whole scalar sector meson masses are subject to some degree of uncertainty. As presented in [109], we have $m_{f_0} = 990 \pm 20\text{MeV}$ and $m_{a_0} = 980 \pm 20\text{MeV}$, and additionally the disputed κ meson with a mass in the range 700 - 900 MeV [100]. Several works propose the existence of the κ as belonging to a low lying scalar nonet, e.g. [23] and [110]. The counterintuitive aspect of this picture is the ordering $m_\kappa < m_{a_0}$, which is reversed with respect to the corresponding members of the pseudoscalar nonet, namely the π and K mesons.

It so appears that this ordering in the masses of the scalar mesons is paramount to the existence of the second first-order transition boundary. If we vary the value of m_κ used in fixing the parameters while keeping all other input unchanged, we can see a huge variation in the behaviour of the second phase transition. Increasing m_κ to values close to m_{a_0} leads to a complete transformation of the first-order line into a smooth crossover, which happens at $m_\kappa \gtrsim 970\text{MeV}$. [111] If we instead try to decrease m_κ too much, the second CEP eventually reaches the temperature axis, which is in contradiction with lattice results indicating a smooth crossover for $\mu = 0$ [106]. This might be used for estimating a lower bound to the value of m_κ, although such a model dependent calculation might not be actually reliable. Regarding the parameterization, this playing around with m_κ is manifested mainly in the value of g_3, which corresponds to a mass-dependent non-flavour-mixing interaction term and whose absolute value changes inversely to the change in m_κ. So, not only are mass-dependent interaction terms important for the correct description of the meson spectra, it appears that these terms are also critical for the thermodynamical features of quark matter.

4.3 Strange Quark Matter

The matter structures of the universe are seemingly void of net strangeness (or charm, beauty and truth), in contrast with the obvious net isospin of atomic nuclei. This situation is easy to accept for the heavier quark flavours, which would require very extreme conditions, but there may be reasonable speculation about the existence of conditions which would favour the formation of quark matter with a net strange component. As was shown in the previous section in the context of an effective model of the strong interaction, at a sufficiently hot or dense region of the phase diagram, strange quarks are expected to populate quark matter. This comes about because of the relatively low mass of the strange quark which, despite being larger than those of the light quarks, is still small enough so that it becomes, at some point, energetically favourable for the system to occupy strange quark states instead of just light ones, lowering the Fermi level of the system. [56]

If this picture is correct, there are actually some physical objects or phenomena where we could expect to find evidences of both the existence of phase transitions and a *strange quark matter* (SQM) phase. For instance, in the very dense core of compact stars, thermodynamical conditions might be able to sustain a SQM phase. There are today several stellar objects which are plausible candidates to hosting SQM, and a number of observational experiments have been proposed to study this possibility. [112] Another possibility is the formation of strangelets in high energy *heavy ion collisions* (HIC), i.e, small *drops* of SQM in a mixed phase with regular non-strange matter. Experiments at RHIC have been unable to find such structures, but there remains a very large portion of the QCD phase diagram to probe. [113] So, compact stars and HIC are probably the two physical systems whose meticulous analysis can substantiate or disprove the possibility of stable SQM. A review of some of the research effort in these areas may be found in [114].

An even more radical view has been conjectured in [115] and later revived in [116]. The proposal is that SQM would be the true ground state of strongly interacting matter, with an energy per baryon lower than that of a stable system of ^{56}Fe nuclei (~ 930MeV) at zero pressure. The empirical fact that matter appears to exist in stable structures formed by nucleons seems to automatically invalidate this hypothesis, as we do not observe nuclei transitioning to SQM as it would be naively expected if nucleons were metastable. However, if we consider that a stable SQM phase would be possible only for a considerable portion of strange quarks (roughly the same as up and down quarks), then we can understand the apparent stability of nuclei, i.e., its large lifetime, as being related with the huge unlikeliness of a large number of weak decays occurring to bring the nuclei across the stability boundary of SQM. In other words, there is a very large energy

barrier between metastable nuclear states and stable SQM, rendering such a phenomenon probabilistically negligeable. Thus, a stable SQM phase with roughly equal numbers of the three lightest quark flavours is not incompatible with the existence of apparently stable nuclei.

Some consequences arising from the hypothesis of absolutely stable SQM have been subjected to investigation, but so far it remains conjectural. The analysis of the extended NJL model performed in the previous section does not seem to allow for such form of stable SQM, but it should be remarked that the model has no confinement mechanism and, thus, it should not be expected to provide an accurate description of the hadronic phase. Such limitation raises doubts on any attempt for rigorous comparisons between quark and hadronic phases.

In the remainder of this section, we will investigate the possiblity of SQM as it is conjectured to arise in the interior of compact stars, i.e., at high density and low temperature. We will focus on the $T = 0$ limit and try to sketch an understanding of how favourable or disfavourable our model is with respect to this possibility.

4.3.1 Beta Equilibrium and Charge Neutrality at $T = 0$

In order to address the prospect of stable SQM, certain sensible physical conditions must be included for adequate modelling. These have been proposed by Farhi and Jaffe [117] in the context of a Bag Model, but they can perfectly be taken over to the NJL model. The quarks are assumed to be in β-equilibrium with respect to their weak electronic decay reactions:

$$d \rightleftharpoons u + e^- + \bar{\nu}_e \rightleftharpoons s \tag{4.28}$$

The equilibrium conditions may be formulated as constraints in the individual quark chemical potentials. The neutrinos are expected to quickly escape the system, so that their contribution is altogether discarded. Using an average baryon chemical potential μ and the electron chemical potential μ_e, we can write

$$\mu_u = \mu - \frac{2}{3}\mu_e \qquad , \qquad \mu_d = \mu_s = \mu + \frac{1}{3}\mu_e \tag{4.29}$$

For the modelling of electrically neutral objects, we must further impose a charge neutrality condition; this is expressed in terms of quark and electron number densities ρ_i as

μ_{crit}	M_{u1}	M_{u2}	M_{d1}	M_{d2}	M_{s1}	M_{s2}	μ_{e1}	μ_{e2}
325	365.5	33.6	365.5	27.4	577.9	504.2	0	69.9
409	13.3	9.9	10.3	9.4	503.7	153.6	89.5	14.1

TABLE 4.3: Critical values at $T = 0$ with β-equilibrium and charge neutrality. The values with subscripts 1 and 2 refer to the upper and lower values at each transition, respectively. All values are given in MeV.

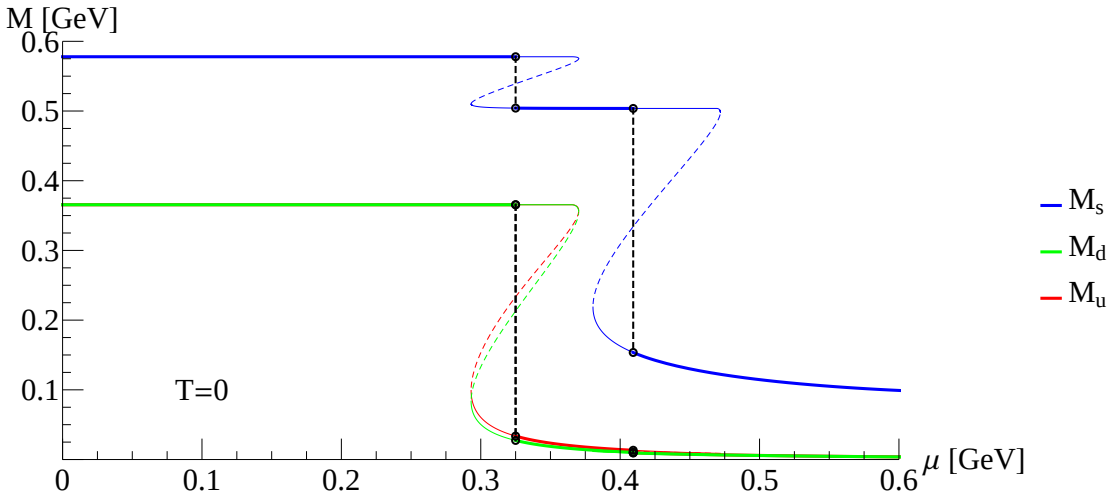

FIGURE 4.15: Mass profiles at $T = 0$ with β-equilibrium and charge neutrality.

$$\frac{2}{3}\rho_u - \frac{1}{3}\left(\rho_d + \rho_s + 3\rho_e\right) = 0 \tag{4.30}$$

We now append (4.29) and (4.30) to our previous conditions (4.27), and use this modified system of equations to solve for the dynamical quark masses and other thermodynamical quantities of interest. Of course, the quark integrals appearing in the gap equations should in this case be written with different chemical potentials for each quark flavour i, $J_0\left(M_i^2, T, \mu_i\right)$.

4.3.2 Quark Number Densities

First of all, the mass profile for fixed $T = 0$ is shown in figure 4.15. There, the two first-order transitions are marked by the black dashed lines. Values of the dynamical masses and of the baryon chemical potential at the critical points are shown in table 4.3. The pattern is overall similar to the previous cases, now with a slight difference in the masses of the light quarks due to the difference in their respective chemical potentials. This difference is largest immediately after the first transition, and gradually decreases for larger baryon chemical potentials. As before, stable solutions are shown in thick lines, while metastable and unstable solutions are shown in thin and dashed lines, respectively.

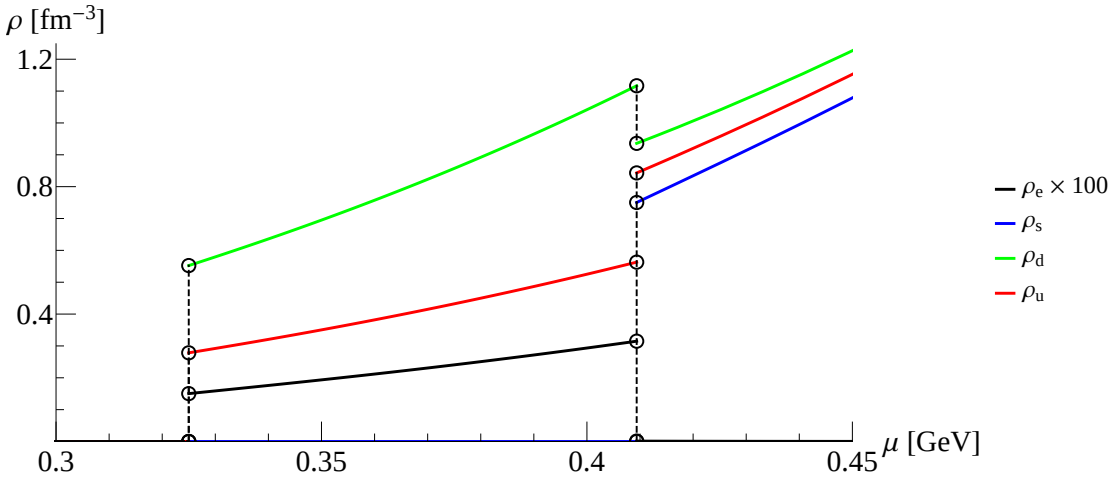

FIGURE 4.16: Quark and electron number densities at $T = 0$ with β-equilibrium and charge neutrality. The electron number density is shown here multiplied by a factor of 100.

We now look at the quark and electron densities as functions of μ, which is shown in figure 4.16. In this figure, only equilibrium solutions are displayed, and the chemical potential domain is restricted to better illustrate the regions of interest. One striking feature is that the electron density is 3 to 4 orders of magnitude smaller than the quark densities. Moreover, it is zero before the first transition and it rapidly falls to zero after the second one.[3] It could be said that, overall, electrons play a very small role in the properties of the system.

The behaviour of the quark number densities is straightforward. At the first transition, a finite density of light quarks appears, with roughly two down quarks for each up quark. This should be expected for negligible electron density in the face of the charge neutrality condition. At the second transition, the light quark densities readjust to account for an emerging finite strange quark density. These densities then rise monotonically with μ, and they appear to get progressively close to each other for higher μ values. This behaviour is best inspected in figure 4.17, where the density fraction of each flavour is displayed as a function of μ. Clearly, between the first and second transitions, we have about 1/3 up quarks and 2/3 down quarks. After the second transition, the fractions get visibly close to 1/3 for each flavour. This feature is referred in [56] as a necessary condition for the existence of stable SQM.

[3]The value of ρ_e after the second transition is so small that it appears to be zero for the resolution of the graphic. However, it has a finite value at the lower end of the transition ($\sim 1.2 \times 10^{-5}\text{fm}^{-3}$), which then quickly approaches zero for larger μ.

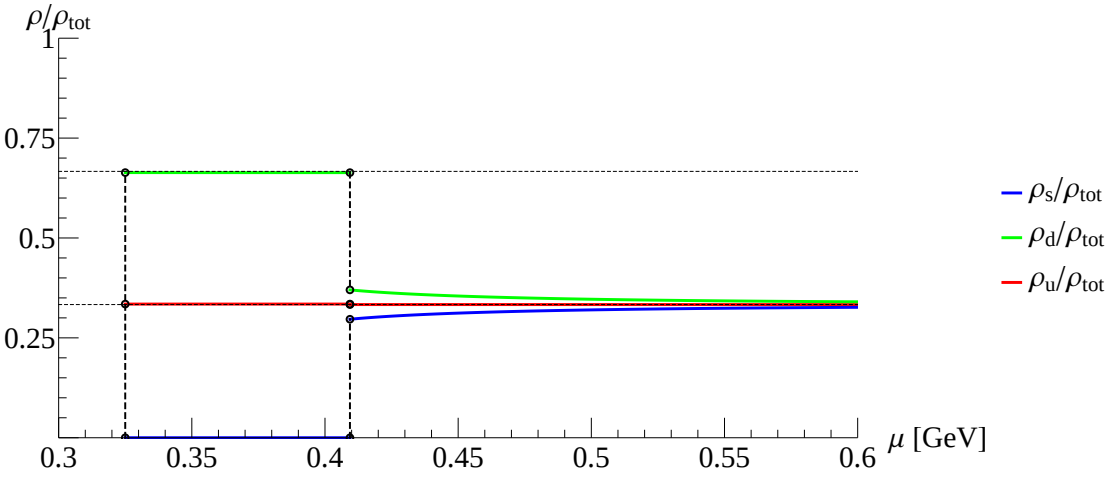

FIGURE 4.17: Quark number fractions at $T = 0$ with β-equilibrium and charge neutrality. Two thin dashed horizontal lines are drawn at fraction values of 1/3 and 2/3.

4.3.3 Energy per Baryon and State Equation

We turn to the energy per baryon E/A as a function of density. The former is defined as ε/ρ_B, where ε is the energy density as defined in (4.26) and ρ_B is the baryon number density defined as

$$\rho_B = \frac{\rho_u + \rho_d + \rho_s}{3} \tag{4.31}$$

In this case, we need to include the contribution arising from the electrons. This means that there is an electronic term in the thermodynamical potential (4.22) which, in the limit of non-interacting massless electrons at $T = 0$, can be simply written as [56]

$$\Omega_e = -\frac{\mu_e^4}{12\pi^2} \tag{4.32}$$

leading to the following relations for $T = 0$:

$$\varepsilon = -\Omega - \Omega_e + \sum_{i=u,d,s,e} \mu_i \rho_i \qquad , \qquad \rho_e = \frac{\mu_e^3}{3\pi^2} \tag{4.33}$$

Also, it is convenient to use densities normalized to the nuclear saturation density $\rho_0 \sim 0.17\text{fm}^{-3}$, which allows us to more easily establish comparisons.

The results are presented in figure 4.18. The thick, thin and dashed lines represent, as before, stable, metastable and unstable solutions, respectively. The two gray areas mark the density ranges where no stable solutions exist; they correspond to mixed phase

ρ_B/ρ_0	1.63	3.30	4.95
E/A	973	1042	1105

TABLE 4.4: Boundary points for the stable solutions in figure 4.18. The energy values are given in MeV.

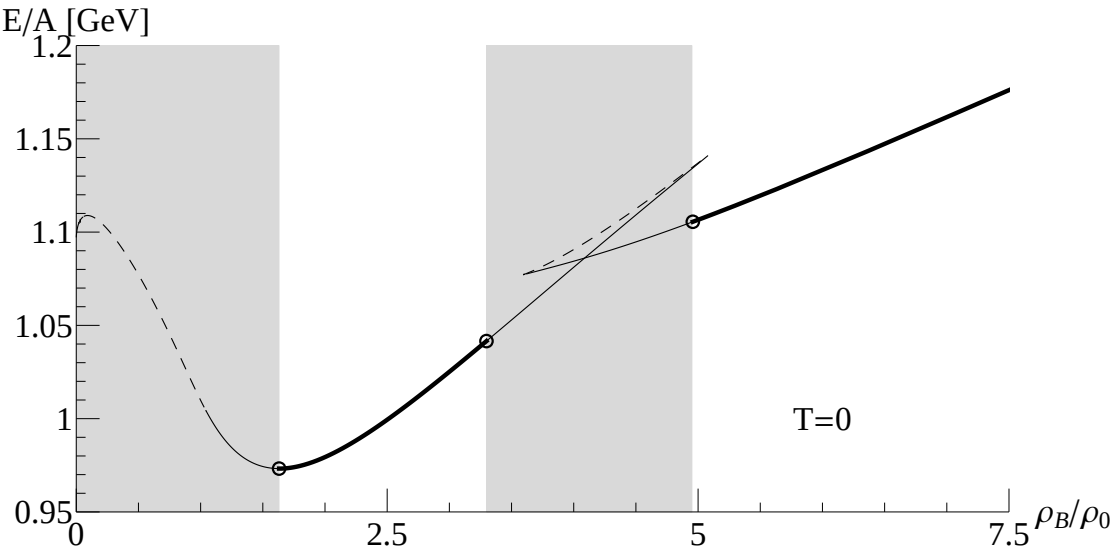

FIGURE 4.18: Energy per baryon as a function of the baryon density normalized to the nuclear saturation density ρ_0 at $T = 0$ with β-equilibrium and charge neutrality.

regions where chunks of matter from both boundary stable solutions coexist. We do not provide a description of these regions associated with the two first-order transitions.

The boundary points for stable solutions are summarized in table 4.4 and are marked in the figure with circles. The first of these points is actually the minimum of the curve, and its coordinates are somewhat lower than those found in similar model calculations. For example, in [56], the minimum is at $\rho_B = 2.25\rho_0$, with $E/A = 1102$MeV. Still, our results remain larger than those associated with nuclear stability ($\rho_B = \rho_0$ and $E/A = 930$MeV). Since this minimum is coincident with the onset of non-strange matter, which we empirically know is unstable, this result is actually within expectations. Also in [56], strange quarks are predicted to appear at $\rho_B = 3.85\rho_0$ with $E/A \sim 1140$MeV. Again, our results are below these values (third column of table 4.4), but still above nuclear stability values. It could then be said that, when compared with the 't Hooft extended NJL model, ours effectively lowers E/A and ρ across the whole plane, pushing the values closer to the nuclear matter stability ones; nevertheless, it does not seem to corroborate Witten's hypothesis of absolutely stable SQM.

We might as well consider what these results might imply regarding SQM at high densities, as it is speculated to exist in compact stars. The theoretical study of these stellar objects is usually performed by means of the Tolman-Oppenheimer-Volkoff (TOV) equations. [118] [119] These equations can be written as

$$\begin{aligned} \frac{dp}{dr} &= -G\frac{\varepsilon + p}{r}\frac{m + 4\pi r^3 p}{r - 2Gm} \\ \frac{dM}{dr} &= 4\pi\varepsilon r^2 \end{aligned} \tag{4.34}$$

where r is the radial distance from the center and $m(r)$ is the mass enclosed by a spherical surface of radius r; $\varepsilon(r)$ and $p(r)$ have the same meaning as before, but are here taken as functions of r. If we know the state equation $p(\varepsilon)$ connecting p and ε, equations (4.34) can be integrated numerically for some central value $\varepsilon(r=0) = \varepsilon_c$ and with boundary conditions

$$M(r=0) = 0 \quad , \quad p(r=0) = p(\varepsilon_c) \quad , \quad p(r=R) = 0 \tag{4.35}$$

where R is the radius of the star and $m(r=R) = M$ is its mass. A Runge-Kutta algorithm stepping in variable r may be employed to perform the numerical integration until the pressure drops to zero, at which time we take the current value of r as the radius of the sphere, and similarly with m for its mass. For each inital value of ε_c, we will get a different point in the R-M plane. Together, these points trace a curve of equilibrium combinations of R and M for stellar objects made up from matter obeying our state equation. One then compares observational data on compact stars to check if there might be some overlap.

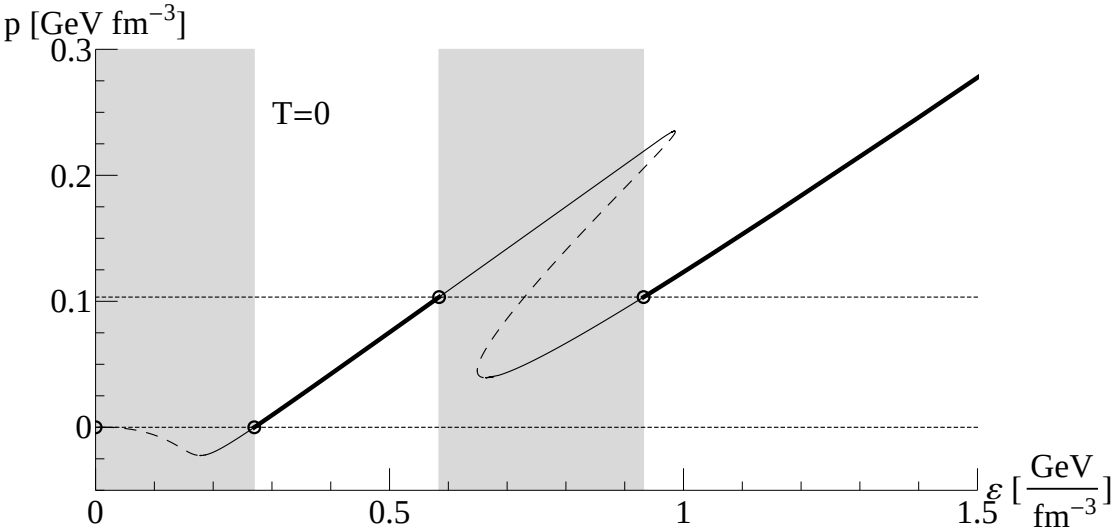

FIGURE 4.19: Pressure as a function of energy density at $T = 0$ with β-equilibrium and charge neutrality.

The state equation of our model is shown graphically in figure 4.19. The meaning of the lines follows precisely the conventions we have used so far. We see the first

transition occurring at zero pressure and the stable light quarks phase beginning at $\varepsilon \sim 270\text{MeVfm}^{-3}$. The second transition occurs at $p \sim 103\text{MeVfm}^{-3}$; the first stability line ends at $\varepsilon \sim 584\text{MeVfm}^{-3}$ and the second stability line begins at $\varepsilon \sim 932\text{MeVfm}^{-3}$. The gray areas correspond again to mixed phases.

However, modelling compact stars on the basis of this state equation should not be taken very seriously, for several reasons. First of all, the model does not actually describe hadronic phases, which are most likely present on the outer layers of these objects where the pressure is not so high. Another issue has to do with the absence of a magnetic field in the model; it is thought that high magnetic fields arise in the interior of compact stars, strongly affecting both the chiral transitions (through magnetic catalysis [120]) and the thermodynamical potential. Also, one has to deal with the singularities associated with the mixed phases, which require an adequate treatment in order to have a reasonable modelling.

In spite of all these issues, some crude qualitative appreciation may be carried through. If we compare the state equation in figure 4.19 with those reported in figure 2 of [112], ours appears to be somewhere between the RH(p,n,H,K) and the RH(p,n,H,Q) curves, although it goes to $p = 0$ at a much larger value of ε. We could say that our state equation is *soft*. From this we can expect a softer curve in the R-M plane with generally lower values for both coordinates than those which are usually required for stiffer state equations (maximum masses of around 2 solar masses and maximum radii from 8 to 12 km). In summary, we expect that our model might accomodate compact stars with SQM cores with very small masses and radii only.

Chapter 5

Conclusion

Here, we recap the main points focused on the course of this thesis, including background material and model related aspects. Also, we highlight the chief results and we make some suggestions on directions for further work on the subject.

5.1 Summary

5.1.1 Background and Model

We have started from the QCD Lagrangian and the description of its symmetries, with particular attention to the approximate chiral symmetry. We have compiled a series of existing theoretical and phenomenological remarks which support the idea that the mechanism of dynamical breaking of chiral symmetry in the light sector of QCD is a powerful tool for the description of strong interactions below an energy scale $\Lambda \sim 1\text{GeV}$. We have argued that such a tool is of importance due to the non-perturbative nature of QCD at that energy scale, and also as a more easily tractable alternative to lattice QCD in respect to computational effort. We have also given a brief account of the construction of EFTs, as well as of the $1/N_c$ expansion of QCD.

From a number of low energy models that have been proposed in roughly 70 years, we have focused on the NJL model. It incorporates the ideas of chiral symmetry breaking (or better, the Nambu-Goldstone realization of chiral symmetry) in a simple and elegant fashion, providing valuable and often accurate insight into the vacuum properties of QCD and the dynamical mass generation of quarks. Its basic features, from its original formulation in terms of nucleon fields to its reinterpretation in terms of quark fields have been reviewed for two flavours. Its extension to three flavours with the inclusion of the strange quark has been explained, introducing the 't Hooft six quark interaction term

which explicitly breaks the $U_A(1)$ anomalous symmetry. We have also illustrated the Bethe-Salpeter description of hadrons and the functional bosonization of the model.

Following reference papers, we have then presented a thorough analysis of a three-flavour version of the model based on its functional bosonization through the introduction of auxiliary and physical bosonic fields. We have shown how to use a SPA with an asymptotic expansion in terms of the physical fields for the functional integration over the auxiliary fields, leading to a set of stationary phase conditions for the expansion coefficients. For the explicit evaluation of the quark functional integral, we have resorted to a proper time heat kernel expansion which has been suitably generalized to the case of a non-degenerate mass matrix. We have then obtained, through standard techniques, the mass gap equations and the effective potential from the tadpole term of the effective bosonized Lagrangian in the mean field approximation. These steps have been carefully exposed because of their relevance to the version of the model we were analyzing afterwards.

Some additional important aspects have been taken from the literature and detailed in order to provide a more complete picture of the developments in NJL models and also to raise a stronger argument in favour of our later treatment. It has been argued that the three-flavour NJL model with the 't Hooft term has no stable ground state, and the introduction of eight quark interaction terms has been suggested to recover the model's stability.

All the previous points converge into the recent formulation of an extended version of the NJL model, which follows in the manner of an EFT and incorporates a complete set of mass-dependent interaction terms in addition to all the other terms already present in the former versions. These terms, which explicitly break chiral symmetry, are included in a way which is completely consistent with dimensional analysis, N_c counting and Λ expansion. The whole functional bosonization scheme which had been employed before was then carried out for this new Lagrangian, determining the stationary phase conditions, the mass gap equations and the effective potential. The procedure for fitting the model's parameters has been outlined as well. It has been highlighted that the inclusion of the mass-dependent interaction terms raised the model to an unprecedented level of accuracy in the description of empirical data, which supports the conclusion that the explicit breaking of chiral symmetry is of paramount importance in strong dynamics.

5.1.2 Thermodynamical Analysis

In the last chapter, we have proposed to analyze the consequences of the new mass-dependent terms for the thermodynamical properties of the model. To that end, we

have included a model dependence on temperature and chemical potential through the Matsubara formalism. This has essentially converted the Euclidean time quark integrals into infinite sums over Matsubara frequencies, which have been explicitly evaluated. Using these results, the thermodynamical potential has been determined in the mean field approximation.

We then solved the coupled system of stationary phase conditions and gap equations numerically for the dynamical quark masses. We have shown a series of mass profiles for fixed values of the chemical potential and we have drawn the phase diagram in the μ-T plane. The most striking observation was the existence of two first-order transition boundaries. In other versions of the NJL model, this feature would only be present either for unphysically low couplings associated with the flavour-mixing interaction terms or with the inclusion of diquark terms. In our case, the non-flavour-mixing term with coupling g_3 was found to be crucial for the emergence of the second first-order transition, somehow counterbalancing the flavour-mixing effects of other terms. This behaviour could also be traced back to the ordering $m_\kappa < m_{a_0}$ in the scalar meson spectrum.

We have also investigated the possibility of stable SQM existing within the model. This study has been carried out by first imposing β-equilibrium and charge neutrality conditions, and then solving the aforementioned coupled system of equations subject to these constraints at zero temperature. We have studied the dependence of quark and electron densities on μ and found that the electrons played almost no role; after the first transition, finite densities of up and down quarks arise in the approximate ratio of 2 downs for each up; the strange quarks appear after the second transition, and the three flavours quickly tend to exist in identical fractions as μ is increased.

The energy per baryon as a function of baryon density and the state equation in the ε-p plane have also been analyzed. In general, both appear to be *softer* than those of other models, although they do not appear to allow for absolutely stable SQM. Consequences for dense SQM inside compact stars have also been speculated, but no conclusive observations have been made.

5.2 Further Work

There is a large room for further investigations involving this model. Of relevance to compact stars is the inclusion of a magnetic field in the Lagrangian, which is expected to significantly alter the results we have obtained in this thesis. This is not a difficult task, but time constraints have precluded the development of this work. Another possiblity is to include the Polyakov loop. The absence of confinement is probably the

main disadvantage of this model, and the Polyakov loop is a standard way of modelling the effects of the confining-deconfining phase at finite temperatures. These could be specially relevant at finite temperatures. Also, it would be nice to check how chiral and deconfinement transitions correlate with each other. Furthermore, we have not provided a suitable description of the mixed phases associated with the first-order transitions. This is yet another aspect that could be investigated in a deeper way.

Aside from thermodynamical considerations, we can study a number of scattering processes, like π-π or π-K scattering, since the considered model Lagrangian is able to account properly for the $SU(3)$ breaking effects in the description of the weak decay constants f_π and f_K, in addition to having the correct empirical masses of the mesons. We can also study decay processes, like the η or η' three pion decays, that require the explicit breaking of isospin symmetry, which can easily be introduced through a parameter refitting with $m_u \neq m_d$.

Further extensions to the model Lagrangian may still be considered, namely the inclusion of vector interaction terms, which would enable the study of a broader set of processes. For example, the results of experiments with stopped antiprotons at LEAR (CERN) gave unexpectedly large violation of the OZI rule by a factor of 30 - 70. The KLOE collaboation at DAΦNE ϕ factory has claimed on the finding of direct OZI violation in the $\phi \longrightarrow \pi^+ + \pi^- + \pi^0$ decay [121]. The amplitude of the direct transition turns out to be as large as 10% of the indirect OZI violation in $\phi \longrightarrow \rho + \pi$. Since the Lagrangian contains multi-fermion vertices which break the OZI rule, one can address this problem and find physical consequences of such interactions. Moreover, with vector modes included in the Lagrangian, one can go beyond the $\eta\,(\eta') \longrightarrow \gamma + \gamma$ decays and study processes like $\eta\,(\eta') \longrightarrow \gamma + V$, where V could be either ρ, ω or ϕ.

Appendix A

SU(3) and U(3) Groups

A.1 SU(3)

The gauge symmetry associated with the strong interactions is encoded in the $SU(3)$ group. Its defining generators T^a may be written in terms of the Gell-Mann matrices which generalize the $SU(2)$ Pauli matrices

$$\lambda_1 = \begin{pmatrix} 0 & 1 & 0 \\ 1 & 0 & 0 \\ 0 & 0 & 0 \end{pmatrix} \qquad \lambda_2 = \begin{pmatrix} 0 & -i & 0 \\ i & 0 & 0 \\ 0 & 0 & 0 \end{pmatrix} \qquad \lambda_3 = \begin{pmatrix} 1 & 0 & 0 \\ 0 & -1 & 0 \\ 0 & 0 & 0 \end{pmatrix}$$

$$\lambda_4 = \begin{pmatrix} 0 & 0 & 1 \\ 0 & 0 & 0 \\ 1 & 0 & 0 \end{pmatrix} \qquad \lambda_5 = \begin{pmatrix} 0 & 0 & -i \\ 0 & 0 & 0 \\ i & 0 & 0 \end{pmatrix} \qquad \lambda_6 = \begin{pmatrix} 0 & 0 & 0 \\ 0 & 0 & 1 \\ 0 & 1 & 0 \end{pmatrix}$$

$$\lambda_7 = \begin{pmatrix} 0 & 0 & 0 \\ 0 & 0 & -i \\ 0 & i & 0 \end{pmatrix} \qquad \lambda_8 = \frac{1}{\sqrt{3}} \begin{pmatrix} 1 & 0 & 0 \\ 0 & 1 & 0 \\ 0 & 0 & -2 \end{pmatrix} \tag{A.1}$$

with $T_a = \lambda_a/2$. These are traceless Hermitean matrices, which additionaly satisfy

$$\mathrm{tr}\,(\lambda_a \lambda_b) = 2\delta_{ab} \tag{A.2}$$

The $SU\,(3)$ Lie algebra is

$$[T_a, T_b] = i f_{abc} T_c \tag{A.3}$$

where the completely antisymmetric f_{abc} are the structure constants of the group. The non-zero components are

$$\begin{gathered} f_{123} = 1 \qquad , \qquad f_{458} = f_{678} = \frac{\sqrt{3}}{2} \\ f_{147} = -f_{156} = f_{246} = f_{257} = f_{345} = -f_{367} = \frac{1}{2} \end{gathered} \tag{A.4}$$

Also, we can define an anticommutator

$$\{T_a, T_b\} = \frac{1}{3}\delta_{ab} + d_{abc} T_c \tag{A.5}$$

where the completely symmetric constants d_{abc} have non-zero components

$$\begin{gathered} d_{118} = d_{228} = d_{338} = -d_{888} = \frac{1}{\sqrt{3}} \\ d_{448} = d_{558} = d_{668} = d_{778} = -\frac{1}{2\sqrt{3}} \\ d_{146} = d_{157} = -d_{247} = d_{256} = d_{344} = -d_{355} = -d_{366} = -d_{377} = \frac{1}{2} \end{gathered} \tag{A.6}$$

A.2 U(3)

We may append to the Gell-Mann matrices (A.1) a multiple of the identity matrix

$$\lambda_0 = \sqrt{\frac{2}{3}}\mathbb{1} = \sqrt{\frac{2}{3}} \begin{pmatrix} 1 & 0 & 0 \\ 0 & 1 & 0 \\ 0 & 0 & 1 \end{pmatrix} \tag{A.7}$$

In this way, we extend our group to $U\,(3)$ with nine defining generators $T_a = \lambda_a/2$, where now the index a runs from 0 to 8. For this extended set of Gell-Mann matrices, we have

$$\mathrm{tr}\lambda_a = \sqrt{6}\delta_{a0} \tag{A.8}$$

and (A.2) still holds. The Lie algebra is given as in (A.3), with the same structure constants (A.1). The anticommutator may be written as

$$\{T_a, T_b\} = d_{abc}T_c \tag{A.9}$$

where in this case we have, in addition to (A.1),

$$d_{0ab} = \sqrt{\frac{2}{3}}\delta_{ab} \tag{A.10}$$

The following relations are useful in calculations and manipulation of expressions

$$\begin{aligned} f_{abe}f_{cde} - f_{ace}f_{bde} + f_{ade}f_{bce} &= 0 \\ f_{abe}d_{cde} + f_{ace}d_{bde} + f_{ade}d_{bce} &= 0 \\ f_{abe}f_{cde} - d_{ace}d_{bde} + d_{ade}d_{bce} &= 0 \end{aligned} \tag{A.11}$$

$$\begin{aligned} d_{abb} &= 3\sqrt{6}\delta_{a0} \\ d_{acd}d_{bcd} &= 3\left(\delta_{ab} + \delta_{a0}\delta_{b0}\right) \\ f_{acd}f_{bcd} &= 3\left(\delta_{ab} - \delta_{a0}\delta_{b0}\right) \end{aligned} \tag{A.12}$$

Another very useful expression is

$$\left(\lambda_a\right)_{ij}\left(\lambda_a\right)_{kl} = 2\delta_{il}\delta_{jk} \tag{A.13}$$

Finally, we define the symmetric coefficients (the ϵ are Levi-Civita symbols)

$$\begin{aligned} A_{abc} &= \frac{1}{3!}\epsilon_{ijk}\epsilon_{mnl}\left(\lambda_a\right)_{im}\left(\lambda_b\right)_{jn}\left(\lambda_c\right)_{kl} \\ &= \frac{2}{3}d_{abc} + \sqrt{\frac{2}{3}}\left(3\delta_{a0}\delta_{b0}\delta_{c0} - \delta_{a0}\delta_{bc} - \delta_{b0}\delta_{ac} - \delta_{c0}\delta_{ab}\right) \end{aligned} \tag{A.14}$$

Appendix B

Dirac Algebra

The description of point-like relativistic spin-1/2 particles is done through the Dirac equation

$$(i\gamma^\mu \partial_\mu - m)\,\psi = 0 \tag{B.1}$$

where ψ belongs to the four-spinor representation of the Lorentz group and the γ^μ matrices obey a Clifford algebra

$$\{\gamma^\mu \gamma^\nu\} = 2g^{\mu\nu} \tag{B.2}$$

Here, $g^{\mu\nu}$ is the Minkowski metric with signature $(+---)$. γ^μ and m are 4×4 matrices. From (B.2) it is evident that

$$(\gamma^\mu)^2 = g^{\mu\mu}\mathbb{1} \tag{B.3}$$

The algebra (B.2) has many possible realizations. In the standard Dirac representation the γ^μ matrices are

$$\gamma^0 = \begin{pmatrix} \mathbb{1} & 0 \\ 0 & -\mathbb{1} \end{pmatrix} \quad , \quad \gamma^i = \begin{pmatrix} 0 & \sigma^i \\ -\sigma^i & 0 \end{pmatrix} \tag{B.4}$$

where $\mathbb{1}$ is the 2×2 unit matrix and σ^i are the Pauli matrices

$$\sigma^1 = \begin{pmatrix} 0 & 1 \\ 1 & 0 \end{pmatrix} \quad , \quad \sigma^2 = \begin{pmatrix} 0 & -i \\ i & 0 \end{pmatrix} \quad , \quad \sigma^3 = \begin{pmatrix} 1 & 0 \\ 0 & -1 \end{pmatrix} \tag{B.5}$$

In this representation, the γ^μ matrices satisfy

$$\gamma^{\mu\dagger} = \gamma^0 \gamma^\mu \gamma^0 \quad \Rightarrow \quad \begin{cases} \gamma^{0\dagger} &= \gamma^0 \\ \gamma^{i\dagger} &= -\gamma^i \end{cases} \tag{B.6}$$

Other common representations are the Weyl and the Majorana representations.

We can use the four matrices (B.4) and the unit matrix $\mathbb{1}$ to define a complete basis spanning the whole space of 4×4 matrices. We have

$$\begin{array}{cccc} 1 & \text{scalar} & & \mathbb{1} \\ 4 & \text{vector} & & \gamma^\mu \\ 6 & \text{tensor} & \sigma^{\mu\nu} = \frac{i}{2}\left[\gamma^\mu, \gamma^\nu\right] & \\ 4 & \text{axial vector} & & \gamma^5 \gamma^\mu \\ 1 & \text{pseudoscalar} & \gamma^5 = i\gamma^0\gamma^1\gamma^2\gamma^3 & \end{array} \tag{B.7}$$

The γ^5 matrix is of special importance because it anticommutes with all other γ^μ

$$\left\{\gamma^\mu, \gamma^5\right\} = 0 \tag{B.8}$$

and, in the Dirac representation, it satisfies

$$\left(\gamma^5\right)^2 = \mathbb{1} \quad , \quad \gamma^{5\dagger} = \gamma^5 \tag{B.9}$$

These properties allow us to define left and right projection operators as

$$P_{R,L} = \frac{1 \pm \gamma^5}{2} \tag{B.10}$$

which obey the usual relations

$$P_R + P_L = 1 \tag{B.11a}$$

$$P_R^2 = P_R \quad , \quad P_L^2 = P_L \tag{B.11b}$$

$$P_L P_R = P_R P_L = 0 \tag{B.11c}$$

Of particular interest for calculations are the trace properties of these matrices. Some of the useful identities are

$$\mathrm{tr}\left(\gamma^{\mu}\right) = \mathrm{tr}\left(\gamma^{5}\right) = 0 \tag{B.12a}$$

$$\text{the trace of any product of an odd number of } \gamma^{\mu} = 0 \tag{B.12b}$$

$$\text{the trace of } \gamma^{5} \text{ times any product of an odd number of } \gamma^{\mu} = 0 \tag{B.12c}$$

$$\mathrm{tr}\left(\gamma^{5}\gamma^{\mu}\gamma^{\nu}\right) = 0 \tag{B.12d}$$

$$\mathrm{tr}\left(\gamma^{\mu}\gamma^{\nu}\right) = 4g^{\mu\nu} \tag{B.12e}$$

$$\mathrm{tr}\left(\gamma^{\mu}\gamma^{\nu}\gamma^{\rho}\gamma^{\sigma}\right) = 4\left(g^{\mu\nu}g^{\rho\sigma} - g^{\mu\rho}g^{\nu\sigma} + g^{\mu\sigma}g^{\nu\rho}\right) \tag{B.12f}$$

Appendix C

Noether's Theorem

Noether's theorem relates the continuous symmetries of a given theory to conserved currents. This is usually formulated on the basis of the Lagrangian of the theory (or the Lagangian density, for field theories). Below we will sketch a simple proof of this theorem.

Suppose that we have a Lagrangian density $\mathcal{L}(\phi, \partial_\mu \phi)$ written in terms of the field $\phi = \left(\phi^1, \phi^2, \ldots \phi^n\right)$ and which is invariant under the infinitesimal field transformations

$$\phi \longrightarrow \phi' = \phi + i\alpha^a X^a \phi \tag{C.1}$$

where the X^a are the transformation generators and the α^a are continuous parameters. If $\mathcal{L}$ is invariant under such transformation, then

$$\delta\mathcal{L} = \frac{\partial \mathcal{L}}{\partial \phi}\delta\phi + \frac{\partial \mathcal{L}}{\partial\left(\partial_\mu \phi\right)}\delta\left(\partial_\mu \phi\right) = 0 \tag{C.2}$$

with

$$\begin{aligned} \delta\phi &= \phi' - \phi = i\alpha^a X^a \phi \\ \delta\left(\partial_\mu \phi\right) &= \partial_\mu\left(\phi' - \phi\right) = \partial_\mu\left(i\alpha^a X^a \phi\right) \end{aligned} \tag{C.3}$$

We then have

$$\frac{\partial \mathcal{L}}{\partial \phi} i\alpha^a X^a \phi + \frac{\partial \mathcal{L}}{\partial\left(\partial_\mu \phi\right)}\partial_\mu\left(i\alpha^a X^a \phi\right) = 0 \tag{C.4}$$

We now use

$$\frac{\partial \mathcal{L}}{\partial \left(\partial_\mu \phi\right)} \partial_\mu \left(i\alpha^a X^a \phi\right) = \partial_\mu \left(\frac{\partial \mathcal{L}}{\partial \left(\partial_\mu \phi\right)} i\alpha^a X^a \phi\right) - \partial_\mu \left(\frac{\partial \mathcal{L}}{\partial \left(\partial_\mu \phi\right)}\right) i\alpha^a X^a \phi \tag{C.5}$$

and the Euler-Lagrange equation

$$\frac{\partial \mathcal{L}}{\partial \phi} = \partial_\mu \left(\frac{\partial \mathcal{L}}{\partial \left(\partial_\mu \phi\right)}\right) \tag{C.6}$$

to arrive at

$$\partial_\mu \left(\frac{\partial \mathcal{L}}{\partial \left(\partial_\mu \phi\right)} i\alpha^a X^a \phi\right) = 0 \tag{C.7}$$

Since this must hold for arbitrary α^a, it means that, to each symmetry generator X^a, there corresponds a conserved current

$$J^a_\mu = i \frac{\partial \mathcal{L}}{\partial \left(\partial_\mu \phi\right)} X^a \phi \tag{C.8}$$

and a respective conserved charge given by

$$Q^a = \int d^3x J^a_0 \tag{C.9}$$

Bibliography

[1] Y. Nambu and G. Jona-Lasinio. Dynamical Model of Elementary Particle Based on an Analogy with Superconductivity. I. *Physical Review*, 122(1):345–358, April 1961. URL doi:10.1103/PhysRev.122.345.

[2] Y. Nambu and G. Jona-Lasinio. Dynamical Model of Elementary Particle Based on an Analogy with Superconductivity. II. *Physical Review*, 124(1):246–254, October 1961. URL doi:10.1103/PhysRev.124.246.

[3] A. A. Osipov, B. Hiller, and A. H. Blin. Light quark masses in multi-quark interactions. *The European Physical Journal A*, 49(1), January 2013. URL doi:10.1140/epja/i2013-13014-y.

[4] A. A. Osipov, B. Hiller, and A. H. Blin. Effective multi-quark interactions with explicit breaking of chiral symmetry. *Physical Review D*, 88, September 2013. URL doi:10.1103/PhysRevD.88.054032.

[5] R. Alkofer and H. Reinhardt. *Chiral Quark Dynamics*. Springer, 1995.

[6] D. J. Gross and F. Wilczek. Ultraviolet Behavior of Non-Abelian Gauge Theories. *Physical Review Letters*, 30, June 1973. URL doi:10.1103/PhysRevLett.30.1343.

[7] W. Greiner, S. Schramm, and E. Stein. *Quantum Chromodynamics*. Springer, 2002.

[8] M. E. Peskin and D. V. Schroeder. *An Introduction to Quantum Field Theory*. Perseus Books, 1995.

[9] E. Fermi. Tentativo di una Teoria Dei Raggi β. *Il Nuovo Cimento*, 11(1):1–19, January 1934. URL doi:10.1007/BF02959820.

[10] W. E. Thirring. A soluble relativistic field theory. *Annals of Physics*, 3(1):91–112, January 1958. URL doi:10.1016/0003-4916(58)90015-0.

[11] D. J. Gross and A. Neveu. Dynamical symmetry breaking in asymptotically free field theories. *Physical Review D*, 10, November 1974. URL doi:10.1103/PhysRevD.10.3235.

[12] M. Soler. Classical, Stable, Nonlinear Spinor Field with Positive Rest Energy. *Physical Review D*, 1, May 1970. URL doi:10.1103/PhysRevD.1.2766.

[13] F. Gürsey. On the symmetries of strong and weak interactions. *Il Nuovo Cimento*, 16(2):230–240, April 1960. URL doi:10.1007/BF02860276.

[14] M. Gell-Mann and M. Lévy. The axial vector current in beta decay. *Il Nuovo Cimento*, 16(4):705–726, May 1960. URL doi:10.1007/BF02859738.

[15] T. H. R. Skyrme. A Non-Linear Field Theory. *Proceedings of the Royal Society A*, 260(1300):127–138, February 1961. URL doi:10.1098/rspa.1961.0018.

[16] J. J. Sakurai. Theory of Strong Interactions. *Annals of Physics*, 11(1):1–48, September 1960. URL doi:10.1016/0003-4916(60)90126-3.

[17] S. Weinberg. A model of leptons. *Physical Review Letters*, 19:1264–1266, November 1967. URL doi:10.1103/PhysRevLett.19.1264.

[18] S. Coleman, J. Wess, and B. Zumino. Structure of Phenomenological Lagrangians. I. *Physical Review*, 177:2239–2246, January 1969. URL doi:10.1103/PhysRev.177.2239.

[19] C. G. Callan, S. Coleman, J. Wess, and B. Zumino. Structure of Phenomenological Lagrangians. II. *Physical Review*, 177:2247–2250, January 1969. URL doi:10.1103/PhysRev.177.2247.

[20] R. Dashen. Chiral SU(3)xSU(3) as a Symmetry of the Strong Interactions. *Physical Review*, 183(5):1245–1260, July 1969. URL doi:10.1103/PhysRev.183.1245.

[21] R. Dashen and M. Weinstein. Soft Pions, Chiral Symmetry, and Phenomenological Lagrangians. *Physical Review*, 183(5):1261–1291, July 1969. URL doi:10.1103/PhysRev.183.1261.

[22] L.-F. Li and H. Pagels. Perturbation Theory about a Goldstone Symmetry. *Physical Review Letters*, 26:1204–1206, May 1971. URL doi:10.1103/PhysRevLett.26.1204.

[23] E. van Beveren, T. A. Rijken, K. Metzger, C. Dullemond, G. Rupp, and J. E. Ribeiro. A low lying scalar meson nonet in a unitarized meson model. *Zeitschrift für Physik C*, 30(4):615–620, December 1986. URL doi:10.1007/BF01571811.

[24] H. Georgi. An effective field theory for heavy quarks at low energies. *Physics Letters B*, 240(3-4):447–450, April 1990. URL doi:10.1016/0370-2693(90)91128-X.

[25] S. Weinberg. Phenomenological Lagrangians. *Physica A: Statistical Mechanics and its Applications*, 96(1-2):327–340, April 1979. URL doi:10.1016/0378-4371(79)90223-1.

[26] G. 't Hooft. A Planar Diagram Theory for Strong Interactions. *Nuclear Physics B*, 72(3):461–473, April 1974. URL doi:10.1016/0550-3213(74)90154-0.

[27] A. V. Manohar. Large N QCD. In F. David and R. Gupta, editors, *Probing the Standard Model of Particle Interactions*. Elsevier, 2008.

[28] A. Hosaka and H. Toki. *Quarks, Baryons and Chiral Symmetry*. World Scientific, 2001.

[29] M. L. Goldberger and S. B. Treiman. Decay of the Pi Meson. *Physical Review*, 110, June 1958. URL doi:10.1103/PhysRev.110.1178.

[30] S. Scherer and M. R. Schindler. *A Primer for Chiral Perturbation Theory*. Springer, 2012.

[31] F. Strocchi. *Symmetry Breaking*. Springer, 2005.

[32] J. Bernstein. Spontaneous symmetry breaking, gauge theories, the Higgs mechanism and all that. *Reviews of Modern Physics*, 46, January 1974. URL doi:10.1103/RevModPhys.46.7.

[33] J. Goldstone. Field theories with "Superconductor" solutions. *Il Nuovo Cimento*, 19(1):154–164, January 1961. URL doi:10.1007/BF02812722.

[34] R. P. Feynman and A. R. Hibbs. *Quantum Mechanics and Path Integrals*. McGraw-Hill, 1965.

[35] R. A. Bertlmann. *Anomalies in Quantum Field Theory*. Oxford Science Publication, 2000.

[36] G. 't Hooft. Symmetry Breaking through Bell-Jackiw Anomalies. *Physical Review Letters*, 37, July 1976. URL doi:10.1103/PhysRevLett.37.8.

[37] G. 't Hooft. Computation of the quantum effects due to a four-dimensional pseudoparticle. *Physical Review D*, 14, December 1976. URL doi:10.1103/PhysRevD.14.3432.

[38] D. Diakonov. Chiral symmetry breaking by instantons. In A. Di Giacomo and D. Diakonov, editors, *Selected topics in nonperturbative QCD. Proceedings, 130th Course of the International School of Physics Enrico Fermi*, pages 397–432, Varenna, Italy, 1995.

[39] S. L. Adler. Axial-Vector Vertex in Spinor Electrodynamics. *Physical Review*, 177, January 1969. URL doi:10.1103/PhysRev.177.2426.

[40] R. Jackiw and K. Johnson. Anomalies of the Axial-Vector Current. *Physical Review*, 182, June 1969. URL doi:10.1103/PhysRev.182.1459.

[41] J. Bardeen, L. N. Cooper, and J. R. Schrieffer. Theory of Superconductivity. *Physical Review*, 108(5):1175–1204, December 1957.

[42] T. Eguchi and H. Sugawara. Extended model of elementary particles based on an analogy with superconductivity. *Physical Review D*, 10, December 1974. URL doi:10.1103/PhysRevD.10.4257.

[43] K. Kikkawa. Quantum Corrections in Superconductor Models. *Progress of Theoretical Physics*, 56(3):947–955, March 1976. URL doi:10.1143/PTP.56.947.

[44] C. M. Bender, F. Cooper, and G. S. Guralnik. Path integral formulation of mean-field perturbation theory. *Annals of Physics*, 109(1):165–209, November 1977. URL doi:10.1016/0003-4916(77)90169-5.

[45] D. Ebert and M. K. Volkov. Composite-meson model with vector dominance based on U(2) invariant four-quark interactions. *Zeitschrift für Physik C Particles and Fields*, 16(3):205–210, 1983. URL doi:10.1007/BF01571607.

[46] M. K. Volkov. Meson Lagrangians in a superconductor quark model. *Annals of Physics*, 157(1):282–303, October 1984. URL doi:10.1016/0003-4916(84)90055-1.

[47] S. I. Kruglov. Renormalization and Ward Identities in a Non-Linear Spinor Model. *Acta Physica Polonica B*, 15(8):725–738, August 1984.

[48] A. Dhar, R. Shankar, and S. R. Wadia. Nambu–Jona-Lasinio–type effective Lagrangian: Anomalies and nonlinear Lagrangian of low-energy, large-N QCD. *Physical Review D*, 31(8):3256–3267, June 1985. URL doi:10.1103/PhysRevD.31.3256.

[49] D. Ebert and H. Reinhardt. Effective Chiral Hadron Lagrangian with anomalies and skyrme terms from quark flavour dynamics. *Nuclear Physics B*, 271(3-4): 188–226, 1986. URL doi:10.1016/S0550-3213(86)80009-8.

[50] V. Bernard, U.-G. Meissner, and I. Zahed. Decoupling of the pion at finite temperature and density. *Physical Review D*, 36, August 1987. URL doi:10.1103/PhysRevD.36.819.

[51] J. da Providência, M. C. Ruivo, and C. A. de Sousa. Time-dependent Hartree-Fock formalism and the excitations of the Dirac sea in the Nambu–Jona-Lasinio model. *Physical Review D*, 36, September 1987. URL doi:10.1103/PhysRevD.36.1882.

[52] T. Kunihiro and T. Hatsuda. Effects of flavour mixing induced by axial anomaly on the quark condensates and meson spectra. *Physics Letters B*, 206(3):385–390, May 1988. URL doi:10.1016/0370-2693(88)91596-1.

[53] S. P. Klevansky. The Nambu-Jona-Lasinio model of quantum chromodynamics. *Reviews of Modern Physics*, 64(3):649–708, July 1992. URL doi:10.1103/RevModPhys.64.649.

[54] U. Vogl and W. Weise. The Nambu and Jona-Lasinio Model: Its Implications for Hadrons and Nuclei. *Progress in Particle and Nuclear Physics*, 27:195–272, 1991. URL doi:10.1016/0146-6410(91)90005-9.

[55] T. Hatsuda and T. Kunihiro. QCD Phenomenology based on a Chiral Effective Lagrangian. *Physics Reports*, 247(5-6):221–367, October 1994. URL doi:10.1016/0370-1573(94)90022-1.

[56] M. Buballa. NJL-model analysis of dense quark matter. *Physics Reports*, 407(4-6): 205–376, February 2005. URL doi:10.1016/j.physrep.2004.11.004.

[57] M. Kobayashi and T. Maskawa. Chiral Symmetry and η-X Mixing. *Progress of Theoretical Physics*, 44(5):1422–1424, August 1970. URL doi:10.1143/PTP.44.1422.

[58] V. Bernard, R. L. Jaffe, and U.-G. Meissner. Strangeness mixing and quenching in the Nambu-Jona-Lasinio model. *Nuclear Physics B*, 308(4):753–790, October 1988. URL doi:10.1016/0550-3213(88)90127-7.

[59] E. E. Salpeter and H. A. Bethe. A Relativistic Equation for Bound-State Problems. *Physical Review*, 84(6):1232–1242, December 1951. URL doi:10.1103/PhysRev.84.1232.

[60] M. Gell-Mann and F. Low. Bound States in Quantum Field Theory. *Physical Review*, 84, October 1951. URL doi:10.1103/PhysRev.84.350.

[61] M. Oettel, G. Hellstern, R. Alkofer, and H. Reinhardt. Octet and decuplet baryons in a covariant and confining diquark-quark model. *Physical Review C*, 58, October 1998. URL doi:10.1103/PhysRevC.58.2459.

[62] R. Alkofer, H. Reinhardt, and H. Weigel. Baryons as chiral solitons in the Nambu-Jona-Lasinio model. *Physics Reports*, 265(3):139–252, February 1996. URL doi:10.1016/0370-1573(95)00018-6.

[63] R. Alkofer and I. Zahed. The pseudoscalar nonet in generalized NJL models. *Physics Letters B*, 238(2-4):149–155, April 1990. URL doi:10.1016/0370-2693(90)91711-J.

[64] R. M. Davidson and E. R. Arriola. Structure functions of pseudoscalar mesons in the SU(3) NJL model. *Physics Letters B*, 348(1-2):163–169, March 1995. URL doi:10.1016/0370-2693(95)00091-X.

[65] K. Goeke. Baryons in the SU(2) and SU(3) NJL model: A review of results. *Progress in Particle and Nuclear Physics*, 36:207–216, 1996. URL doi:10.1016/0146-6410(96)00025-7.

[66] D. Ebert, T. Feldmann, and H. Reinhardt. Extended NJL model for light and heavy mesons without thresholds. *Physics Letters B*, 388(1):154–160, November 1996. URL doi:10.1016/0370-2693(96)01158-6.

[67] M. K. Volkov, V. L. Yudichev, and D. Ebert. Decays of excited strange mesons in the extended NJL model. *Journal of Physics G: Nuclear and Particle Physics*, 25 (10), May 1999. URL doi:10.1088/0954-3899/25/10/303.

[68] A. L. Mota, M. C. Nemes, B. Hiller, and H. Walliser. Meson properties in a renormalizable version of the NJL model. *Nuclear Physics A*, 652(1):73–87, May 1999. URL doi:10.1016/S0375-9474(99)00147-5.

[69] M. K. Volkov, A. B. Arbuzov, and D. G. Kostunin. The decay $\tau \to \pi\omega\nu$ in the extended NJL model. *Physical Review D*, 86, September 2012. URL doi:10.1103/PhysRevD.86.057301.

[70] A. A. Osipov, H. Hansen, and B. Hiller. Long distance expansion for the NJL model with SU(3) and UA(1) breaking. *Nuclear Physics A*, 745(1-2):81–103, November 2004. URL doi:10.1016/j.nuclphysa.2004.08.022.

[71] C. M. Bender, F. Cooper, and G. S. Guralnik. Path integral formulation of mean-field perturbation theory. *Annals of Physics*, 109(1):165–209, November 1977. URL doi:10.1016/0003-4916(77)90169-5.

[72] H. Reinhardt and R. Alkofer. Instanton-induced flavour mixing in mesons. *Physics Letters B*, 207(4):482–488, June 1988. URL doi:10.1016/0370-2693(88)90687-9.

[73] N. Bleistein and R. A. Handelsmann. *Asymptotic Expansions of Integrals*. Dover Publications, 1975.

[74] A. A. Osipov and B. Hiller. Path integral bosonization of the 't Hooft determinant: fluctuations and multiple vacua. *Physics Letters B*, 539(1-2):76–84, July 2002. URL doi:10.1016/S0370-2693(02)02041-5.

[75] A. A. Osipov and B. Hiller. Path integral bosonization of the 't Hooft determinant: quasi-classical corrections. *The European Physical Journal C - Particles and Fields*, 35(2):223–241, June 2004. URL 10.1140/epjc/s2004-01779-3.

[76] G. V. Dunne. Functional determinants in quantum field theory. *Journal of Physics A: Mathematical and Theoretical*, 41(30), August 2008. URL doi:10.1088/1751-8113/41/30/304006.

[77] D. V. Vassilevich. Heat kernel expansion: user's manual. *Physics Reports*, 388 (5-6):279–360, December 2003. URL doi:10.1016/j.physrep.2003.09.002.

[78] J. Schwinger. On Gauge Invariance and Vacuum Polarization. *Physical Review*, 82(5):664–679, June 1951. URL doi:10.1103/PhysRev.82.664.

[79] B. S. DeWitt. *Dynamical Theory of Groups and Fields*. Gordon and Breach, 1965.

[80] S. W. Hawking. Zeta function regularization of path integrals in curved spacetime. *Communications in Mathematical Physics*, 55(2):133–148, June 1977. URL doi:10.1007/BF01626516.

[81] G. Esposito. Asymptotic heat kernels in quantum field theory. In A.P. Samokhin and G.L. Rcheulishvili, editors, *Problems on high energy physics and field theory: proceedings of the 17th Workshop.*, volume 17th Workshop, pages 127–134, Protvino, Russia, 1995.

[82] V. A. Slobodenyuk. Asymptotics of Expansion of the Evolution Operator Kernel in Powers of Time Interval Δt. *Theoretical and Mathematical Physics*, 105(2): 1387–1395, November 1995. URL doi:10.1007/BF02070934.

[83] A. A. Bytsenko et al. *Analytic Aspects of Quantum Fields*. World Scientific, 2003.

[84] R. D. Ball. Chiral gauge theory. *Physics Reports*, 182(1-2):1–186, October 1989. URL doi:10.1016/0370-1573(89)90027-6.

[85] A. A. Osipov and B. Hiller. Generalized proper-time approach for the case of broken isospin symmetry. *Physical Review D*, 63, March 2001. URL doi:10.1103/PhysRevD.63.094009.

[86] A. A. Osipov and B. Hiller. Inverse mass expansion of the one-loop effective action. *Physics Letters B*, 515(3-4):458–462, August 2001. URL doi:10.1016/S0370-2693(01)00889-9.

[87] A. A. Osipov and B. Hiller. Large mass invariant asymptotics of the effective action. *Physical Review D*, 64, September 2001. URL doi:10.1103/PhysRevD.64.087701.

[88] W. Pauli and F. Villars. On the Invariant Regularization in Relativistic Quantum Theory. *Reviews of Modern Physics*, 21, July 1949. URL doi:10.1103/RevModPhys.21.434.

[89] A. A. Osipov and M. K. Volkov. *Soviet Journal of Nuclear Physics*, 41(3), 1985.

[90] F. J. Dyson. The Radiation Theories of Tomonaga, Schwinger, and Feynman. *Physical Review*, 75(3):486–502, February 1949. URL doi:10.1103/PhysRev.75.486.

[91] A. A. Osipov, B. Hiller, V. Bernard, and A. H. Blin. Aspects of $U_A(1)$ breaking in the Nambu and Jona-Lasinio model. *Annals of Physics*, 321(11):2504–2534, November 2006. URL doi:10.1016/j.aop.2006.02.010.

[92] A. A. Osipov, B. Hiller, and J. da Providência. Multi-quark interactions with a globally stable vacuum. *Physics Letters B*, 634(1):48–54, March 2006. URL doi:10.1016/j.physletb.2006.01.008.

[93] A. A. Osipov, B. Hiller, A. H. Blin, and J. da Providência. Effects of eight-quark interactions on the hadronic vacuum and mass spectra of light mesons. *Annals of Physics*, 322(9):2021—-2054, September 2007. URL doi:10.1016/j.aop.2006.08.004.

[94] J. Gasser and H. Leutwyler. Chiral perturbation theory to one loop. *Annals of Physics*, 158(1):142–210, November 1984. URL doi:10.1016/0003-4916(84)90242-2.

[95] J. Gasser and H. Leutwyler. Chiral perturbation theory: Expansions in the mass of the strange quark. *Nuclear Physics B*, 250(1-4):465–516, 1985. URL doi:10.1016/0550-3213(85)90492-4.

[96] J. Bijnens. Chiral Lagrangians and Nambu-Jona-Lasinio like models. *Physics Reports*, 265(6):370–446, February 1996. URL doi:10.1016/0370-1573(95)00051-8.

[97] S. Scherer. Introduction to chiral perturbation theory. In J. W. Negele and E. Vogt, editors, *Advances in Nuclear Physics*, volume 27 of *Advances in Nuclear Physics*, pages 277–538. Springer, July 2002.

[98] A. V. Manohar. Effective field theories. In H. Latal and W. Schweiger, editors, *Perturbative and Nonperturbative Aspects of Quantum Field Theory*, volume 479 of *Lecture Notes in Physics*, pages 311–362, Schladming, Austria, 1997.

[99] D. B. Kaplan and A. V. Manohar. Current-Mass Ratios of the Light Quarks. *Physical Review Letters*, 56, May 1986. URL doi:10.1103/PhysRevLett.56.2004.

[100] J. Beringer et al. (Particle Data Group). Review of particle physics. *Physical Review D*, 86, July 2012. URL doi:10.1103/PhysRevD.86.010001.

[101] T. Matsubara. A New Approach to Quantum-Statistical Mechanics. *Progress of Theoretical Physics*, 14(4):351–378, 1955. URL doi:10.1143/PTP.14.351.

[102] C. W. Bernard. Feynman rules for gauge theories at finite temperature. *Physical Review D*, 9, June 1974. URL doi:10.1103/PhysRevD.9.3312.

[103] J. I. Kapusta. *Finite-Temperature Field Theory*. Cambridge University Press, 1989.

[104] M. Le Bellac. *Thermal Field Theory*. Cambridge University Press, 1996.

[105] B. Hiller, J. Moreira, A. A. Osipov, and A. H. Blin. Phase diagram for the Nambu–Jona-Lasinio model with 't Hooft and eight-quark interactions. *Physical Review D*, 81(11), June 2010. URL doi:10.1103/PhysRevD.81.116005.

[106] K. Fukushima and T. Hatsuda. The phase diagram of dense QCD. *Reports on Progress in Physics*, 74(1), December 2010. URL doi:10.1088/0034-4885/74/1/014001.

[107] M. A. Stephanov. QCD Phase Diagram and the Critical Point. *International Journal of Modern Physics A*, 20(19), July 2005. URL doi:10.1142/S0217751X05027965.

[108] Z. Fodor and S. D. Katz. Critical point of QCD at finite T and μ, lattice results for physical quark masses. *Journal of High Energy Physics*, 04(4), May 2004. URL doi:10.1088/1126-6708/2004/04/050.

[109] K. A. Olive et al. Review of particle physics. *Chinese Physics C*, 38, September 2014.

[110] J. A. Oller. The mixing angle of the lightest scalar nonet. *Nuclear Physics A*, 727 (3-4):353–369, November 2003. URL doi:10.1016/j.nuclphysa.2003.08.002.

[111] J. Moreira, J. Morais, B. Hiller, A. A. Osipov, and A. H. Blin. Strange quark matter in the presence of explicit symmetry breaking interactions. September 2014. URL arXiv:1409.0336[hep-ph].

[112] F. Weber. Strange quark matter and compact stars. *Progress in Particle and Nuclear Physics*, 54(1):193–288, March 2005. URL doi:10.1016/j.ppnp.2004.07.001.

[113] B. I. Abelev et al. (STAR Collaboration). Strangelet search in Au+Au collisions at $\sqrt{s_{NN}} = 200$ GeV. *Physical Review C*, 76, July 2007. URL doi:10.1103/PhysRevC.76.011901.

[114] K. Rajagopal. The phases of QCD in heavy ion collisions and compact stars. *Acta Physica Polonica B*, 31:29, May 2000. URL doi:10.1063/1.1345236.

[115] A. R. Bodmer. Collapsed Nuclei. *Physical Review D*, 4, September 1971. URL doi:10.1103/PhysRevD.4.1601.

[116] E. Witten. Cosmic separation of phases. *Physical Review D*, 30(272), July 1984. URL doi:10.1103/PhysRevD.30.272.

[117] E. Farhi and R. L. Jaffe. Strange matter. *Physical Review D*, 30, December 1984. URL doi:10.1103/PhysRevD.30.2379.

[118] R. C. Tolman. Static Solutions of Einstein's Field Equations for Spheres of Fluid. *Physical Review*, 55, February 1939. URL doi:10.1103/PhysRev.55.364.

[119] J. R. Oppenheimer and G. M. Volkoff. On Massive Neutron Cores. *Physical Review*, 55, February 1939. URL doi:10.1103/PhysRev.55.374.

[120] V. P. Gusynin, V. A. Miransky, and I. A. Shovkovy. Dimensional reduction and catalysis of dynamical symmetry breaking by a magnetic field. *Nuclear Physics B*, 462(2-3):249–290, March 1996. URL doi:10.1016/0550-3213(96)00021-1.

[121] M. Adinolfi et al. (KLOE Collaboration. KLOE first results on hadronic physics. In C. S. Lim and Y. Yamanaka, editors, *High energy physics. Proceedings, 30th International Conference*, pages 374–376, Osaka, Japan, July 2000. ICHEP.